

6-8-2005

Fuel Model Development and Fire Simulation Analysis in the Wildland-Urban Interface: The Case of Forest Park, Portland, Oregon

David Malcolm Kuhn
Portland State University

Follow this and additional works at: https://pdxscholar.library.pdx.edu/open_access_etds



Part of the [Geography Commons](#)

Let us know how access to this document benefits you.

Recommended Citation

Kuhn, David Malcolm, "Fuel Model Development and Fire Simulation Analysis in the Wildland-Urban Interface: The Case of Forest Park, Portland, Oregon" (2005). *Dissertations and Theses*. Paper 4309. <https://doi.org/10.15760/etd.6192>

This Thesis is brought to you for free and open access. It has been accepted for inclusion in Dissertations and Theses by an authorized administrator of PDXScholar. Please contact us if we can make this document more accessible: pdxscholar@pdx.edu.

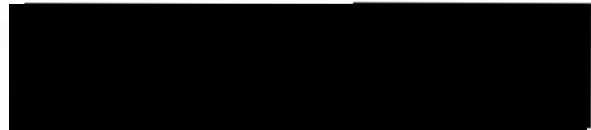
THESIS APPROVAL

The abstract and thesis of David Malcolm Kuhn for the Master of Science in Geography were presented June 8, 2005, and accepted by the thesis committee and the department.

COMMITTEE APPROVALS:



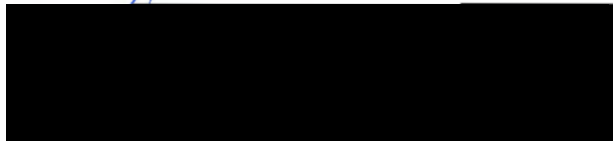
Joseph Poracsky, Chair



Jiunn-Der Geoffrey Duh

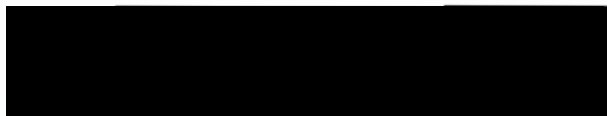


Michael C. Houck



Linda George
Representative of the Office of Graduate Studies

DEPARTMENT APPROVAL:



Teresa L. Bulman, Chair
Department of Geography

ABSTRACT

An abstract of the thesis of David Malcolm Kuhn for the Master of Science in Geography presented June 8, 2005.

Title: Fuel Model Development and Fire Simulation Analysis in the Wildland-Urban Interface: The Case of Forest Park, Portland, Oregon

Forest Park, a 5,000 acre heavily-forested park within the city limits of Portland, Oregon was selected as the study area for performing a fire simulation analysis. A well-documented fire swept over a large area of the park in 1951, and provides both direct inputs, including the ignition point, and context for the present day fire simulations. The goal of the research was two fold. First, determine the difference between small area simulations using standard and custom surface fuel models. Second, determine if fire simulation can be an effective tool in assessing fire danger and behavior in a wildland-urban interface environment like Forest Park.

Two separate simulations were performed. One used standard wildland fuel models (standard simulation) and the other used custom fuel models (custom

simulation) based on in situ fuel assessment. All other simulation inputs and parameters were the same. The primary difference between the fuel models was the live fuel components. The custom fuel models had substantially more live fuel loading and this caused the simulations to have notably different results. The standard simulation remained a low-intensity surface burn with uniform spread, an unlikely result given the weather inputs and topography of the study area. The custom simulation had a more natural spread pattern given the environmental inputs. The high intensity fire produced by the custom fuels culminated in large-scale spotting.

The results pointed to weather being the key factor in fire potential and behavior in Forest Park. A drought, such as that experienced in 1951, could create a dangerous situation because the majority of the herbaceous live fuel would lose substantial levels of moisture leading to a much drier understory. With reduced fuel moisture in the live fuels the risk of fire increases. The results supported the development of custom fuel models for small scale fire simulations. Furthermore, the results demonstrated that fire simulation can be used as an effective management tool in the wildland-urban interface that Forest Park represents.

FUEL MODEL DEVELOPMENT AND FIRE SIMULATION ANALYSIS IN
THE WILDLAND-URBAN INTERFACE:
THE CASE OF FOREST PARK, PORTLAND, OREGON

by

DAVID MALCOLM KUHN

A thesis submitted in partial fulfillment of the
requirements for the degree of

MASTER OF SCIENCE
in
GEOGRAPHY

Portland State University
2005

For the love and support while on this adventure,
I dedicate this thesis to my family

Adrienne, Sydney, and Lucy

ACKNOWLEDGEMENTS

There are many groups of individuals without whose support this thesis would not have gotten off the ground. I would first like to thank Fred Nilsen from Portland Parks. Fred not only gave me access to the park, but also a group of highly motivated and wonderful volunteers. I would also like to thank Sandra Diedrich at the Ivy Removal Project. She and Fred coordinated the use of the “No Ivy League” summer crew of 2004. Without the help of these 18 young, motivated, and intelligent people the fieldwork necessary to complete this thesis would have been an insurmountable task. In this regard I would also like to thank Melissa Severini for her work in the forest.

A special thanks to Paul Ries at the Oregon Department of Forestry. A grant from the ODF supporting this project provided the funds to acquire weather equipment to monitor weather conditions during the field research. This data was subsequently used in simulations for this study. I would also like to thank the Holmstrom and Rogers families for allowing me to set up the weather monitoring stations on their property adjacent to the park.

I would like to acknowledge the professors that challenged and enabled me to acquire the skills required to complete this study; Geoffrey Duh, Keith Hadley, Tom Harvey, Mike Emch, and Barbara Brower. A very special thank you is required for Joe Poracsky for all his efforts as my advisor and professor throughout the last 3 years at Portland State. Without his editorial comments and suggestions this thesis may have been incomprehensible.

TABLE OF CONTENTS

ACKNOWLEDGMENTS	ii
LIST OF TABLES	v
LIST OF FIGURES	vi
CHAPTER 1: FIRE IN THE WILDLAND-URBAN INTERFACE	1
CHAPTER 2: THE DANGER AND COST OF URBAN WILDFIRE	7
Economic Growth and Land Development	7
A Spatial Framework for WUI Environments and Fire Risk	8
Urban Wildfire Disasters	10
Urban Wildfire Mitigation Strategy	13
Fire Simulation as a Tool	13
Summary	15
CHAPTER 3: FOREST ECOLOGY AND FIRE MECHANICS	16
Regional and Local Species Composition	16
Regional and Local Forest Succession	19
Invasive Species at the Interface	22
Understanding the Cycle of Fire	23
Factors and Mechanics of Forest Fire	29
Factors and Mechanics of Fire Environments	32
Summary	37
CHAPTER 4: PORTLAND'S FOREST PARK: A CASE STUDY	38
Pre-Park History	38
Historic Land Use and Development	48
Human Impact Fire Factors of Forest Park	56
Fire History of Forest Park	60
Management Objectives	73
Summary	77
CHAPTER 5: MODEL IMPLEMENTATION: STEPS AND RESULTS	78
Fire Model History	78
Fire Modeling Applications	83
Farsite in the Field	90
Farsite Inputs	91
Fuel Map Development: Standard Fuel Models Selection Process	95
Fuel Map Development: Remote Sensing and Vegetation Index	106
Fuel Map Accuracy Assessment	108
	iii

Spatial Alignment of All Inputs	112
Farsite Input Preparation and Simulation Ignition	115
Summary	116
CHAPTER 6: MODEL RESULTS	118
The Fire Model Results for Forest Park	118
Simulation Results Compared to the 1951 Fire	135
Potential Property Loss in Forest Park’s Wildland-Urban Interface	146
CHAPTER 7: DISCUSSION AND RECOMMENDATIONS	149
Summary	149
Fire Mitigation Techniques	150
Additional Fire Simulation Scenarios within the Study Area	153
Analysis Limitations and Recommended Model Improvements	158
Improved Fire Planning and Management of Forest Park	159
Conclusion	160
REFERENCES	162
APPENDIX A	167
Farsite Algorithms and Inputs	167
APPENDIX B	175
Weather and Wind Files	175
Conditional Fuel Files	177
The Landscape File	179
Landscape File: Topographic Themes	179
Landscape File: Fuel Map Development Process	179
Landscape File: Canopy Themes	185
Fieldwork Data Collection and Vegetation Sampling	188
APPENDIX C	204
Vegetation Index Technical Information	204

LIST OF TABLES

Table 1: The top 5 most-costly wildfires in U.S. history all occurred between 1991 and 2003.	11
Table 2: Recommended Firemon Landscape Assessment strata type and sub-components.	30
Table 3: Table includes all development within a 1.24 mile (2km) buffer around Forest Park.	54
Table 4: Description of fuel model fields derived from Firemon and Behave output.	84
Table 5: Explanation of the raster inputs to Farsite.	86
Table 6: Stand composition of each plot.	97
Table 7: Comparing the fuel loading quantities between Anderson’s standard fuel models and the custom fuel model equivalents for the study area.	106
Table 8: Accuracy assessment of the WDVI classification of study area	110
Table 9: A comparison of fire behavior parameters between the standard and custom simulation results and the reconstructed 1951 fire.	136
Table 10: The values in the table are based on tax assessment records and therefore do not reflect the real value of the properties.	147

LIST OF FIGURES

Figure 1: Graphs showing the general trend of wildland fires and acres burned since 1960.	4
Figure 2: Examples of the four WUI environment types.	9
Figure 3: Photo taken during the fires that raged through San Diego County October 25 th through November 4 th , 2003.	12
Figure 4: Two views of the western hemlock zone using the national atlas forest cover type classification.	17
Figure 5: Western Hemlock Zone Forest Succession Pattern.	20
Figure 6: Photo taken by author of invasive English ivy.	22
Figure 7: 230 year series represents a FRI more similar to the dynamic observed in Forest Park since the time of settlement and logging.	24
Figure 8: Fire movement through a forest.	32
Figure 9: Surface fuel exposure based on open wind conditions aloft and canopy cover.	34
Figure 10: Visual aid of general topographic features found in the Tualatin Mountains and Forest Park.	35
Figure 11: 3D image of the canyons and other topographic features just South of Saltzman Road.	36
Figure 12: The Tualatin Mountains dominate Portland's Westside.	39
Figure 13: Elevation profiles at three points across the Tualatin Mountains ridge.	41
Figure 14: Original trails that traversed the Tualatin Mountain ridge.	43
Figure 15: Census 2000 urbanized area (UA) and urban clusters (UC).	47
Figure 16: Development around the southern end of Forest Park since 1870.	49
Figure 17: Development around the northern end of Forest Park since 1870.	50

Figure 18: Building zone designation around the southern half of Forest Park based on 2004 metro taxlot data.	51
Figure 19: Building zone designation around the northern half of Forest Park based on 2004 metro taxlot data.	52
Figure 20: The aerial photo shows the intersection of Highway 30 and St. Helens Rd.	55
Figure 21: A transient fire lit on the side of a trail in Hoyt Arboretum.	57
Figure 22: Two utility corridors transect the park.....	59
Figure 23: The orange shaded area is a rough estimate of the 1889 fire extent, overlaid on the current roads.	62
Figure 24: The orange shaded area is a rough estimate of the 1940 fire extent overlaid on the current roads.	64
Figure 25: Red shaded area represents the 1951 fire extent.	66
Figure 26: Large scale fires to burn in or around Forest Park since Anglo-American settlement.	68
Figure 27: Photo taken on August 22 nd , 1951 of burned area on the western slopes of the Tualatin range, west of Skyline Blvd.	72
Figure 28: Photo taken on August 22 nd , 1951 of burned area on the western slopes of the Tualatin range, west of Skyline Blvd looking down onto Bonny Slope.	73
Figure 29: Vertical fuel structures that can lead to crown fires.	75
Figure 30: Shaded fuel breaks are placed at strategic locations to minimize fire's ability to ladder into tree crowns.	76
Figure 31: Fire simulation model types, inputs, and output generation schematic.	82
Figure 33: Farsite project view.....	92
Figure 34: Anderson's photo of fuel model 5.	99
Figure 35: Visual comparison and a walk-through of areas in the study area confirmed that fuel model 5 had appropriate fuel loading values.	99

Figure 36: Anderson’s photo of fuel model 8.	101
Figure 37: Photo taken by Author of a sampling plot selected to represent fuel model 8.	101
Figure 38: Anderson’s photo of fuel model 10.	103
Figure 39: Photo taken by Author of a maturing stand dominated by Douglas-fir. There is little old growth environment in the study area.	103
Figure 40: Anderson’s photo of fuel model 9.	105
Figure 41: The fall litter potential for this stand type in the study area is most likely less than that expected by Anderson for this fuel model.	105
Figure 43: 1,000 points were randomly generated over the WDVI image.	111
Figure 44: The majority rule processing of the 1.1 meter original fuel map to the resampled 10 meter Farsite input.	112
Figure 45: The output of the majority rule function applied to the classified WDVI image was used as the base fuel layer for all other fuel inputs.	114
Figure 46: Burnt area shared by both simulations within the first 48 hours of the simulation runs.	120
Figure 47: Time of arrival spread of the standard simulation.	123
Figure 48: Time of arrival spread of the custom simulation.	124
Figure 49: Rate of spread across the entire standard simulation extent.	125
Figure 50: Rate of spread calculated for the custom simulation.	126
Figure 51: Fire line intensity of the custom simulation.	128
Figure 52: Heat per area of the custom simulation.	129
Figure 53: The flame length of the standard simulation.	132
Figure 54: Flame lengths of the custom simulation.	133
Figure 55: High correlation between elevated fire intensity and flame lengths on slopes with northeastern aspects.	135

Figure 56: Shaded areas represent areas that both simulated fires and 1951 fire burned.137

Figure 57: Circles represent the total area burned during the fires.....138

Figure 58: Images show a four hour sequence (hours 57 to 60) in the fire spread of the custom simulation.140

Figure 59: Images from the Standard simulation represent hours 57 and 58.141

Figure 60: Time of arrival (TOA) comparison between the predicted TOA values of the 1951 fire and the TOA values of the custom simulation.143

Figure 61: Histogram of the distribution of pixels for the time of arrival difference map comparing the 1951 fire and the custom simulation.144

Figure 62: Time of arrival (TOA) comparison between the predicted TOA values of the 1951 fire and the TOA values of the standard simulation.145

Figure 63: Histogram of the distribution of pixels for the time of arrival difference map comparing the 1951 fire and the standard simulation.146

Figure 64: Accidental fire start in green belt within a residential development.154

Figure 65: Accidental fire start from power line-tree contact.....157

CHAPTER 1: FIRE IN THE WILDLAND-URBAN INTERFACE

From an environmental perspective, there are three general types of fire: wildland, wildland-urban interface, and urban/building fire. In each environment the fuel types and amounts, the potential spread area, and the degree of economic damage are all different. For example, a wildland fire occurs in a wilderness area, burning only trees and vegetation over potentially thousands of acres. On the other end of the spectrum, an urban fire will typically consume a single structure on a street surrounded by other buildings and limited vegetation. Fire in a wildland-urban interface (WUI) combines these two scenarios and may occur in physical environments that vary along a gradient from more wildland to more urban. The focus of this study is to assess the use of fire models built for wildland fire environments on a WUI fire environment. However, before the discussion narrows in on fire in the WUI, a brief overview of wildland fire is required.

Fire is a fundamental part of most forest ecosystems in the Western United States. In the short term fire is damaging and destructive; but, over the long term, fire enables the forest to develop through a natural progression and remain healthy. Forests have a natural pattern of succession which is dependent on a cycle of fire as a cleansing component. Fire frees nutrients back into the soil, thins out trees to prevent fuel accumulation, and allows some species to become dominant while removing others. The threat of catastrophic fire in wildland areas stems from a historical policy of fire exclusion in our national forests and other wilderness environments.

Many Western U.S. forests are adjacent to urban areas. The exclusion of fire from these previously fire-dependent ecosystems has led to unprecedented accumulation of fuel and a change in successional patterns away from fire climax communities (Miller and Wade 2003). Among the negatives of removing fire from the natural cycle are that: tree and understory vegetation become overcrowded; the risk of insect infestation, disease, and blowdown due to weakened trees increases; and overall stand health declines. The cumulative effect has been increased dead fuel as well as larger numbers of live trees, producing an increased fire hazard. National wildland fire statistics have been compiled dating back to 1960 and these data point to fewer but larger fires, at least over the past 45 years (Figure 1). Federal agency expenditures to fight fire have steadily increased, with the 2002 fire season setting the record at \$1.66 billion (NIFC).

Most wildfires are caused by humans, and not always accidentally. A Texas A&M study conducted on causes of Texas wildfires in 1993 found that 40% were arson (<http://agnews.tamu.edu/graphics/newsgraph/tfsv/firecaus.html>). It thus stands to reason that an increased number of people in an area will possibly lead to an increase in fire hazard. The October 2003 fires in Southern California were a stark reminder of the devastating effects of human-caused wildfire in an urban environment.

The forest ecology and climate of Northwest Oregon are substantially different than that of Southern California, especially with respect to fuel moisture levels and fuel composition. Nonetheless, the temperate rain forests of Northwest Oregon are part of a fire dependent ecosystem, albeit one with a much longer fire cycle than that of the Southern California oak-grassland and chaparral. Fires will continue to occur in

Oregon's forests and, in the case where forests are part of a Wildland-Urban Interface (WUI) environment, fire frequency and intensity will likely increase.

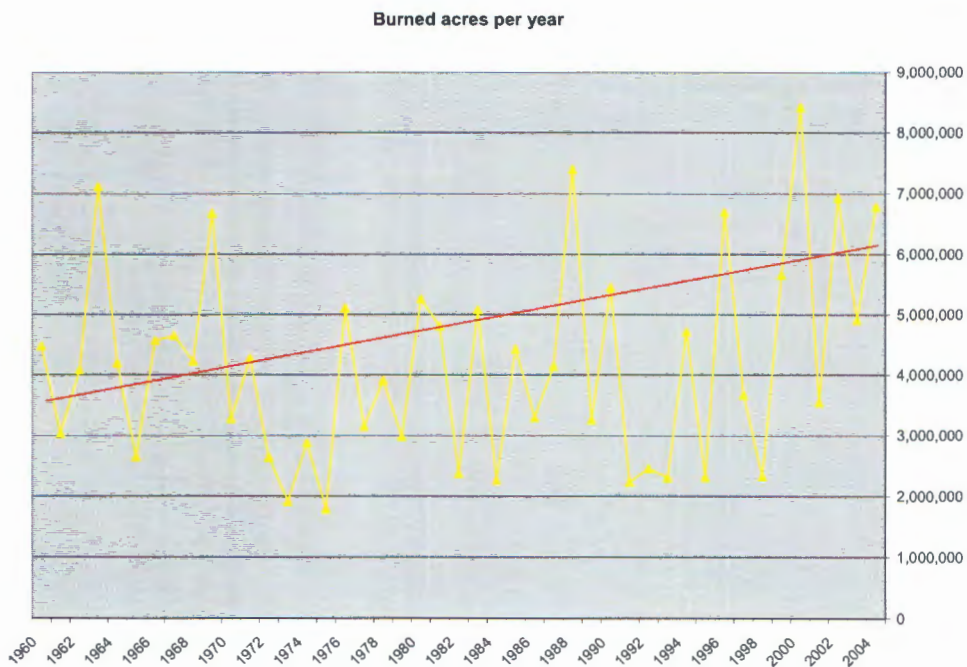
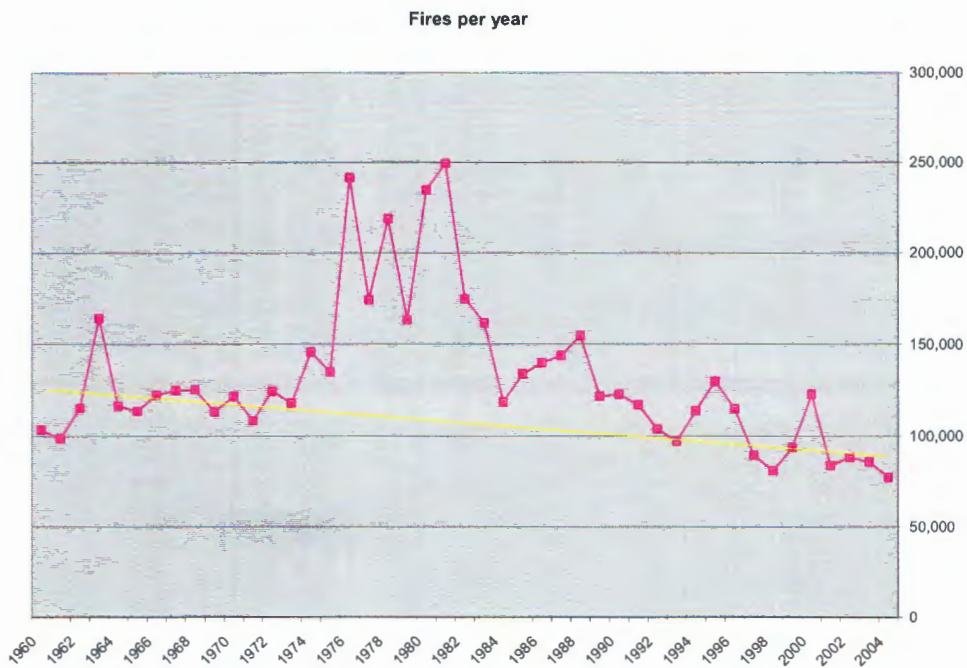


Figure 1: Graphs showing the general trend of wildland fires and acres burned since 1960. Compiled by the National Interagency Fire Center based on data from Bureau of Land Management, Bureau of Indian Affairs, National Park Service, US Fish and Wildlife Service, USDA Forest Service and all State Lands. (Source: <http://www.nifc.gov/stats/wildlandfirestats.html> .)

Forest Park - a heavily forested park within the city limits of Portland, Oregon - represents an environment where an urban forest fire could endanger thousands of people and result in substantial property loss. The ability to analyze the probability and behavior of a forest fire under different ignition scenarios would assist local officials to develop appropriate treatment, evacuation, and suppression plans.

One tool that could be used to simulate such a set of fire scenarios is the Farsite fire simulation model. Developed by the USFS, Farsite is used to predict the behavior of fire in wildland environment for past, present, and future fires. The model uses thirteen standard fuel models, each based on a different vegetation environment. Additionally, custom fuel models can be developed for field-identified conditions in a local area, and then be analyzed by the application. The Farsite model was used in this research to examine possible scenarios for Forest Park.

The goals of this research are two-fold. First, to determine the accuracy of custom surface fuel models versus standard wildland fuel models applied to the same urban forest environment. In this regard, is there negligible difference in the simulation outcome when using either standard fuel models or custom fuel models based on in situ fuel assessment? The different fuel models will be tested using the inputs from a 1951 fire that burned through a central area of the park. The ignition point, spread pattern, and final extent of the 1951 fire were documented. Each simulation will use the 1951 weather inputs prior to and during the fire. The results of the simulations will then be compared with each other and with the reconstructed 1951 fire extent. This first goal can be accomplished within the course of this study.

The second goal of this research is to determine if fire simulation can be an effective management and planning tool in predicting urban forest fire behavior, specifically in Forest Park. The answer to the first question enables city officials to assess if the model can be used as the foundation for a comprehensive fire mitigation strategy. If the model is reliable enough to locate threats it can be used as a decision support tool to plan mitigation. Furthermore, the City of Portland can use this study as the basis for assessing the cost of applying similar analysis to other park areas. This study is thus the first step in incorporating fire modeling into a fire mitigation strategy that can be applied in the context of the City of Portland's 1995 Natural Resource Management Plan.

CHAPTER 2: THE DANGER AND COST OF URBAN WILDFIRE

This chapter explains why fire is a growing threat to urban environments and how development in specific locations increases the threat. The different types of WUI environments are defined and aerial images are used as examples. Wildfires that occurred in WUI environments illustrate the potential for property and human loss. The chapter continues with an introduction to the use of fire behavior simulation as a tool for identifying areas that would be best served by active management.

Economic Growth and Land Development

Economic factors have led to an increase in development in areas considered part of the WUI. Economic prosperity of the last several decades has led to unprecedented growth in real estate development throughout the West. Established communities within WUI environments, such as the Oakland-Berkeley Hills in the Bay area or the West Hills in Portland, Oregon, have seen housing prices grow 10% or more year-after-year in the past decade, according to the National Association of Realtors. This level of growth has increased insurance risk and priced many moderate-income people out of these increasingly expensive neighborhoods. Part of what makes the established neighborhoods in WUI environments appealing is their location and setting.

With the rise in real estate values, more affordable “suburban” housing has been developed further from urban centers. Many new developments are being put on rural or ex-agricultural land. However, developments are being placed on previously forested land. Even when the developments are clearcut prior to building, the adjacent

land remains forested. In some cases the latter developments are being built in areas that have the highest risk of fire, such as hillsides, in canyons, or on bluffs surrounded by nearby greenbelts or forests.

A Spatial Framework for WUI Environments and Fire Risk

The WUI can be defined by a variety of development density scales. Many state agencies in the west have adopted a set of definitions for four different types of WUI condition: including interface, intermix, occluded, and rural conditions (Figure 2). The *interface* condition is defined by clear demarcation between structures and wildland fuels along constructed borders (e.g. roads or fences). Wildland fuels do not continue into developed areas where an interface condition exists. In an *intermix* condition there is no clear line of demarcation between development or wildland fuels, and structures are scattered throughout the wildland area. Typically an intermix environment will consist of resort or residential development. An *occluded* condition exists primarily in urban forest, greenbelt, park or open space environments where an island of wildland fuels is surrounded by development. *Rural* conditions exist where small clusters of development, such as ranches or farms, are exposed to wildland fuels. Rural conditions are typically defined by their being embedded in a working landscape (Weatherford 2002).



Interface environment: clear demarcation exists between forested and urban development



Occluded environment: Forested area is surrounded by urban development



Intermix environment: Small clusters of development are nestled within areas dominated by forest



Rural environment: Pockets of development and cleared land extend through areas dominated by forest

Figure 2: Examples of the four WUI environment types using remote sensing images (1m B&W DOQQ). The examples used came from images taken within the Portland metropolitan area or immediate environs. (Source: EROS Data Center, USGS Seamless Data Distribution Delivery System.)

Intermix and rural WUI environments by definition consist of more wildland than development. In intermix or rural environments only individual houses or small clusters of structures can be considered when employing mitigation practices. The surrounding wildland area may be treated, but only to the extent of avoiding the loss of tens or hundreds of thousands of acres to conflagration.

The WUI environments that are focused upon in this paper are interface and occluded environments. The subject area of this paper is primarily an interface environment. However, patches of occluded environments abut the larger interface landscape. The danger posed by an occluded environment can be deceptive; the forested area does not have to be very large and may snake through areas of high density development.

Occluded areas will also tend to have increased pressures; higher vegetation density, greater ignition potential, and potentially more non-native and less fire-resistant trees and shrubs. For example, pre-settlement vegetation in the hills around Oakland and Berkeley consisted of oak-savannah grassland. However, the fuel that burned there in 1991 consisted largely of planted groves and escaped ornamental shrubs, all of which were fire-prone species.

Urban Wildfire Disasters

According to the Insurance Information Institute (2005), four of the five most costly wildfires in U.S. history occurred in interface or occluded conditions. A table of the most devastating urban wildfires reveals that fire in the WUI is becoming more frequent, property losses are increasing, and the size of the fires are growing (Table 2).

Table 1: The top 5 most-costly wildfires in U.S. history all occurred between 1991 and 2003. The ranking is based on 2003 value of lost property. Of the 16 most costly urban wildfires, 8 have occurred since 1991, and none occurred before 1970. It is estimated that 2.3% of all insurance claims stem from wildfire. (Source: Insurance Information Institute.)

Fire Dates	Rank	Fire Location Type	Fire Location "Fire Name"	Acres Burned	Dollars when occurred (millions)	In 2003 dollars (millions)
Oct 20-21, 1991	1	Occluded	Oakland/Alameda Counties, California "Tunnel"	1,520	\$1,700	\$2,296
Oct. 25-Nov. 4, 2003	2	Interface	San Diego County, California "Cedar"	273,246	\$1,060	\$1,060
Oct. 25-Nov. 3, 2003	3	Intermix/Interface	San Bernardino County, California "Old"	91,281	\$975	\$975
Nov. 2-3, 1993	4	Interface	Los Angeles County, California "Old Topanga"	16,500	\$375	\$478
Oct 27-28, 1993	5	Interface	Orange County, California "Laguna Hills"	14,437	\$350	\$446

The 1991 Oakland-Berkeley Hills "Tunnel Fire" was one of the most costly and deadly urban wildfires, burning only 1,520 acres (615 hectares), but destroying 2,843 homes and killing 25 people. As a result, the Oakland-Berkeley Hills is considered one of the most costly natural catastrophes of all time (Cleaves 2001). Comparatively, the 1991 fire would have represented a small area in the "Cedar Fire" of 2003 in San Diego County, which occurred over a month after the end of the fire season and destroyed 3,570 homes (Figure 3).



Figure 3: Photo by John Gibbins from the San Diego Union-Tribune taken during the fires that raged through San Diego County October 25th through November 4th, 2003. The picture shows one of the fire fronts of the “Cedar Fire” in San Diego county, which killed 14, destroyed 2,232 homes, and consumed 273,246 acres (110,579 hectares). The “Paradise” and “Old” Fires, which burned during the same time in adjacent San Bernardino County killed 2 and 6, destroyed over 221 and 993 homes, and consumed 56,700 (22,946) and 91,281 (36,940) acres (hectares) respectively. The three fires consumed a total of 421,227 acres (170,465 hectares).

The Oakland-Berkeley Hills fire is a prime example of the danger posed by a fire-prone greenbelt inside an urban environment. The historic approach to fire in WUI conditions has been prevention through public education: providing residents in high-risk areas with information on creating fire-safe zones around their homes. This approach alone will not work in occluded and interface environments. With ever increasing density, fire outbreak in these areas may destroy homes and threaten people in minutes, despite an immediate and massive response. Fire mitigation needs to start inside the occluded or interface environment. Information about fire mitigation techniques, such as fire-safe zones, must be coupled with information about landscape

scale fire management. The public needs to be made aware that fire itself can play a role in the prevention process in the form of prescribed burns (Miller 1997).

Urban Wildfire Mitigation Strategy

The effect of development on fuel composition in an occluded environment takes years to manifest in the forest succession and ecology. With regular monitoring the impact can be measured over time. The monitoring data can be used to determine appropriate management solutions. However, increasing development can make mitigation management more difficult to accomplish because along with development comes increased land use regulation and designation to special categories (Miller and Wade 2003). Occluded environments are quickly designated “sensitive areas” and the ability to apply any kind of fuel treatments becomes difficult, legally and politically.

An occluded environment is most likely a highly valued landscape for the surrounding developments. The loss of just that environment, let alone the surrounding homes and businesses, would have profound economic, social, and emotional impact on the population. Therefore, introducing “destructive” fire management practices into the environment is difficult without providing the public with proper justification. Fire management plans need to prove themselves ecologically and economically, while minimizing aesthetic impact. The easiest way to demonstrate the effectiveness of a comprehensive fire management plan is to show the potential fire behavior in the environment.

Fire Simulation as a Tool

Urban areas with interface or occluded environments need to prioritize the use of fire behavior modeling and simulation in the development of fire management

plans. Fires have many elements of uncertainty, especially in spread behavior at the point of interface and through developed areas. It has been proven that, at recognizable thresholds, the proper combination of weather and fuel produces and sustains simultaneous outbreaks of fires across the wilderness. Recognizing these conditions and assessing the potential of fire risks in WUI environments using simulation has been largely ignored as a pre-disaster strategy. However, historical review and development of local models could provide better decision support during real emergencies (Cleaves 2001).

Fire behavior simulation was developed for use in wildland fire management. The original fire models were used to draw most likely spread rates and directions on maps for use by firefighters in planning suppression activities. Eventually the advent of computers enabled the models to be represented in algorithms with digital output. Fire simulations were no longer specifically for active fires, but could be used to analyze past fires, and compare events that occurred in the same location. In this regard, fire simulation became a tool for analyzing fire ecology. Today, fire simulation is used to analyze past, present, and potential fires. However, the use of this technology has focused on wildland environments and fuels. With increasing cost associated with the rising number of fires in the WUI, the need for effective tools in developing pre-disaster mitigation strategies is required.

The ability to simulate and visualize fire behavior is a powerful tool for fire management planning in WUI environments. For example, fire simulation enables urban planners to assess an entire landscape, and pinpoint the locations of greatest threat and potential treatment. The simulation results can be used as input in cost-

benefit analysis of various treatment protocols. As treatments are completed, additional simulations can be run to determine their effectiveness. Ecological assessment is made possible by the data collected during pre-treatment and post-treatment field work. The assessment data is fundamental in determining how the ecosystem is reacting to the treatment regime, especially if prescribed fire is used (Agee 2000). All the science, management, and planning aside, the most useful aspect of the simulation output is the educational value in demonstrating to the public the risks of doing nothing.

Summary

In this chapter we discussed how economic growth in the past 20 years has led to increasing home prices and rapid development in WUI environments across the West. Interface and occluded WUI environments have been the sites of the most devastating urban wildfires. Traditionally, mitigation strategy has been employed at the interface boundary, in the immediate vicinity of structures. However, firebrands and lofted embers can travel great distances during more intense fires. Therefore mitigation strategy needs to extend beyond the interface boundary and into the wildland environment. Fire simulation can be used to assess and demonstrate fire behavior at the landscape scale. Simulation output can be used by multiple stakeholders to determine the most appropriate locations, extent, and types of mitigation technique to employ.

CHAPTER 3: FOREST ECOLOGY AND FIRE MECHANICS

This chapter is focused on the fire ecology of the western hemlock zone and the mechanics of fire movement. Agee, Fahnestock, and Flewelling are among the many researchers who have established theory on the cycle of fire in the forests west of the Cascade crest. Their efforts have shown that fire plays an integral role in the long-term health and development of these forests.

Regional and Local Species Composition

Douglas-fir typically regenerates and establishes itself as the dominant coniferous species in the foothills and low mountains west of the Cascades after a high intensity fire or other disturbance that kills all of the vegetation in a forest. Such a disturbance is typically referred to as a *stand replacing event*, and these are rare in the western Pacific Northwest. Much of this area is considered to be a part of the western hemlock vegetation zone, a classification based on western hemlock being considered the self-perpetuating and climax species (Figure 4). Typically the western hemlock zone is bounded by elevations ranging from 750 to 3,500 feet (Franklin and Dyrness 1988). Forest Park is part of this zone, though in the lower elevation portion. However, the park's placement in a WUI environment has produced a somewhat non-standard species composition.



Figure 4: Two views of the Western Hemlock Zone using the national atlas forest cover type classification. The map on the left displays forests classed as Douglas-fir and western hemlock. The map on the right displays only the western hemlock forests. The red box outlines the Tualatin Mountains. Douglas-fir and western hemlock classes are found in the box. However, Douglas-fir and western hardwoods would be considered dominate at the current stage of development. (Source: National Atlas of the United States, the USDA Forest Service.)

A fire protection plan written in 1950 concluded that the whole area had been logged within 50 to 70 years prior. Considerable logging had also been completed in the area between Germantown Road and Newberry Road between 1945 and 1950 (Marshall 1950). Multiple fires of variable intensity have burned large portions of the Tualatin Mountains in the last 150 years since Euro-American settlement. Many of them started from slash pile burning. The repeated disturbance pattern has continually altered the natural succession. This cycle of fire has established a mixed hardwood forest composed of large stands of red alder (*Alnus rubra*), and bigleaf maple (*Acer*

macrophyllum), interspersed with stands of Douglas-fir (*Pseudotsuga menziesii* Mirb.), western hemlock (*Tsuga heterophylla*), and younger western red cedar (*Thuja plicata*), and grand fir (*Abies grandis*). The current hardwood-conifer mix, based on percentage of total trees per hectare measurements acquired from sampling plots, is 51% hardwood and 49% conifer.

A natural, undisturbed, and mature western hemlock vegetation zone forest at an age of about 250 years would consist of three primary species: Douglas-fir, western hemlock, and western red cedar. Secondary species interspersed with the primaries would consist of grand fir, black cottonwood, red alder, bigleaf maple, madrone, and western yew. The hardwood species would start to be excluded from a maturing forest or relegated to riparian or edge environments once the conifers began over topping them. The forest understory would consist of a variety of well developed shrubs; sword fern, salal, Oregon grape, lady fern, red huckleberry, western hazel and vine maple (along trails and edges). Wildflowers such as wild ginger, Hooker's fairy bells, vanilla leaf, trillium, evergreen violet, and inside-out flower would also grow among the shrubs, primarily during the summer (Houle 1996).

Bigleaf maple has become unusually dominant through out the park, but not abnormally so. Bigleaf maple was present prior to logging and abundant in areas that did not burn. In areas that were logged or burned Bigleaf maple stumps remained vital and re-sprouted, growing more quickly than other pioneer species and building a larger seed source. Conversely the repeated logging and burning reduced the seed source of conifers.

Red alder has dominated some areas of the park. In a natural environment red alder would be a pioneer species and grow primarily on riparian slopes. However, areas where humans have disturbed the successional pattern, either by intensive logging and subsequent repeated fires, the soils are leached of nutrients. At this point red alder can invade adjacent areas and out-compete all conifer trees. Young Douglas-fir, the pioneer evergreen after a disturbance, needs bare soil to gain a foothold and develop into a stand. If red alder gets there concurrently then it will take a long time for Douglas-fir to overtop the alder and develop into stands. In the environments devoid of Douglas-fir, shade-tolerant evergreen (western hemlock, western red cedar) struggle to survive in small numbers or are excluded from the area (Newton 1967).

Regional and Local Forest Succession

In remnant forests of the Pacific Northwest, hardwoods pioneer the early successional landscape. Hardwoods may continue to dominate along edges. Eventually the genetic predisposition of conifers to overtop hardwoods will cause the decline of the hardwoods during the stem exclusion stage. Hardwood decline will accelerate as stands transition through the understory reinitiation stage into a multiple cohort stand. A cohort simply refers to groups of trees of similar character, such as age. Typical of mixed Douglas-fir/hardwood forests, the disturbance events lead to a patchwork of multi-modal, and even-aged and –sized stands (Wills and Stuart 1994). Eventually the stand reaches equilibrium in biomass and productivity, and enters into an old-growth stage (Figure 5).

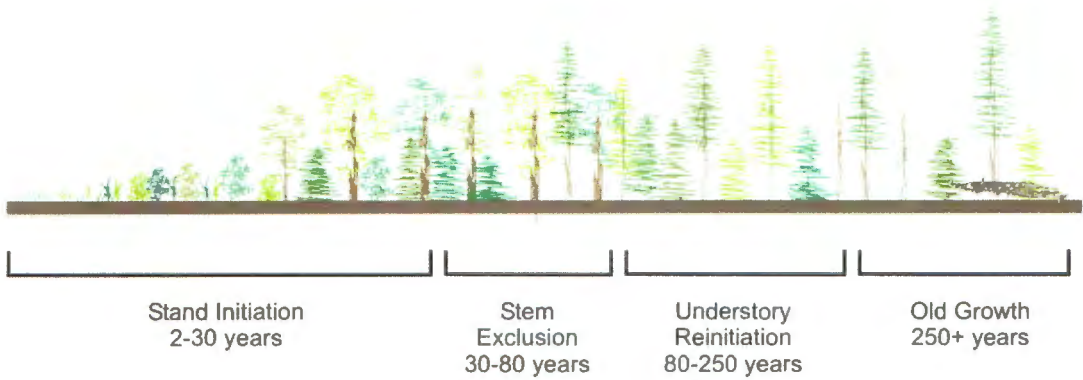


Figure 5: Western Hemlock Zone Forest Succession Pattern. About 20% of Forest Park is in the stand initiation stage, dominated by abundant Alder and Bigleaf maple. Over 50% of the park is in the stem-exclusion stage, in which Douglas-fir over 40 years old, is beginning to top the hardwoods, and the upper reaches of the canopy are about 100 feet tall. About 25% of the park has transitioned into the understory reinitiation stage, with hardwoods beginning to drop out of the stand. There are only a few acres of old-growth in the park, constituting less than 5% of the park area. (Source: concept by Houle 1996, illustration drawn by Author.)

The successional pattern for western hemlock zone forest involves 4 major stages. In the case of fire, for the first few years after a stand replacing event the landscape consists of burned snags and grasses that are able to quickly regenerate. This stage is called the stand initiation stage and will last for up to 30 years. Shrubs will establish and persist in the understory. At lower elevations hardwoods will pioneer the tree growth along with shade-intolerant conifers, such as Douglas-fir. For the first 30 years hardwood will dominate the canopy.

Between 30 and 80 years Douglas-fir will top the hardwood and the successional pattern will shift into the stem exclusion stage. The stem exclusion stage is described as exhibiting decreasing stand density accompanied by canopy closure. Lower branches interlock and lateral expansion slows. As the canopy closes, less light is available to suppressed trees and lower branches. Unless the suppressed trees are very shade tolerant, their ability to photosynthesize is hindered and they die. Leaves

on lower branches die and the limbs become non-functional and die. The net effect is that dominant trees become less randomly distributed throughout the stand (Oliver and Larson 1990).

The understory reinitiation stage begins when trees in the upper canopy begin to succumb in small groups or individually. The gaps left by these trees enable shade tolerant trees to release and ascend into the overstory. Individual stands may stay in this stage for a long time. Young and old trees coexist and occasional disturbances, such as wind throw, insects, or disease, clear trees gradually to let climax species grow into dominance. As gaps in a stand are created and filled, a stable balance of trees of different species, sizes, and ages will become established (Baker, et.al. 1996).

The pattern of increasing conifer dominance should persist for 250 years, at which time an old growth environment becomes established as Douglas-fir gives way to western hemlock and more shade tolerant species. This model only applies as long as no other severe disturbance events occur as the process is unfolding (Franklin and Dyrness 1988).

The succession pattern that has emerged in Forest Park after the frequent disturbances of the late 1800s and first half of the last century is normal, given the elevation and orientation of the area. Past analysis estimates that the majority of the park is in the stem-exclusion stage of development (City of Portland 1995). The City's assertion that the 5,000 acre forest is mostly in a single stage of development is a generalization. This is especially true given the witnessed disturbance history and placement in an urban interface.

There are areas of the park that are well described by the stem-exclusion definition, but others that have begun to transition to understory reinitiation of a single cohort. However, the 50/50 canopy mix is likely to continue for some time, even without further disturbance.

Invasive Species at the Interface

The herbaceous understory of Forest Park is most impacted by its interface condition. There is widespread evidence of ornamental escape in the form of English ivy (*Hedera helix L.*), which has overtaken areas of the forest along the southern edges of the park. Yellow Clematis (*Clematis tangutica*) has also invaded the same areas and grown high into the canopy. Unchecked, these vines will choke trees to death or add enough weight to cause blowdown during a storm (Figure 6).



Figure 6: Photo taken by author of invasive English ivy. Ivy will out-compete other ground cover and eventually grow up into the canopy via tree trunks and out onto limbs. The added weight can bring down trees during storms, creating forest openings, and causing ecological change.

Another invasive of particular concern is Garlic mustard (*Alliaria petiolata*), which is able to compete independent of the presence or cover of native species can alter habitat suitability for native insects. These types of invasive species can eventually alter the fauna and flora of the environments they invade. However, the most dominant understory species in Forest Park is the Sword fern (*Polystichum munitum*). The Sword fern accounted for over 80% of the ground cover measured at sampling plots within the park.

Understanding the Cycle of Fire.

Fire cycle modeling is used to predict regularly occurring fire patterns. In this regard two concepts are critical. The first is the fire cycle, which is used to suggest that fire returns to an area with some regularity and in some instances leads to stand replacement. Second is fire return interval (FRI), the time between fires in a specified area of forest. The FRI is typically how fire cycles are gauged. Even a low intensity surface burn that may only kill a handful of seedlings resets the FRI. In many cases there will be multiple FRIs in a fire cycle (Figure 7).

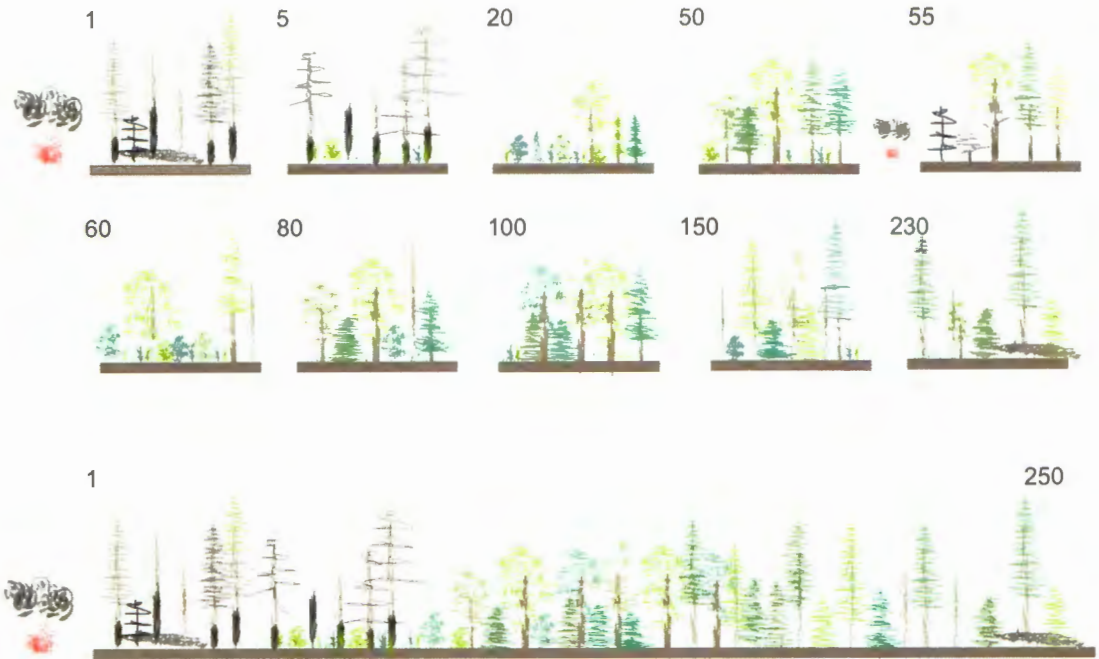


Figure 7: The 230 year series represents a FRI more similar to the dynamic observed in Forest Park since the time of settlement and logging. The bottom series represents a single “natural” FRI, where fire of any intensity has not returned to the forest in 250 years. (Source: concept by Agee 1991, illustration drawn by Author)

Many studies have attempted to establish a fire cycle for the forests west of the Cascades crest. Most studies have found that the fire cycle in wet-to-mesic forests is far more complex than the drier environments east of the Cascade Range. A regional average FRI for the western and coastal Pacific Northwest forests dominated by Douglas-fir was determined to be approximately 230 years. This average was based on an analysis of forest survey records from the 1930s. The study used the records to calculate the time between fires for the various stands from which the samples were collected. This information can then be extrapolated to establish the average FRI for the larger areas. The results of the modeling suggest that substantial spatial variability is included in the estimate, as well as considerable temporal variability due to climatic

shifts (Fahnestock and Agee 1983).

Studies of the long-term fire history of the western Pacific Northwest have been based on lightning as the ignition source. The lightning ignition portion of a fire cycle model developed for the Olympic peninsula (Agee and Flewelling 1983) was applied to 4 locations in western Washington and Oregon. The model parameters used were probability of long-term drought, a rain exceeding 0.25 cm, occurrence of a thunderstorm, and an east wind, which is usually drier and stronger than the typical westerly flow. The model results were presented as the probability of ignition per year that would result in a fire that would grow beyond 1 hectare.

The model was applied to areas of 175,000 hectares (675 mi²) across the entire region. The general trend showed that probability of ignition increases in an easterly and southerly direction from the western Olympics through the Siskiyou Mountains of southwest Oregon. Results from the 4 test sites indicated that ignition per year in the Western Olympics was equal to 0.1, Wind River area equal to 0.3, McKenzie River area equal to 0.5, and the Siskiyou equal to 1.0, ten times the likelihood of ignition relative to the Western Olympics. Agee cautions that the model results should be interpreted as relative numbers between sites, rather than an absolute estimate at any one site.

The fire history of the Pacific Northwest is undoubtedly tied to weather. The fire season typically extends from June to September, largely due to the maritime climate, which produces moderate temperature and humidity, and only light precipitation during these months. It is during droughts that major fires occur and will often burn with great intensity. Because the region is wet most of the year fuel loads

can exceed several hundred tons per acre, from understory growth. The overstory fuels are not the cause for concern as much as the prodigious understory, which can dry out during drought. Additionally, severe weather can blow down large swaths of forest. The Columbus Day storm, in 1962, felled 7 billion board feet worth of trees over several hundred square miles in Oregon and southwest Washington. This level of dead fuel can develop into a cycle of reburns that can extend over decades. The Tillamook burns are a good example of this phenomenon (Pyne 1998).

Little evidence exists that fires lit by Native Americans culminated in large stand replacing events. Furthermore, these events could not have altered the fire cycle of the western Pacific Northwest in any meaningful way. Stories of catastrophic fires can be found in Native American legend. However, the case for widespread aboriginal fires throughout the region can not be established (Agee 1991). Most anthropogenic fires were surface burns lit by Native Americans to clear lowland and non-forested areas for the purpose of game management. Many of these fires burned vast areas, especially in the Willamette Valley. The frequency with which they were set served to establish prairies in the river valley bottoms with isolated groups or individual ash, oak, pine, and fir in special conditions, usually on the margins of the valleys or along streams. At the time of the first survey of the Willamette Valley in 1853 the surveyors frequently found no trees on the flats of the valley (Johannessen et al. 1971).

Conversely, the upland areas adjacent to the valleys had abundant forest cover. In the period 1845-1855 seven times as much land was deforested as in any of the three previous decades as large scale Euro-American settlement of the Willamette

Valley occurred. During this same time period anecdotal accounts exist of great fires occurring from escaped cooking or slash fires throughout the coastal areas of Oregon. Some of these events have been corroborated by journals kept by expeditions dispatched to the southern coast (Morris 1934).

Finding evidence of fires on living trees is also troublesome in Douglas-fir forests, since fire scars tend to be buried in the tree record. Most scars used to reconstruct fire history occur after the tree is 50 years old (Barrett and Arno 1988). Because of the growth rates experienced in the wetter climate, scars heal within the first 5-15 years after a moderate severity fire. Moderate severity fires burn only the small deep furrows of the bark which end up being recorded in the tree's growth rings.

Species dominance changes as the FRI lengthens in wet-to-mesic Douglas-fir forests. Douglas-fir will drop out of a stand if fire is absent for over 700 years and western hemlock and Pacific silver fir will take over as the dominant species. Areas with 300 to 600 year FRI will typically produce stands of mixed-dominance of Douglas-fir and western hemlock or Pacific silver fir. Areas with FRI of less than 300 years maintain forests dominated by Douglas-fir. While, FRI of under 100 years on drier or warmer environments may exclude western hemlock (Agee 1991).

Mesic-to-dry Douglas-fir forests found on the western slopes of the Cascades are dominated by a moderate severity fire cycle. This type of fire cycle is represented by more frequent but less intense fires, which leave substantial survivorship within a stand. The survivors may represent multiple age classes, adding to the patchwork of stands at the landscape scale (Stewart 1984, Agee and Krusemark 2001). Medium size canopy gaps are created by moderate severity FRI leading to stands of mixed

dominance and multi-modal age structure. Stand composition resulting from such fire cycles are correlated more heavily with the fire events than successional stand development dynamics (Wills and Stuart 1994). Even in a moderate severity FRI zone canopy gaps can vary in size, leading to release of suppressed trees within a single stand after lower intensity fires. Alternatively, after more intense fires, regeneration of pioneers may take place on a more coarse scale (Spies and Franklin 1989).

A more localized study conducted on 4,800 acre area of western hemlock zone forest in the central western Cascades revealed an average FRI of 95 years for the years 1150 to 1985. The topography of the study area consisted of steep, dissected slopes. A consequence of a moderate severity fire regime is that old growth characteristics can be sustained or established at both the stand (area of single age class) and landscape (large area of multiple stands) scale over time. Human influence on the fire record was also reviewed within the study area. It was found that the time of least human inhabitation in the area (1810 to 1850) yielded the shortest FRI at 72 years, while the period of most rapid settlement (1850 to 1910) had a 213 FRI (Morrison and Swanson 1990).

Human influence (native or foreign) on the regional fire cycle is negligible. An explanation for this may be that fire history in the Western Hemlock Zone is such a long-term cycle of moderate burns that human influence either by suppression or ignition has not had time to show up in the record. 150 years of settlement, and 100 years of active suppression is not a long time considering that the complete fire cycle in these forests can be over 1000 years. The alternative is that few human-caused fires burned large enough areas to significantly alter the fire cycle. Working from the

perspective of an urban forest fire cycle, the regional fire cycle established from the study of large wildland environments may be of limited utility, which strengthens the case for conducting more fire cycle analysis in WUI environments.

Factors and Mechanics of Forest Fire

Fuels are the most fundamental fire behavior factors, representing the organic material consumed during a fire. Fuels are typically stratified vertically through the forest canopy. The arrangement and components of a stratified canopy determine the character and connectivity of fuel loads. Once the fuel load is established, fuel moisture content can be quantified. The fuel load and fuel moisture components help determine the seasonal variation in flammability. This data becomes a primary input to fire simulation.

When evaluating fire potential at the landscape and regional scale, fuel and fire behavior relationships are emphasized, while species composition is less important (Key and Benson 2001). Therefore, when developing fuel models for a small, localized fire, fuel data will more strongly reflect the ecological components of the forest. Simulation results will enable the analysis of ecological processes, as well as the general fire behavior.

Plant composition, population, and cover data from the overstory to the substrate is used to stratify, quantify, and aggregate fuel loads. A typical strata structure consists of substrates, understory, and overstory (Table 3/Figure 8). Substrate material consists of dead woody debris, as well as litter and duff. Substrate measurements provide the majority of the fuel loading information that makes up a surface fuel model. The forest understory consists of herbs, low shrubs, and small

trees including all grasses and forbs under a meter in height. Herbs are plants that die back each year. Shrubs retain perennial woody stems and grow year to year. Small trees, including tree seedlings, typically have only one central stem, and potentially grow out of the understory. The understory provides much of the ecological context of a plot and is representative of the forests successional health. The overstory consists of trees that make up the various levels of the canopy. Intermediate trees receive little direct sunlight from above. In this regard the actual size of the intermediate trees is relative to height of upper levels of the canopy. Big trees occupy the uppermost canopy, and usually receive direct sunlight from above.

Table 2: Recommended Firemon Landscape Assessment strata type and sub-components. (Source: Firemon.)

Strata	Components
Substrate	inert surface materials, duff, litter, downed woody fuels
Understory	herbs, low shrubs, saplings, small trees
Overstory	intermediate trees (pole-sized, subcanopy), big trees (mature, dominant, upper canopy)

The process of how fire behaves under certain conditions is well understood. Forest fires have some basic behavior regardless of the fuel type that makes up the forest being consumed. Surface, crown, and spot fires are the three types of fire that fire behavior analysis attempts to simulate.

Surface fires (Figure 8a) are the most common and the easiest fires to suppress. Fire will remain on the floor of the forest for a variety of reasons. The first may be because the fuel load is light and therefore the fire does not burn with great intensity.

Second, the surface fuel may be sufficient for more intense burning, but the wind at the surface may not be strong enough to push the fire along to take advantage

of the heavier fuel load. In some circumstances ladder fuel may be available to the surface fire, but only ladder and torch individual trees (Figure 8b).

Third, the surface fuel load may be moderately heavy and the wind may be sufficient enough to create a more intense and rapidly spreading fireline, but the canopy base height may be too high for the surface fire flame length to reach the canopy (Figure 8c).

If an active crown fire does not result from laddering then the canopy density may not be sufficient to support the spread of fire or the wind may not be strong enough to sustain the spread into surrounding tree crowns. However, an active crown fire has the ability to loft embers high into the air, which can be carried by the wind above the canopy and start spot fires ahead of an advancing fire (Figure 8d).

Lastly, the forest composition may be such that the canopy base height is high and no ladder fuels exist that will enable the surface fire to ladder up into the canopy structure. However, when the right conditions exist a surface fire will transition into a crown fire (Figure 8e). Spot fires that start in the right fuel conditions will spread and grow like any other surface fire.

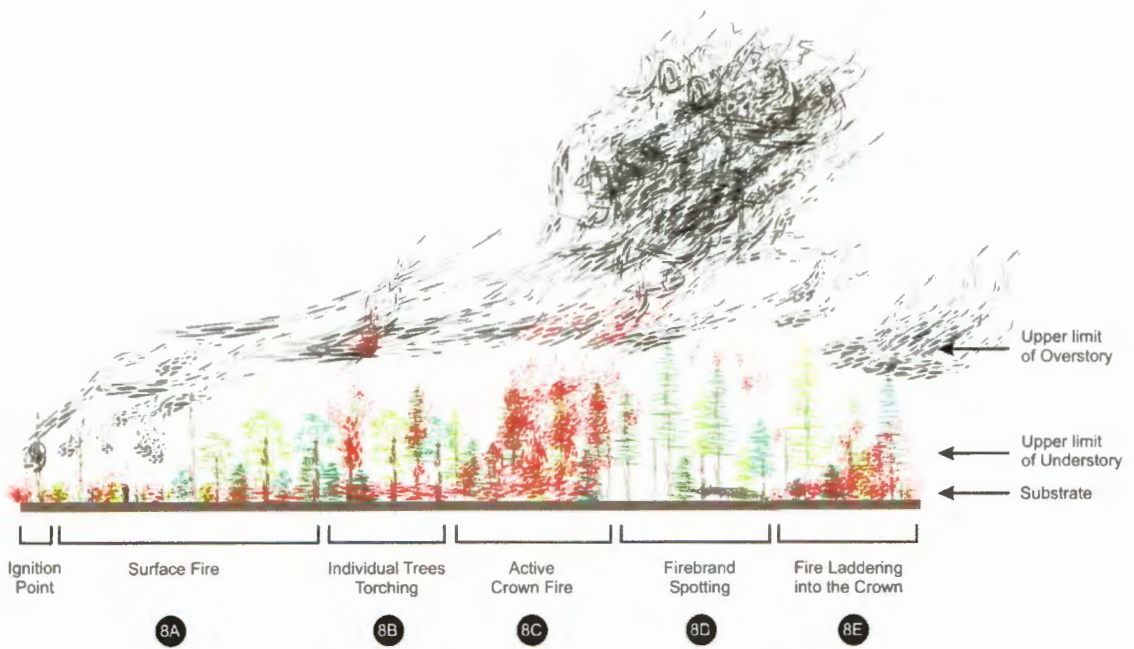


Figure 8: Fire movement through a forest. Fire needs ladder fuel and canopy cover to transition into a crown fire. Some areas have ladder fuels, but the canopy is sparse enough and weather conditions only permit torching of individual or small groups of trees. Locations that have the right set of ladder, canopy, and weather conditions will develop into active crown fire. Crown fires may produce firebrands that will create spot fires ahead of the advancing fire. (Source: illustration drawn by Author)

Factors and Mechanics of Fire Environments

Fire simulation attempts to predict fire behavior by using a set of known fire environment factors as inputs. Weather, wind, topography, and fuel are the primary fire behavior factors, each of which has multiple themes. The topographic themes are the first data layers developed for a fire behavior model. Changes in elevation, aspect, and slope impact wind movement and vegetation growth. Therefore, topographic data for fire simulation has a significant effect on the pattern of fire spread. Weather and wind make up the next set of themes. Wind and weather data is used as a data stream directly into the fire simulation model. Weather parameters include the daily minimum and maximum temperature and relative humidity, the time and elevation at

which the observations were taken, and any precipitation. These parameters are used to establish fuel moisture levels. The wind data is fed into the simulation on a much smaller temporal scale, a 10-minute average is preferred, but hourly readings will suffice. Wind parameters include open conditions for wind speed, wind direction, and percent cloud cover. A typical model may have to rely on data collected from a weather station that is tens of kilometers away from the fire area. Therefore, the data are assumed to apply uniformly over the entire area.

Weather has a direct effect on fuel moisture levels and therefore ignition potential. In most cases these daily figures would be used to approximate the diurnal pattern of temperature and humidity variation. However, in an urban environment several stations may be available within a few kilometers of the fire area. Hourly or sub-hourly data could provide the real diurnal pattern, as well as wind data in close proximity to the projection point. When combined with stand height the wind data is used for computing spotting distances, wind reduction to midflame height, and crown fire characteristics. The midflame height is the point at which the middle of the flame length is above the fuel bed. Open conditions reflect the conditions at 6.1 meters (20 feet) above the vegetation layer. However, wind is slower near the surface and must be adjusted to represent wind conditions at the midflame height. The midflame height is obtained by multiplying the 6.1 meter wind by an adjustment factor (Rothermel 1983). The adjustment factor is based on the level of sheltering the surface fuels have from direct exposure to the open wind speed (Figure 9).

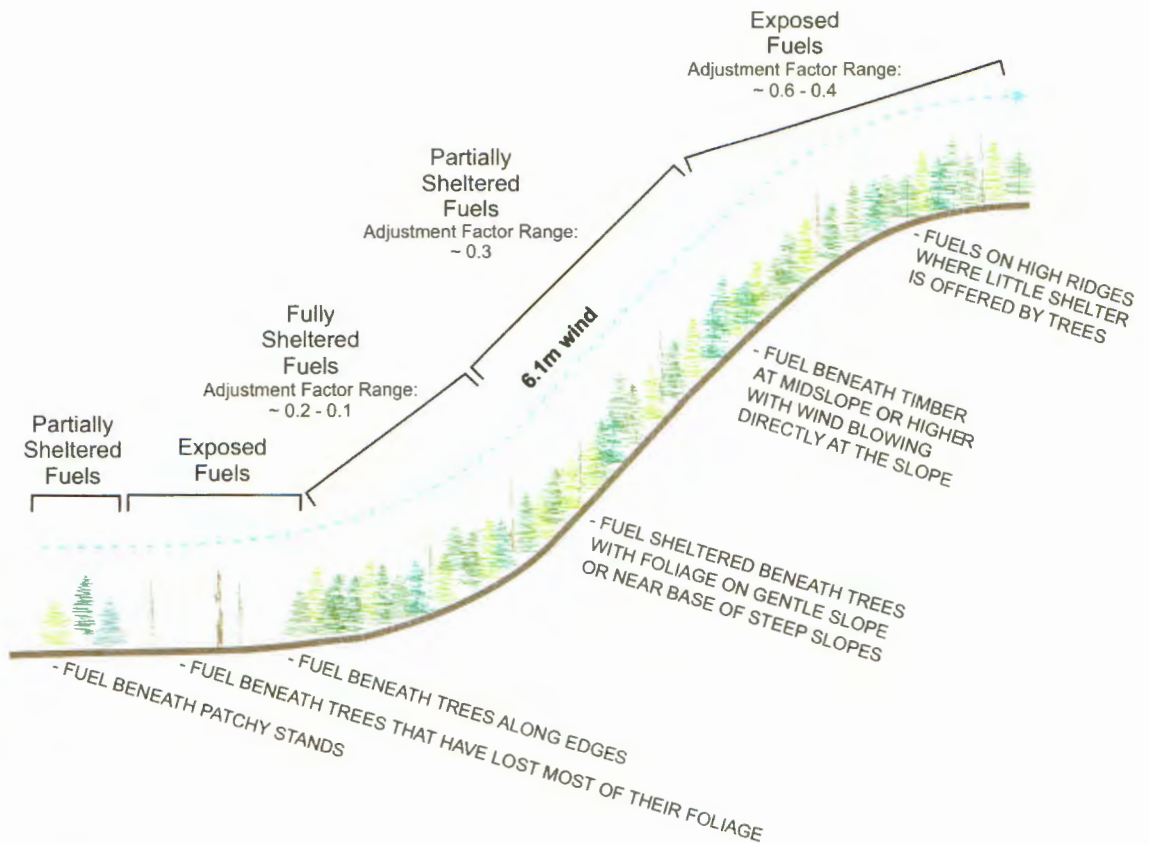


Figure 9: Surface fuel exposure based on open wind conditions aloft and canopy cover. Adjustment factors are applied to the 6.1 m winds to predict the wind speed closer to the surface and where the fire would experience its influence most (midflame height). (Source: concept and language by Rothermel 1983, illustration by Author)

The topography of Forest Park would be a serious concern for any fire suppression efforts. The Tualatin Mountain ridge has topographic features that positively influence fire spread and negatively impact fire suppression (Figure 10). The park area has a series of steep slope that poses potential rapid upslope spread and downhill spotting due to rolling burning material. The steep terrain of the park consists of topographic features such as box canyons, chutes, and chimneys that have potentially rapid upslope spread fed by updrafts of air called “the chimney effect.” Saddles can also be found in the park along the more prominent ridges (Figure 11). Wildfires get

pushed through saddles faster during upslope fire runs due to the squeezing action the terrain has on the air feeding the fire.

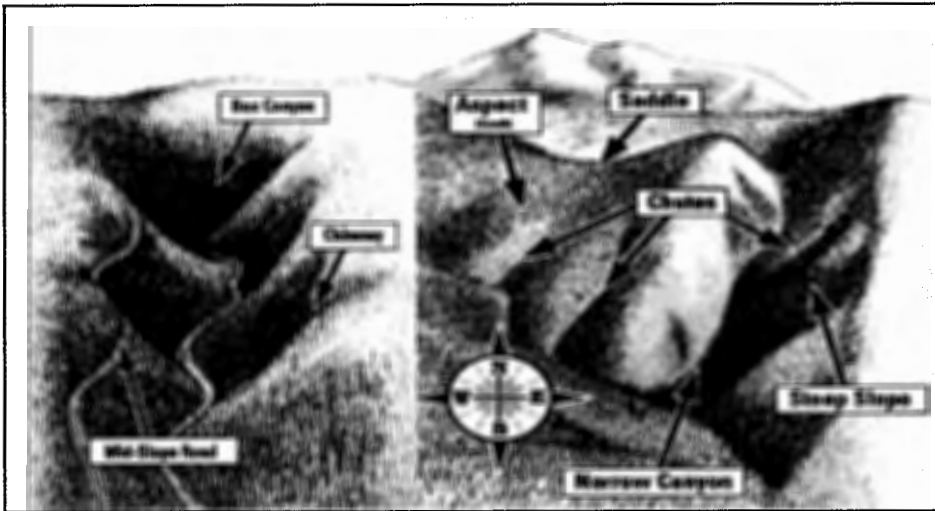


Figure 10: Visual aid of general topographic features found in the Tualatin Mountains and Forest Park. (Source: The reporter's hazardous assignment handbook: wildfires.)

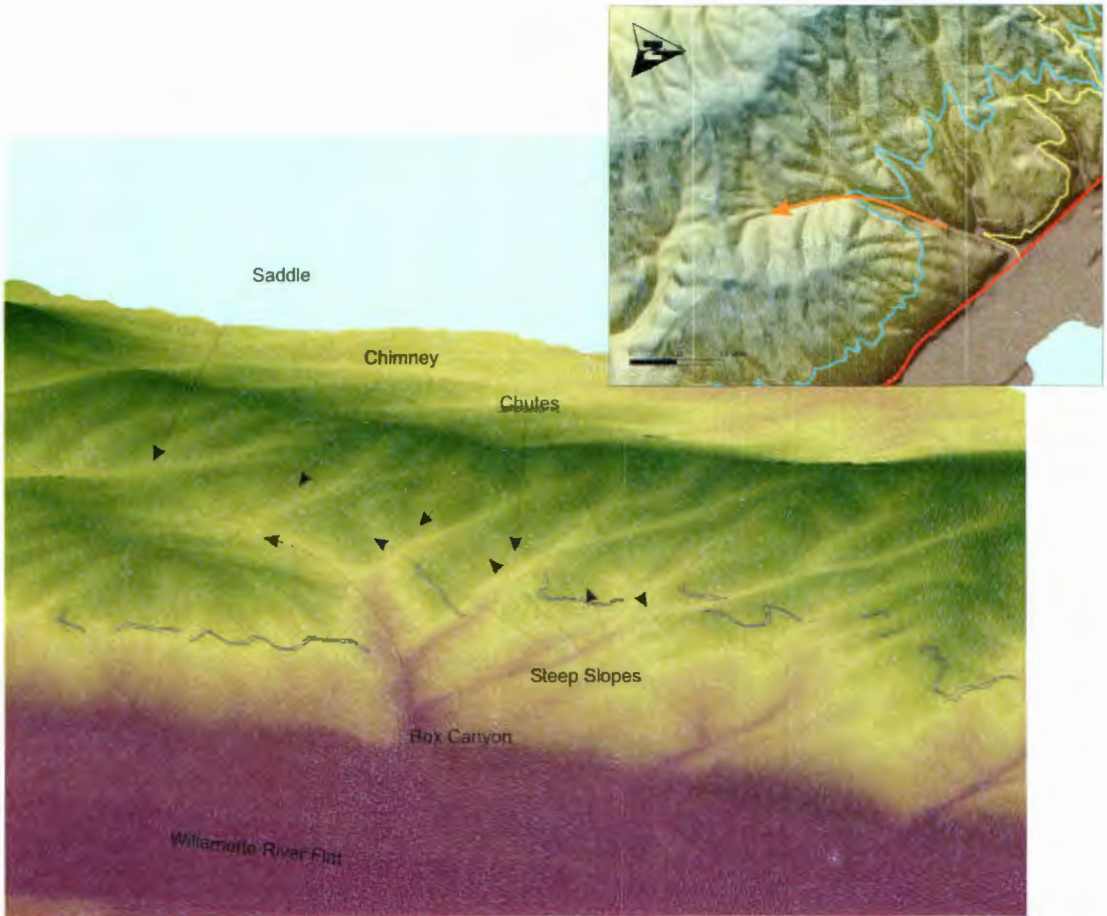


Figure 11: Perspective view of the canyons and other topographic features just South of Saltzman Road. The black double line represents Leif Erickson Drive. This image in upper right corner represents the same area from a planimetric view with shaded relief. The orange arrow indicates the box canyon for visual reference. The blue line is Leif Erickson. The yellow line is Saltzman. The red line is Highway 30 along the Willamette River. (Base Map Source: USGS)

Narrow canyons also dot the landscape. Narrow canyons pose two potential possibilities for rapid fire spread. The first possibility is radiant or convection spotting up slope or across the canyon. The second is in the form of fire backing down one slope and suddenly running up the other. The combination of topographic features and heat build up in front of the leading edge of fire can cause erratic wind patterns

and severe microclimatic effects. Many mid-slope roads cut through the park, which increases access, but an active crown fire could easily bridge the gap.

Summary

This chapter discussed the merits and shortcomings of understanding the regional fire cycle to better interpret the results of fire simulation for specific forests within the region. The fire cycle of the Douglas-fir and western hemlock forests of the western Pacific Northwest has been studied extensively. There is substantial evidence that anthropogenic fires have had no impact on the fire cycle. Furthermore, the fire cycle and FRI lengthens the farther north and west the forest extends. The FRI of these forests is typically longer than the fire cycle of most other types of forests throughout the west. The established fire cycle for Pacific Northwest forests may be of limited utility for the examination of Forest Park. The pressures placed on the park because of its placement in a WUI environment coupled with the forests elevation in the Tualatin Mountains make it difficult to apply the Western Hemlock Zone fire cycle characteristics in their entirety to the area.

CHAPTER 4: PORTLAND'S FOREST PARK: A CASE STUDY

As a study area this research will examine Portland's Forest Park, a more than 5,000 acre second-growth forest on the edge of downtown. To better understand the site, a brief history of the forest and surrounding development will be presented. Historic fires will also be examined to demonstrate how large fires have altered the landscape. Finally, City of Portland planning and natural resources management, focusing on a 1995 plan will be discussed.

Pre-Park History

The Tualatin Mountain ridge trends in a northwesterly-southeasterly direction along the west bank of the Willamette River. Dixie Mountain is the highest point of the ridge at 1,609 feet, and represents the northern terminus of the range. The ridge rises steeply along the eastern side and averages between 1000 and 1,200 feet along the ridge line (Figure 12). Forest Park is situated on the southeastern slopes of the Tualatin Mountains.

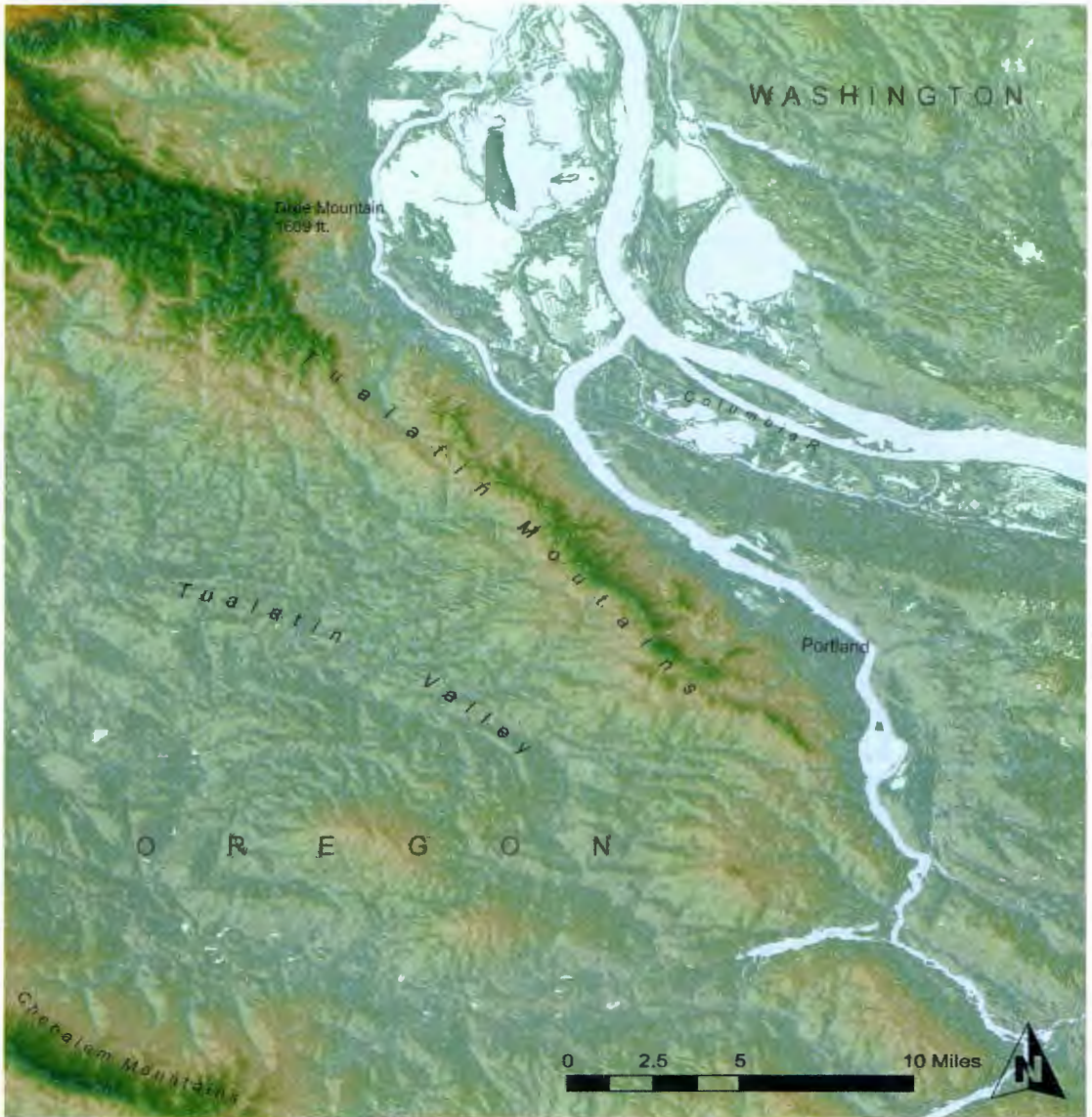


Figure 12: The Tualatin Mountains dominate Portland’s Westside. They separate the Tualatin Valley from the Columbia basin. Forest Park boundary is outlined in orange. The subdivisions in the outline are due to roads and private property that bisect the park. (Base Map Source: USGS, City of Portland)

Steepness varies between the western and eastern slopes. Slopes are generally 20% or less on the western side of the range. The eastern slopes, including the area of Forest Park, are far steeper and frequently in the 25% range. The east side is bisected by numerous chutes and narrow canyons, and slopes in many of these ravines are 75% or greater. Figure 13 illustrates the steepness of the Tualatin Mountains through 3 sample elevation profiles.

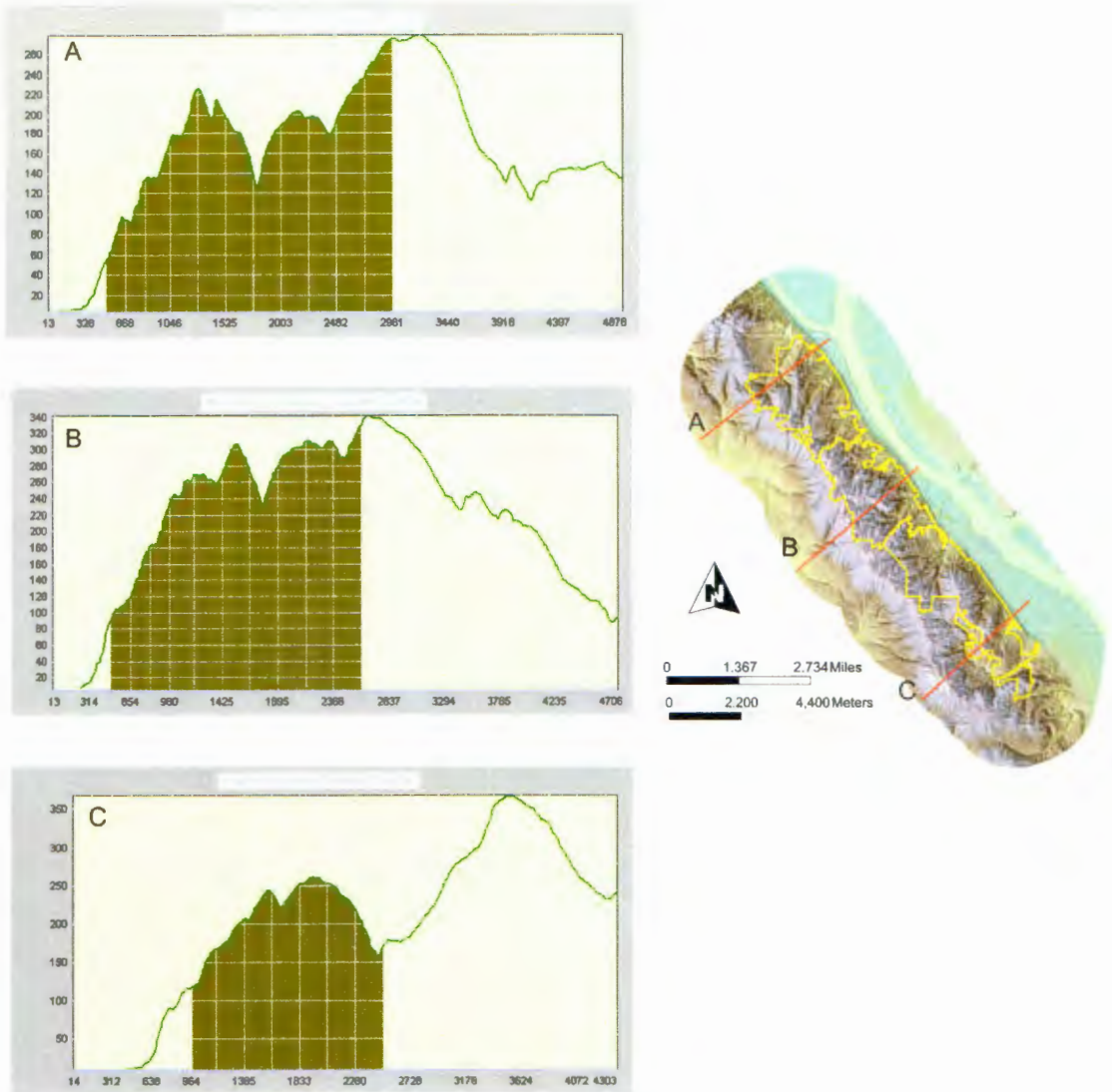


Figure 13: Elevation profiles at three points across the Tualatin Mountains ridge. A two-times vertical exaggeration has been added to the profiles. The olive green shaded areas in the profiles indicate slopes inside Forest Park's boundary. The elevation is in meters, as well as the transect lengths. (Base Map Source: USGS, City of Portland, RLIS; elevation data from Idrisi output by Author.)

In the early 1840s, pioneer farmers constructed trails that traversed the Tualatin Mountain ridge, situated between the Tualatin Valley to the west and the Willamette River to the east. They used the trails to traverse the steep ridge and deliver wheat and produce to settlements along the Willamette, including Portland. Between 1845 and 1849 the trails were widened and improved. The paths of these trails became the foundations for future roads, most notably Cornell, Germantown, and Newberry (Figure 14).

In this initial period all of the land was considered property of the Federal government, but through donation land claims most of the Tualatin Mountains was deeded to settlers between 1850 and 1855. Homestead development increased on the level land along the ridge and farms extended to the base of the hillsides. The steeper, slide-prone land on both sides of the range between the ridge and the Tualatin Valley and the Willamette River was left either undeveloped or logged (Munger 1960).

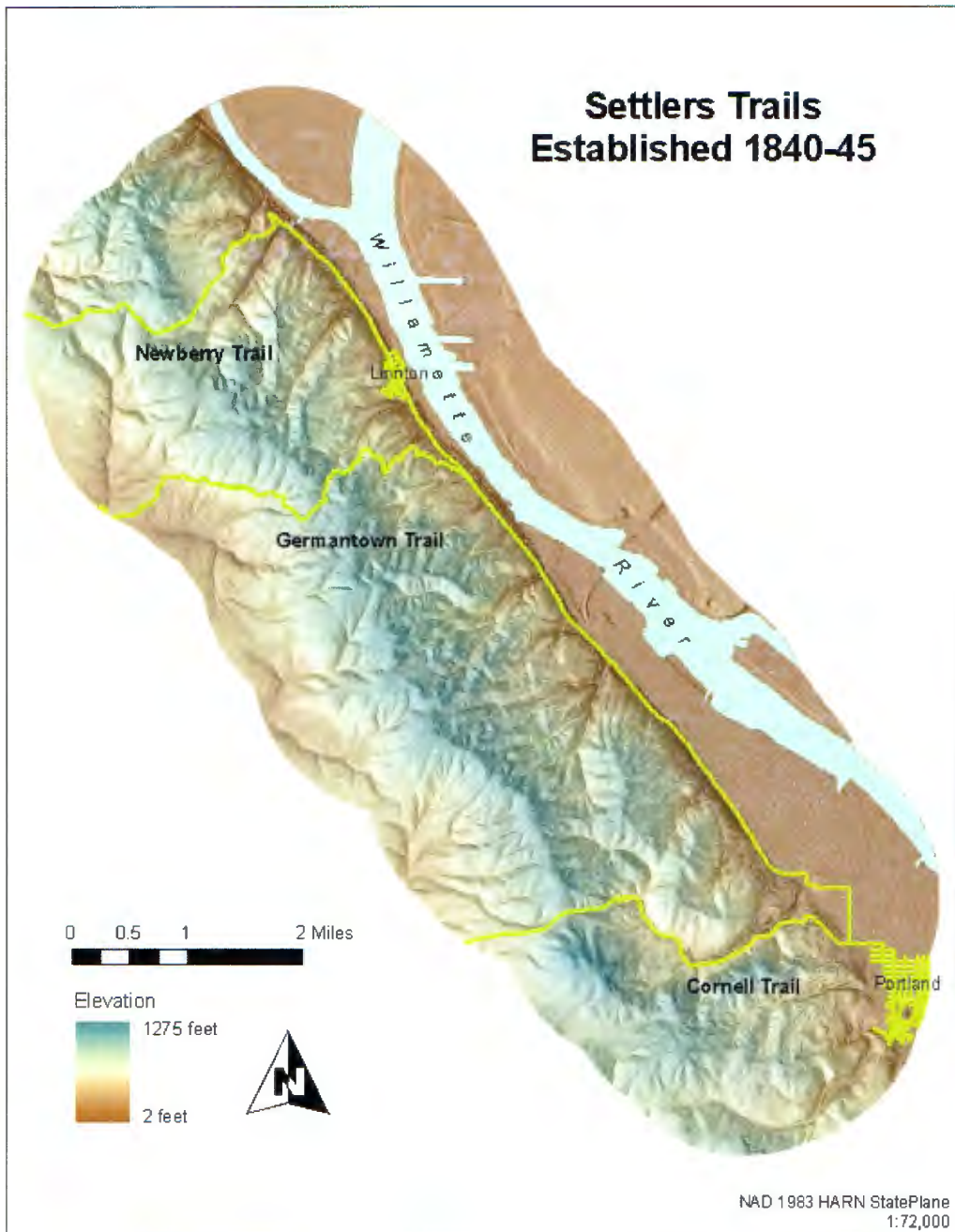


Figure 14: Original trails that traversed the Tualatin Mountain ridge. These trails have subsequently become the Major Roads from the Tualatin Valley to the Willamette River and Portland. All of these trails (roads) wind through Forest Park. (Munger 1960; Base Map Source: USGS, Metro RLIS.)

In 1899 the Municipal Park Commission for Portland was established. Through personal connection, the founder of the Commission, Rev. Thomas Eliot, established a relationship with John Charles Olmsted of the respected Olmsted Brothers, landscape architecture firm, from Brookline, Massachusetts. The Olmsted Brothers firm was contracted to develop a comprehensive park plan for the rapidly growing City of Portland and in March of 1903 John Charles Olmsted and an assistant visited Portland. The plan was eventually submitted to the Commission in December of 1903. In reference to the Tualatin Mountain ridge John Charles Olmsted wrote,

“...such primeval woods will become rare about Portland as they are now about Boston. If these woods are preserved, they will surely come to be regarded as marvelously beautiful... No use to which this tract of land could be put would begin to be as sensible or as profitable to the city as that of making it a public park or reservation, leaving out of it, if it should be found necessary for economy, the top of the ridge, which might come to have special value for country residences.” (1903, 41)

Forty-four years later Olmsted’s vision was realized with the dedication of Forest Park. However, the land for the park was available not because of a conscious acquisition effort and careful planning, but only because of a real estate fiasco. In 1910 the city of Linnton incorporated on the Willamette River at the foot of the Tualatin ridge. Its city limits included most of the park area. Richard Shepard, a member of the Linnton town council and realtor, promoted the idea that a scenic Hillside Drive be constructed along a contour at about the mid-point of the ridge

running from Germantown Road to the end of Thurman Street in northwest Portland. In speculation of the construction of the Drive linking to Portland, residential subdivisions were platted all along the river front, on either side of Germantown Road and Springville Road, and along Skyline Road. However, only the lots at the foot of the mountain along the river were built on (Wilson 1945).

In 1914-1915 Hillside Drive was quickly graded; unfortunately the cost of construction was almost twice what the engineers had expected. In July of 1915 Portland annexed Linnton and, in January of 1916, to pay for the road grading work the newly platted subdivisions were each assessed a fee. At the time there were thousands of lots, but only a third of the assessments were ever paid. Liens were put on the properties, and all were eventually foreclosed on (Munger 1960).

In the meantime, the steep hillside proved too much for Hillside Drive. The road quickly fell into disrepair as winter landslides came down on it, and the cost of maintenance increased. In 1933 Hillside Drive was renamed Leif Erickson Drive through a city ordinance sponsored by the Sons of Norway.

The City Club, a powerful civic-minded group, formed a committee of five in 1944 to address the repeated demands that the northwest hills be granted park status. The City Club report was originally printed in the City Club bulletin of August 31, 1945. The recommendations in the report were approved by the membership on September 7, 1945.

The City Club's recommendations were not officially acted upon until November 12, 1946, when a public meeting was held to formulate a plan to create the proposed park. Soon after, a permanent committee of fifty representatives, forty of

which represented various civic, commercial, educational and recreational agencies, were mobilized to finalize detailed plans for the park.

The first meeting of the “Committee of Fifty” was held on February 5, 1947. Dated June 9, 1947 the committee made a recommendation that the city dedicate all city-owned land in the Tualatin Mountains to the park, asked Multnomah County to convey the city its land, and urged adopting a policy of acquiring private lands within the park boundary. The City Planning Commission also endorsed the recommendations and drafted large scale maps of the proposed park boundary. On July 9, 1947 the City Council held a public hearing on the recommendation and adopted unanimously the recommendations of the Planning Commission and the Committee of Fifty. The transfer and consolidation of the land holdings to the city parks bureau was cumbersome, but on September 25, 1948 Forest Park was formally dedicated (Munger 1960).

The area within the original exterior boundary was estimated at 6,168 acres (2,496 hectares), but because of extensive private inholdings, only 4,200 acres (1,700 hectares) was actual park land (Munger 1960). The park stretches north-northwest for 7.5 miles along the east side of the Tualatin Mountain ridge. It is approximately bordered by Skyline Road to the west and St. Helens Road/Highway 30 at the edge of the Willamette to the east. The City of Portland has continued to acquire private land adjacent to the park and within the original boundary. Today, there are 5,004 acres (2,025 hectares) of park land. However, the City’s ability to expand the park is limited given the surrounding urbanization (Figure 15).



Figure 15: Forest Park is outlined in orange. The yellow shading represents Census 2000 urbanized area (UA) and urban clusters (UC). A UA consists of contiguous, densely settled census block groups (BGs) and census blocks that meet minimum population density requirements (1000 persons per square mile/500 ppsm), along with adjacent densely settled census blocks that together encompass a population of at least 50,000 people. A UC consists of contiguous, densely settled census BGs and census blocks that meet minimum population density requirements, along with adjacent densely settled census blocks that together encompass a population of at least 2,500 people, but fewer than 50,000 people. However, much area not shaded still has substantial development. Parcels Northwest of the park offer the only significant expansion. (Source: USGS, City of Portland, Census 2000)

Historic Land Use and Development

In 1806, during the return trip of the Lewis and Clark expedition eastward, Captain William Clark and a few members of the expedition made a side trip up the Willamette River and are believed to have camped in the area where University of Portland now stands. Looking from the bluff upon which he stood Clark would have looked at the hillside that is now a part of Forest Park. He wrote, “The timber on them [Tualatin Mountains] is abundant and consists almost exclusively of the several species of fir already described [Douglas-fir, grand fir, and western hemlock], and some of which grow to a great height (Lewis and Clark, 1961).”

The virgin forest described by Captain Clark was exploited early by settlers, with most of the big timber being removed by the 1860s. Wood-cutting camps for the unemployed and needy were sponsored by the city in 1914 and again in 1937. High-lead logging was in progress up until 1951 (Munger 1960). Today, only a small patch of old-growth forest exists in the extreme north end of the park area.

Even though most of the land within the modern park boundary was platted for development, only a few small private parcels within the park were ever developed. The only development on park land has been road building and logging activity. However, development has continuously occurred right up to the park boundary since its dedication. A map of the southern half of the park area illustrates the patchwork pattern and type of development over time (Figure 16). Figure 17 is the same type of map for the northern half of the park. Much simpler in pattern are the maps of current land use, portrayed in Figure 18 and 19.

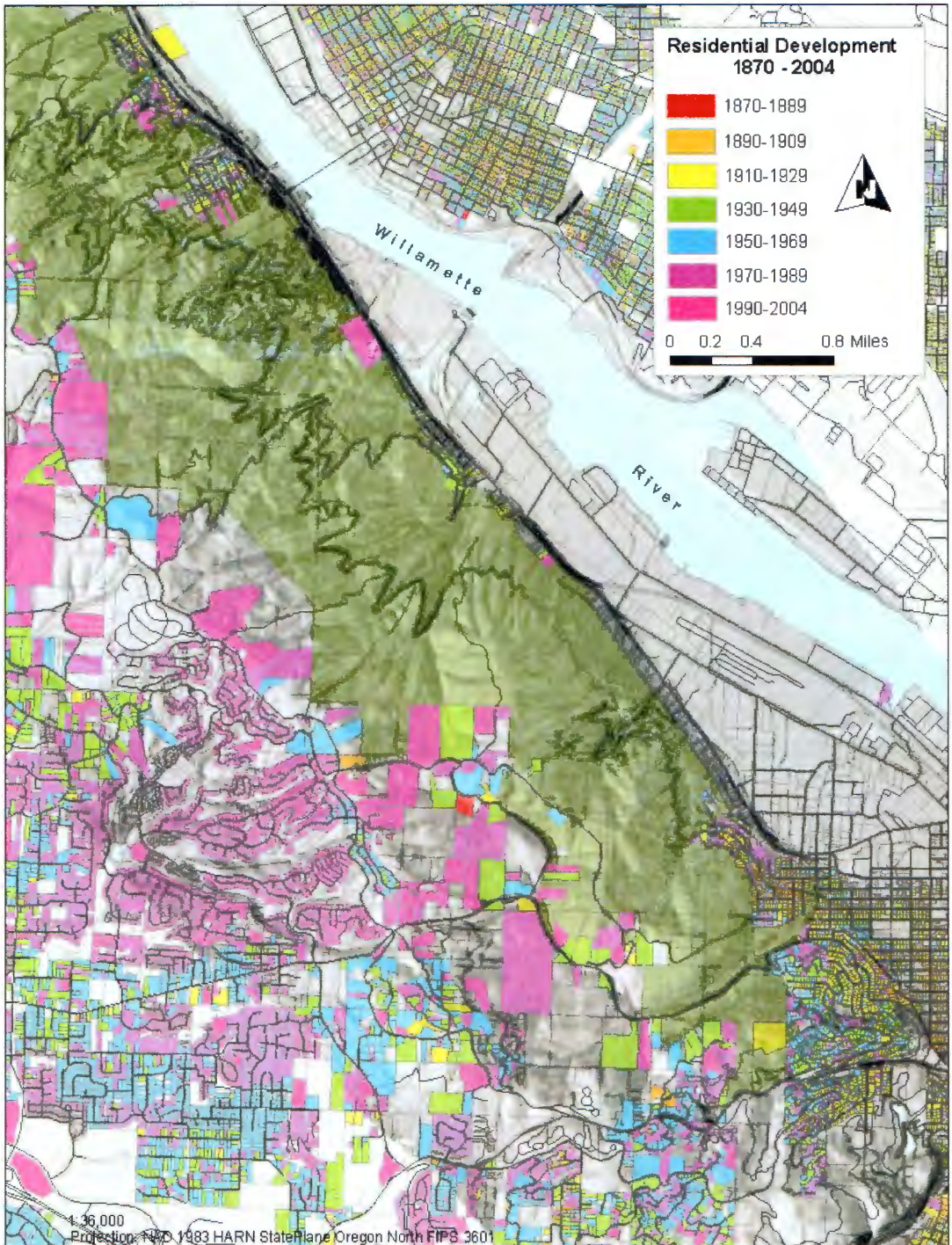


Figure 16: Development around the southern end of Forest Park since 1870. The first parcel developed into a homestead is located just below the center of the map. The majority of the development on the western slope (Bonny Slope) has been completed since 1990. The green shading represents park land. (Source: USGS, Metro RLIS)

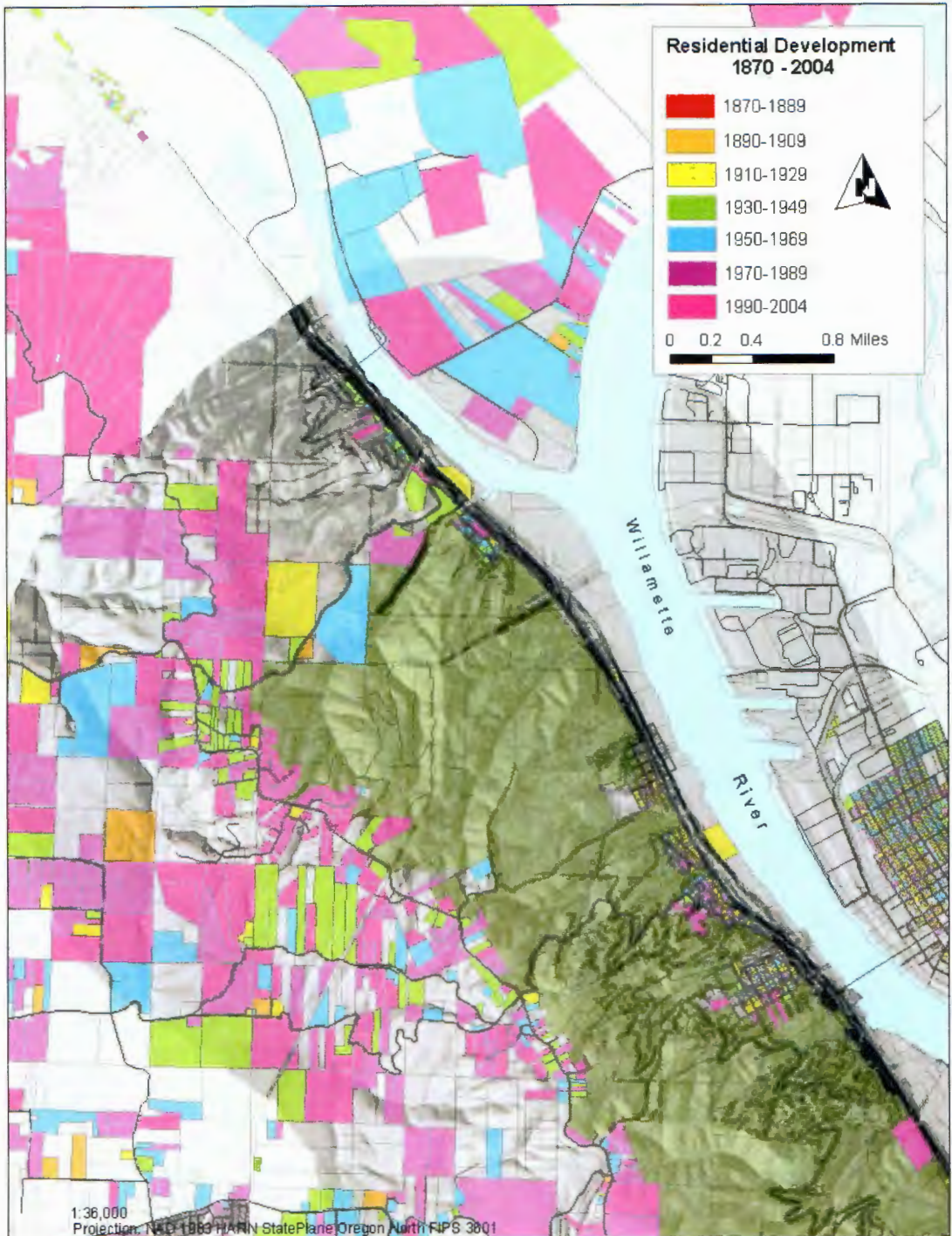


Figure 17: Development around the northern end of Forest Park since 1870. The green shading represents park land. The parcels of land tend to be larger than around the southern half of the park. As in the southern end the majority of the development has been completed since 1990. The hillshade extends 1.24 miles from the Park's boundary; this represents the buffer used throughout the study. (Source: USGS, Metro RLIS)

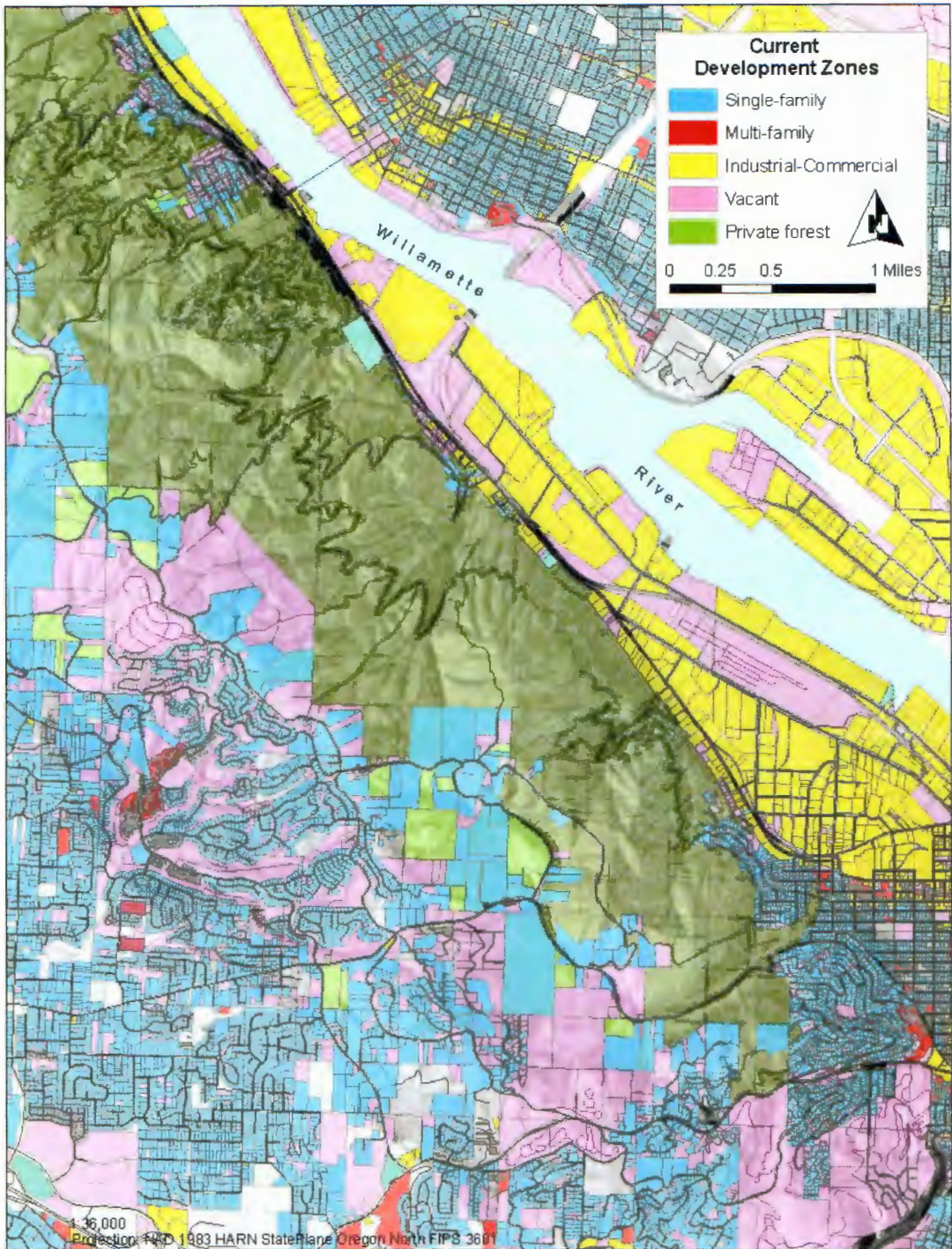


Figure 18: Building zone designation around the southern half of Forest Park based on 2004 metro taxlot data. The figure illustrates the dominance of residential interface on the western slopes of the Tualatin Ridge and abutting the park. The industrial zone is dominated by petroleum refineries, and rail operations. (Source: USGS, Metro RLIS)

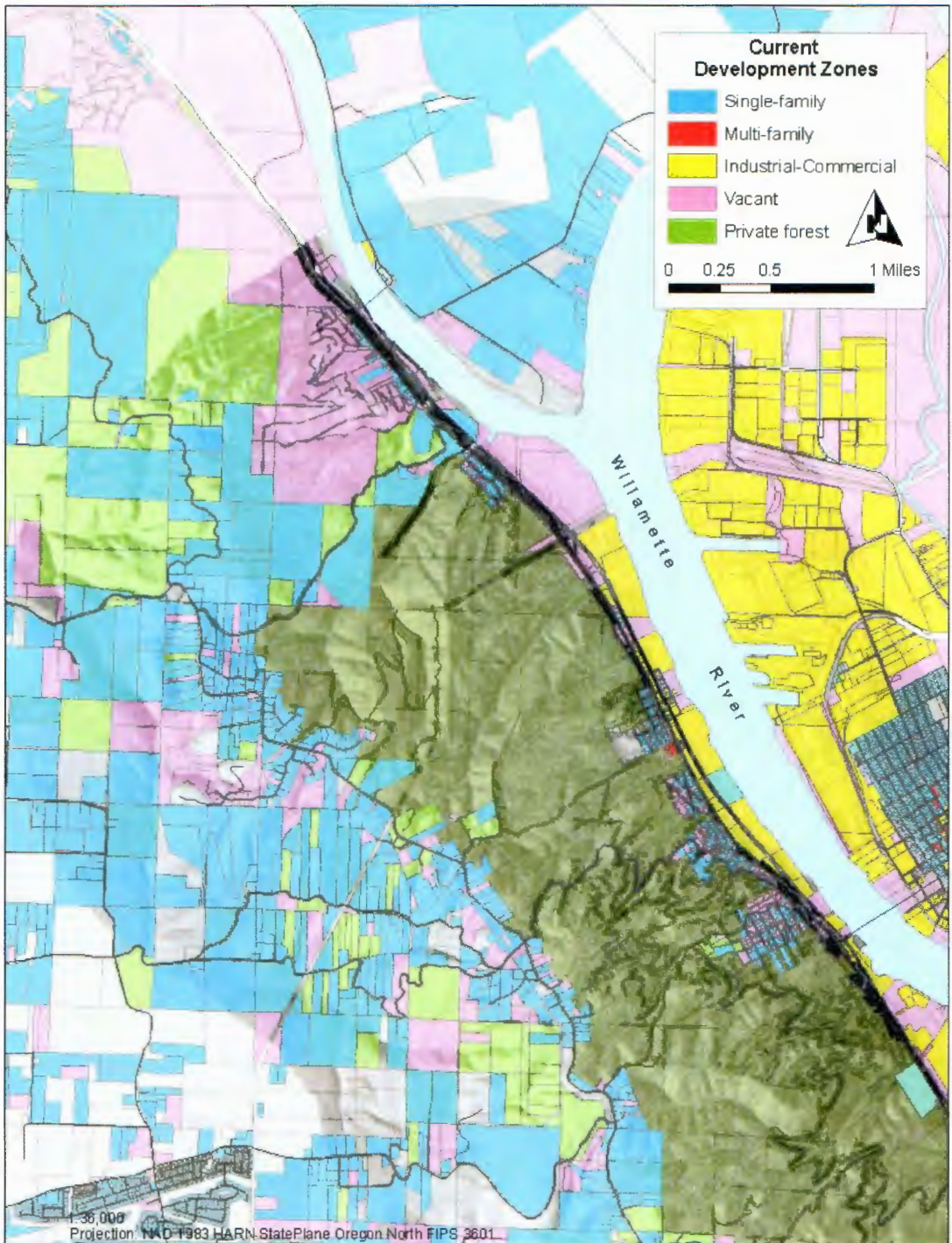


Figure 19: Building zone designation around the northern half of Forest Park based on 2004 metro taxlot data. The green shading represents park land. The figure illustrates the dominance of estate size parcels in around the northern end of the park. Substantial parcels of private forest are also present. Many of the larger parcels designated as single-family and vacant have significant forest cover. (Source: USGS, Metro RLIS)

Figure 18 illustrates the pattern of residential dominance south and west of the ridge, while commercial and industrial dominates the southeastern area. A significant amount of land is also set aside as green space and right-of-way. For example, the majority of vacant property intermixed with the residential zones adjacent to the southern park area is environmental greenbelt and other mandated set aside. The largest vacant parcel in the industrial zone is railroad right-of-way. Figure 19 clarifies the pattern of larger land holdings, estates, and private forests adjacent to the northern section of the park.

Development along the southeastern boundary (Northwest Portland) was largely in place in 1948. Development in this area consists of neighborhoods of single and multi-family development perched on the hills and slopes adjacent to the park. No new development is likely in the northwest hills, which has reached a limit in allowed density.

The western boundary, along the top of the ridge, is largely developed as single family homes. The development becomes more sparse and rural as you move north along Skyline Road. Eventually large estates, farms, horse stables, and private forests dominate the development to the north and west. The extreme northern boundary is structurally undefined, in that the stand continues into privately held properties where management has ranged from unmanaged growth to clearcutting.

A large industrial zone lies along the park's eastern boundary and the Willamette River. Originally the industrial area was a large lake called Guilds Lake and was home to the 1905 Lewis and Clark Exposition. Olmsted's 1903 plan had

called for the whole site to be converted to public open space. However, due to a lack of funds and the interest of the business community in the land for industrial use the site was not converted to a park. The Portland Development Company bought the land and most of the major buildings built for the expo were cleared by 1906. Construction on the hills above the lake caused silt to fill it in between 1910-1913. Little development was completed in the area with the exception of the Montgomery Ward building in 1921. Emergency war housing was constructed on the western portion of the mudflats in 1942 (Abbott 2004).

Today the industrial zone consists of light and heavy manufacturing, shipping, and fuel refining operations. The businesses that back up to the park include a heating oil depot, wood pallet dump, and welding company (Figure 20). The development figures in Table 4 demonstrate the explosive growth that has occurred adjacent to the park. The period between 1990 and 2004 has experienced almost three times the development than any other 20-year period prior, dating back to the 1870s.

Table 3: Table includes all development within a 1.24 mile (2 km) buffer around Forest Park. The Willamette River delineates the eastern boundary of development included in the table. The table includes residential, commercial, and industrial development. Developed acreage includes only residential development (source: Metro RLIS)

Time Period	Lots/Parcels Developed	Residential Acreage Developed
1870 - 1889	100	8
1890 - 1909	1038	115
1910 - 1929	1244	233
1930 - 1949	853	279
1950 - 1969	1071	281
1970 - 1989	1146	248
1990 - 2004	3299	632



Figure 20: The aerial photo shows the intersection of Highway 30 and St. Helens Rd. The North Pacific Railyard can be seen next to Chevron and Phillips refinery storage facilities in the upper left corner of the image. Taxlot lines overlay the photo and Forest Park is shaded green. Inset photo, taken by Author, shows a wood pallet depot that abuts the park boundary on St. Helens Rd. Many businesses on St. Helens Rd. transfer or use hazardous and flammable materials, including fueling stations, fuel distribution and storage. (Source: air-photo courtesy of Spencer B. Gross, Inc.)

Human Impact Fire Factors of Forest Park

Quantifying the impact of the wildland-urban interface (WUI) on Forest Park as it relates or contributes to the forest's combustibility is largely subjective. How various urban pressures, such as pollution or development, impact the vegetation and microclimate of Forest Park is beyond the scope of this study. However, the degree and variety of human-park interaction as dictated by WUI development has implications in terms of the probability and location of potential ignition sites. A network of trails and roads traverse the park, facilitating human access for recreational activities such as hiking, biking, jogging, wildlife observation, and solitary contemplation. A large transient population camps within the park and evidence of campfires is present (Figure 21).



Figure 21: A transient fire lit on the side of a trail in Hoyt Arboretum, which is part of the Forest Park complex. (Source: Photo Taken by Dan Moeller, Plant Collections Manager, Hoyt Arboretum, April 2005)

According to the park managers and Portland Fire Bureau, transient caused fires have set small areas (>5 acres) on fire in the last five years. Additionally, rail lines run parallel to the park's boundary. Sparks from dragging chains or metal-to-metal friction can ignite brush that is not cleared from the rail right of way. Utility corridors, both gas lines and high voltage power lines run through the park and across the ridge at several locations (Figure 22). Residential or industrial development borders the park on two sides. As the level of potential threats have increased

precautions have been taken to improve firefighting access to all areas of the park.

Some trails have been turned into roads and numerous fire lanes have been built since the park's dedication.



Figure 22: Two utility corridors transect the park, one at the extreme northern end of the park and the other in the central management unit, which includes a subterranean gas line. Wood is naturally a poor conductor of electricity, except at extremely high voltages. The utility owners clear many of the trees and branches from the area under the power lines. However, during hot summer days lines sag and in windy conditions trees can blow into or fall across power lines and creating potential for arcing and fire. After larger fires occurred in the park, firelanes and roads were improved to support firefighting efforts within the park. (Source: City of Portland, Metro RLIS, Friends of Forest Park)

Fire History of Forest Park

An unfortunate result of logging and road building was more frequent fires. There have been three large fires in recent record in the Tualatin Mountains - 1889, 1940, and 1951. Newspaper articles, aerial photos, and city archives provide enough details to establish an ignition point and burned area for each fire. The information on these fires is of importance for this study but of varying utility.

The first fire broke out several days prior to September 18th, 1889 on the Irving tract between Barnes and Cornell Roads. The cause of the fire was never determined. The fire spread northwest toward Guilds Lake, currently the northwest industrial district, and southwest through the Kings tract, which are now the developments of Willamette and Kings Heights. The fire continued to spread in a westerly direction to Cedar Mill (Miller 1928). The fire burned through the canyons and over the hills along Canyon, Barnes, and Cornell Roads (Figure 23). The most intense fire was along Cornell and Barnes, destroying most everything in its path except for the largest trees (Oregonian 1889). The reason the fire was so intense in this area was the chimney effect that the steep chutes and canyons of the area had on the fire spread. The fire extent as illustrated in Figure 23 has been compiled by the author based on descriptions from the 1889 Oregonian article. The arrows on Figure 23 indicate the spread direction, and the width of each arrow indicates the relative intensity. The arrows have been placed as general guides of fire spread and intensity based on The Oregonian article, which offered details about the spread of the fire. The article

included the time at which farms and homes were damaged or destroyed by the fire, which helped determine the rate and direction of spread.

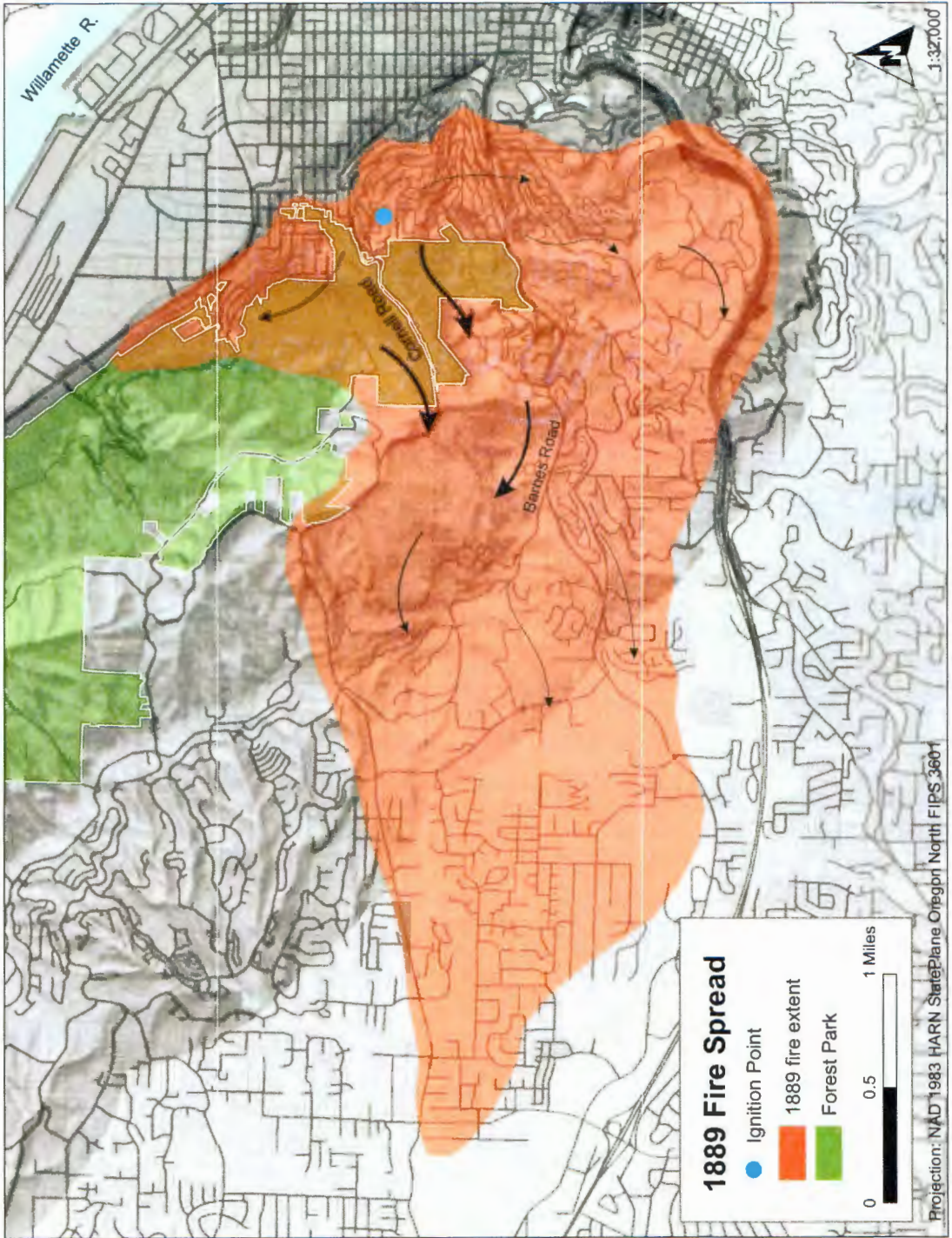


Figure 23: The orange shaded area is a rough estimate of the 1889 fire extent, overlaid on the current roads. White line indicates Forest Park boundary. The arrows represent fire spread as described by the Oregonian article. The width of the arrow indicates areas of greater fire intensity. (Base map source: USGS, Metro RLIS; fire boundary information: The Oregonian 1889; fire boundary drawn by Author)

However, the landscape of the area affected by this fire has been modified and developed extensively over the past 125 years. In addition, the majority of the burned area is outside of Forest Park. Though this fire is not being used for analysis, it is of historical significance and did affect the southern tip of the modern park. Based on the reconstructed fire boundary it would appear that less than 400 acres of park area burned. However, the exact fire extent can not be documented, and it is unclear if timber that may have survived the fire was subsequently logged.

The second large fire in the Forest Park area began August 17th, 1940, and is known as the Bonny Slope fire (Figure 24). This fire devastated about 1000 acres both east and west of the ridge, with most of the area south of Saltzman Road (Munger 1960). The fire also destroyed 11 buildings on the western slope, Bonny Slope area. The cause of the fire could not be determined. The fire burned for less than two days (Morris 1954). The fire was poorly documented, except for a map that was drawn in 1948 that outlined the Bonny Slope burn and few smaller subsequent fires in the same area. The map was drawn to outline the Mazama forest, an area where the Mazama Club had supposedly planted 9,000 trees. A fire protection plan written in 1950 described the landscape created by the Bonny Slope fire as being dominated by snags that left little protective cover for surviving trees and shrubs. The plan highlighted Bonny Slope as the second most hazardous fuel type after logging slash, even after the 1940 fire. The report stated that “fire occurring in this area would have a high rate of spread and be very difficult to control” (Marshall 1950).

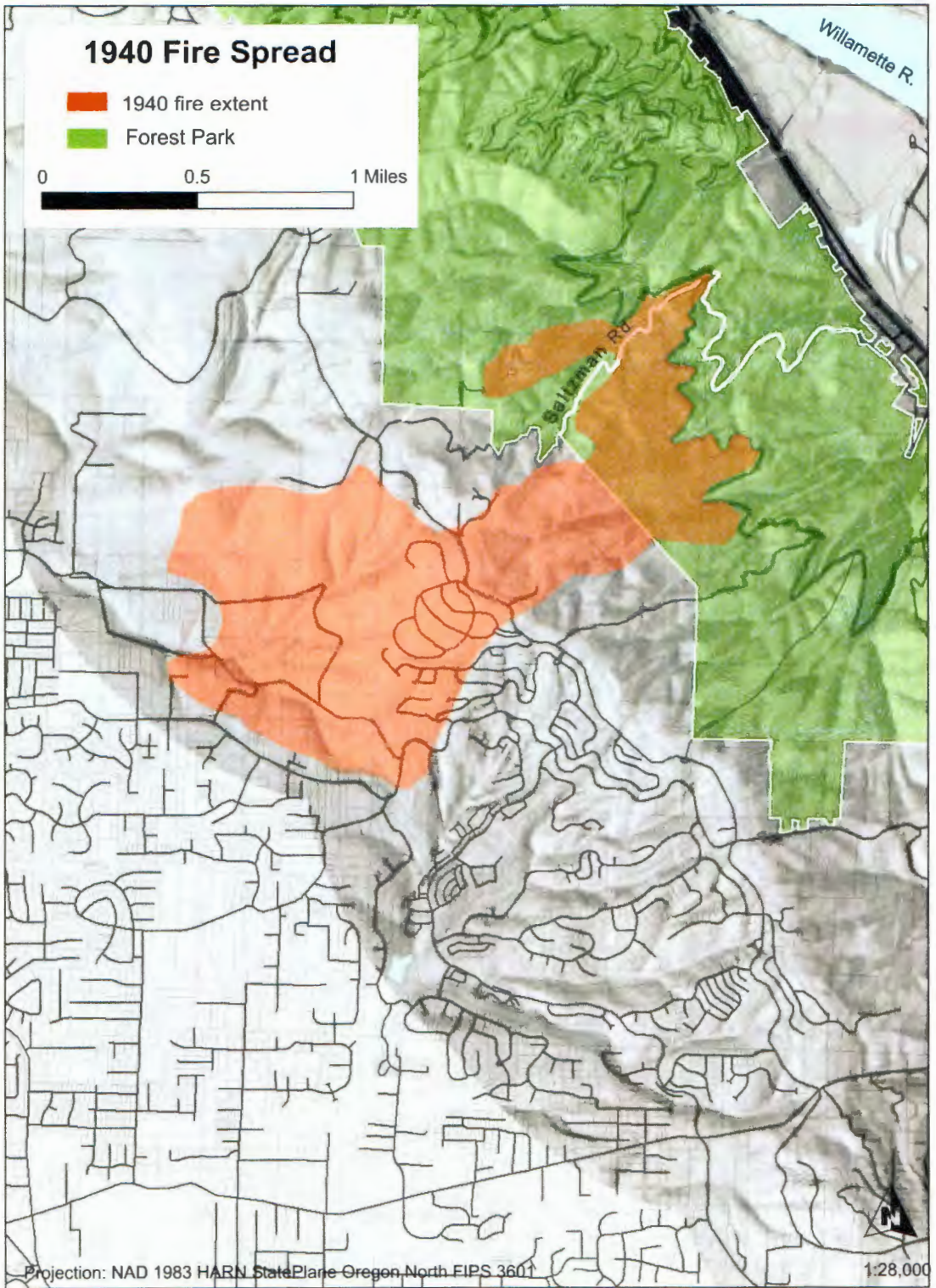


Figure 24: The orange shaded area is a rough estimate of the 1940 fire extent overlaid on the current roads. White line indicates Forest Park boundary. Although the fire was of significant size it was poorly documented. (Base map source: USGS, Metro RLIS; fire boundary information: Mazama map 1948; fire boundary drawn by Author)

The third large fire to occur in the Tualatin Mountains originated in the park and burned for five days from Saturday, August 18th through August 22nd, 1951. Weather during the spring and summer of 1951 played a critical role in the outbreak of the fire. Only two inches of rain fell between April 1st and August 18th, compared to an average at the time of 7.5 inches. There were only 17 days with measurable rain compared to a normal of 42. The fire originated about two-thirds the way up the ridge in an area between Leif Erickson and Skyline Boulevard, north of Saltzman Road near city reservoir number 4 (Figure 25). The prevailing winds during the fire were from north-northeast.

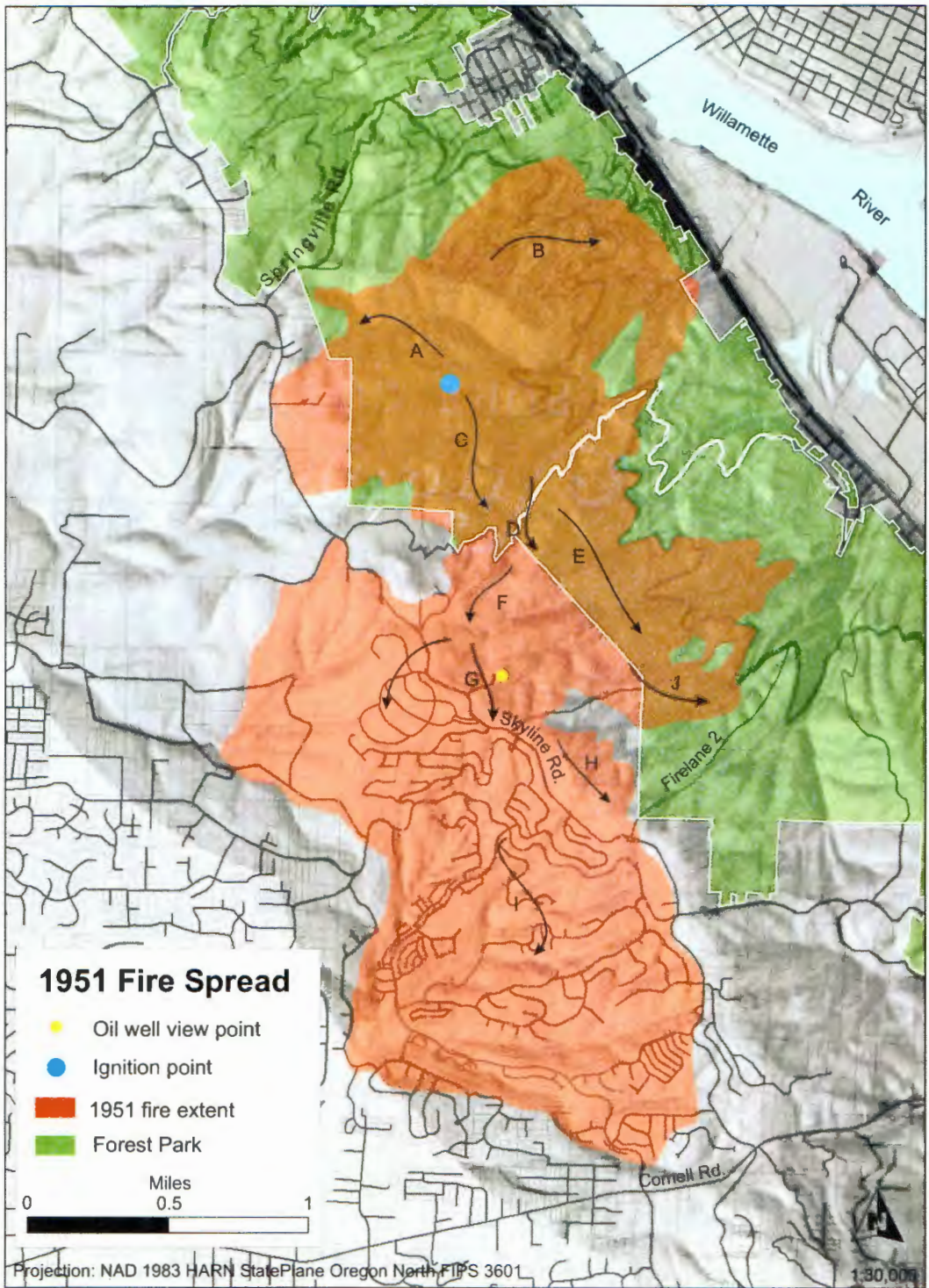


Figure 25: Red shaded area represents the 1951 fire extent. White line indicates Forest Park boundary. 2004 taxlots are included in the map to demonstrate the development that has occurred since the fire. The arrows represent fire spread as described by the William Morris from the USFS who observed the fire. (Base map source: USGS, Metro RLIS; fire boundary information: Morris 1954, The Oregonian 1951; fire boundary drawn by Author)

The fire is believed to have been started by a maintenance crew working near a small tank reservoir in a gully off of Leif Erickson. It is unknown if the ignition was a result of the work they were doing or carelessness during a cigarette break, but it is likely that the fire smoldered in that area for several days before it broke away during the afternoon of the 18th. Regardless, the fire burned over 2,200 acres, about 900 of which were in the park. The fire was not brought under control until the evening of Tuesday, August 21st. As figure 26 illustrates the 1951 fire over-burned the majority of the 1940 fire area.

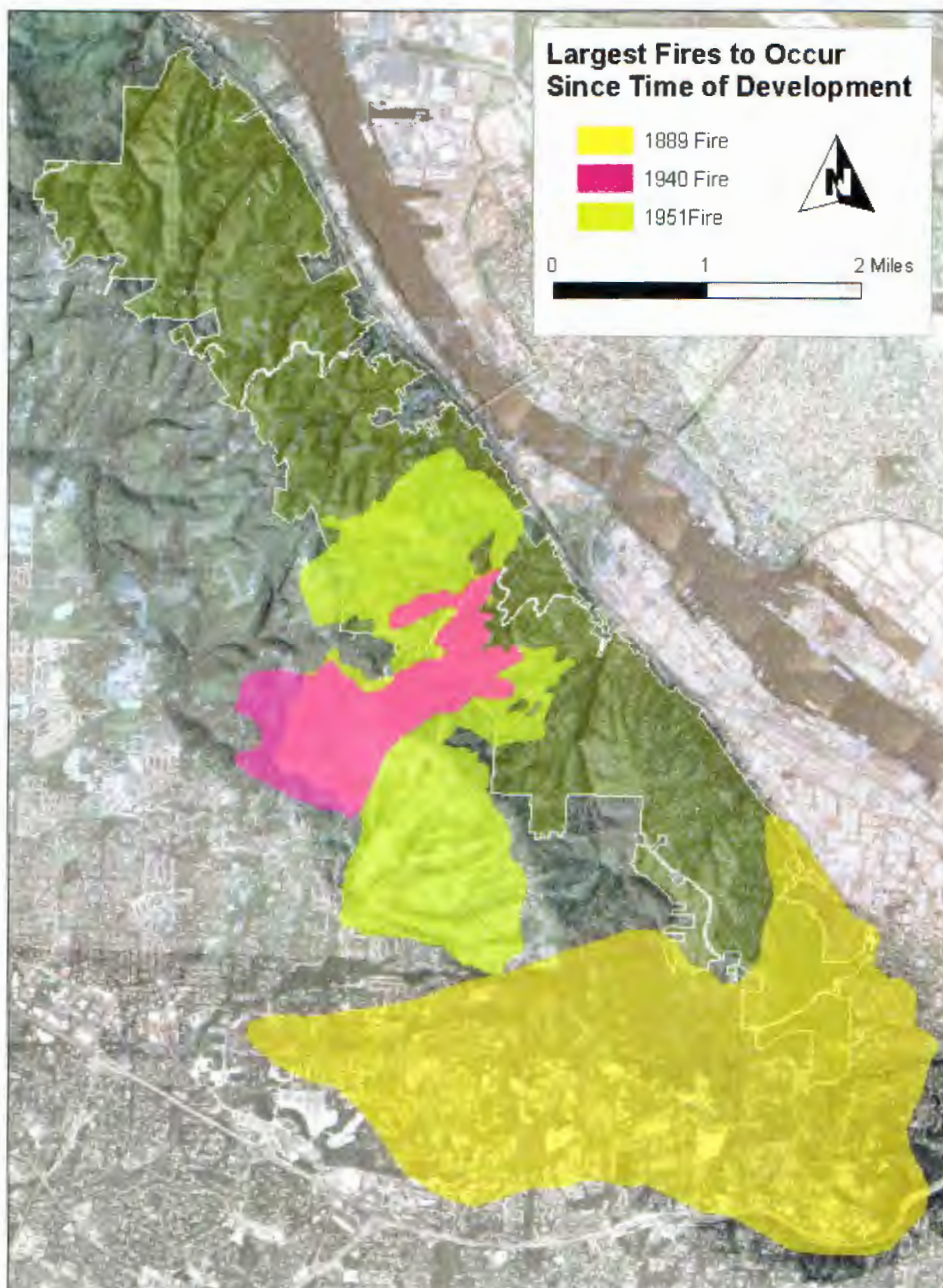


Figure 26: Large scale fires to burn in or around Forest Park since Anglo-American settlement. The white outline is the park boundary. (Source: USGS, City of Portland, fire boundaries drawn by Author)

The northerly spread of the fire was slow and left largely unattended throughout the fire's duration. The fire did eventually spread north nearing Springville Road, where it was presumably extinguished (Figure 25: arrow A). Fire also spread slowly down slope from the point of origin primarily to the northeast (arrow B). Little is known about the tactics or force that was brought to fight the northern fire lines. It is assumed that the fire burned slowly and controllably through most of the area.

The southern and western spread of the fire was far more active and unpredictable. U.S. Forester William Morris observed the fire along this front from Saturday, August 18th until Wednesday morning, August 22nd. He wrote detailed descriptions of the weather, vegetation, and spread rate from the point of ignition until it was brought under control during the evening of August 21st. The first night of his observation he wrote,

From 10:30 that night [August 18th] to 3:00 a.m. the temperature in the vicinity of the fire ranged from 66° to 71°, the relative humidity ranged from 28% to 37%, and the wind on exposed ridges was north 8 to 16 miles per hour. The fuel was the usual mixture of brush and weeds, scattered Douglas-fir saplings, snags, and old logs found on poorly stocked old cuttings in this region. (1953, 2)

The fire moved south about 0.4 miles in the first 12 hours after it broke away (arrow C). By 10 a.m. on Sunday the 19th the fire had spotted a short distance across a gully and moved only ¼ mile south of its overnight position (arrow D). However, by Sunday night the terrain and weather combined to produce the most rapid rate of spread.

The afternoon temperature reached a maximum of 88° and at 8 p.m. the temperature was still 79° with a relative humidity of 34%. At the same time gusts across the ridge top were 20 miles per hour. By this time the fire had spread south-southeast an additional $\frac{3}{4}$ of a mile (arrow E). The fire crossed Skyline road for the first time about $\frac{1}{2}$ a mile northwest of the oil well. At this point the fire spread on both sides of the ridge. Morris observed the eastern flank of the fire from the oil well view point from 8 p.m. until 10:45 p.m. and wrote,

At 8 p.m. the nearest point of the flank was 0.4 miles northwest near the top of the main ridge [along Skyline]. The fuel was largely standing and fallen poles killed by [the 1940 Bonny Slope fire]... This part of the flank spread only about 0.2 miles per hour because it was moving along the contours interrupted by several small gullies... Another finger from the main flank appeared farther down the spur ridge toward the river 0.4 miles north-northwest from the view point, and within 15 minutes two spots appeared 0.1 and $\frac{1}{4}$ mile south of that finger [arrow F]. (1953, 4)

Morris stayed at the oil well view point with the fire burning toward him. He was eventually forced to leave the location because of continued spot fires. At 10:30 p.m. he made his final observation from the oil well site,

...a spot started in the nearest gully about 0.1 miles north of the observation point. It spread at about $\frac{3}{8}$ of a mile per hour up the [nearest drainage gully] where it received the full force of the wind and passed over the view point ridge and oil well road at 10:45. Flames on the slope were about 50 feet high. The wind and draft soon increased from the 20 mile per hour gusts that had prevailed all evening to gusts estimated at 40 miles per hour. Standing snags cracked. New spots quickly appeared on a north slope $\frac{1}{4}$ mile farther south [arrow G]... (1953, 5)

At 11:30 p.m. the temperature was still 72° and the relative humidity was 42%. By 3 a.m. Monday morning the fire, that had passed the oil well, moved

farther south where it entered a large block of Douglas-fir south-southeast of the oil well. Most of the spot fires that had started northeast of the view point reached a partial canopy of trees, where spread slowed (arrow H).

The western flank of the fire consisted of several prongs that had developed from spot fires. By noon on Monday, August 20th fire was still active about ½ mile west of the Skyline-Thompson Road intersection (arrow I). According to Morris the fuel was consistent with a post-burn mixture of tall brush, bracken, and weeds. Flames were 4 to 10 feet high in 3 to 4 foot high green bracken.

The southeastern flank had been slowed once it entered the taller timber and thinner ground fuel. By Monday afternoon the temperature had reached 92° and relative humidity was at 23% with winds north-northeast 8 to 10 miles per hour. At this point the fire was backing down the slopes with flames only 1 foot high in the litter and sword fern. The boundary of the fire was eventually contained by the construction of a fire road, now called Firelane 2. Backfires lit along Firelane 2 stopped the advancing fire within 200 yards of the newly constructed road (arrow J). The fire continued to slowly spread throughout Monday, but by Tuesday the fire was under control and mop up had begun.

The 1951 fire was the most recent large-scale stand replacing fire to burn in the Tualatin Mountains and is central to this study because it is well-documented. The detail provided by Morris on the fire's development, combined with the weather data he collected at the fire, provides a real-world situation against which to test the fire simulation model.

The factors necessary to run the fire simulation model include: ignition source, wind, temperature, relative humidity, topography, and fuel. Taken together these factors produce a particular outcome in terms of areal extent of a burn. For the 1951 fire Morris provides the details of the outcome, as well as the wind, temperature, and humidity information. The ignition location is known and topographic data is available in digital map form. Although the fuel composition of 1951 is not known, the general characteristic of the vegetation that burned is described by Morris. His fuel composition descriptions are detailed enough to compare the simulation results with the actual 1951 fire outcome (Figure 27 and 28).



Figure 27: Photo taken on August 22nd, 1951 of burned area on the western slopes of the Tualatin range, west of Skyline Blvd. The photo indicates the view is to the west (Source: City of Portland Archives).



Figure 28: Photo taken on August 22nd, 1951 of burned area on the western slopes of the Tualatin range, west of Skyline Blvd looking down onto Bonny Slope. The photo is taken from an almost due west aspect (Source: City of Portland Archives)

Assumptions regarding the 1951 fire spread can be made based on Morris's fuel description. Even though it does not enable scientific analysis or simulation recreation because field data can not be collected, it provides a better understanding of how fire moves over the landscape and highlights specific areas that, given the right combination of fuel, exposure, and weather, could support a high intensity fire. This enables the study's fire simulation results to be compared to an actual event.

Management Objectives

An interdepartmental team from Portland Parks and Recreation and the Bureau of Planning, with additional support from citizen and technical advisory committees

developed a comprehensive natural resource management plan (NRMP) in 1994. The city felt that without a revised plan in place, overuse and encroachment would place too much pressure on the park's resources. Adopted by the Portland City Council in 1995, the NRMP outlines objectives for resource inventory, impact assessment, resource management, use management, monitoring, and environmental regulation compliance.

The NRMP recommends the implementation of a sustainable resource program that would monitor vegetation (exotic and native) and wildlife (native and pests), establish core preserves, and implement ecological restoration projects as necessary. Within the context of this program the issue of fire hazard management is to be addressed. Fire simulation modeling would support recommendations outlined in the Forest Park Natural Resource Management Plan by enabling park managers to prevent or minimize the impact of fire. The plan states,

...Fire hazard should be evaluated at regular intervals. Monitor significant risk factors including illegal camps, ignition from adjacent areas, overhead utility lines, and arson. Take appropriate action to eliminate or reduce risk factors. (1995, 48)

The NRMP is primarily concerned with sustainability and access. The report has a one-page synopsis of the fire hazard risk in the park. The plan's authors suggest that the "current and short-term projection of wildfire hazard is low, due to lack of snags, large woody debris and fine fuels as compared with natural forest residues in similar forest types" (City of Portland 1995).

The NRMP bases most of its fire hazard assessment on a shaded fuel break concept. According to the NRMP a shaded fuel break requires high overstory canopy

that keeps the humidity and moisture content of the understory relatively high. The shaded fuel break would usually be cleared of flash fuels (e.g. litter) and heavier ladder fuels (e.g. snags, blowdown logs) (Figure 29). This also assumes “moderate” burning conditions exist. Moderate conditions would include less than normal fuel moisture, low humidity, and above average temperature. An alternative definition is that a shaded fuel break is created by altering surface fuels, increasing the height to the base of the live crown, and opening the canopy by removing trees (Figure 30). Typically a shaded fuel break is also used with additional area treatment such as prescribed burn to reduce the understory fuel load (Agee, et al 2000).

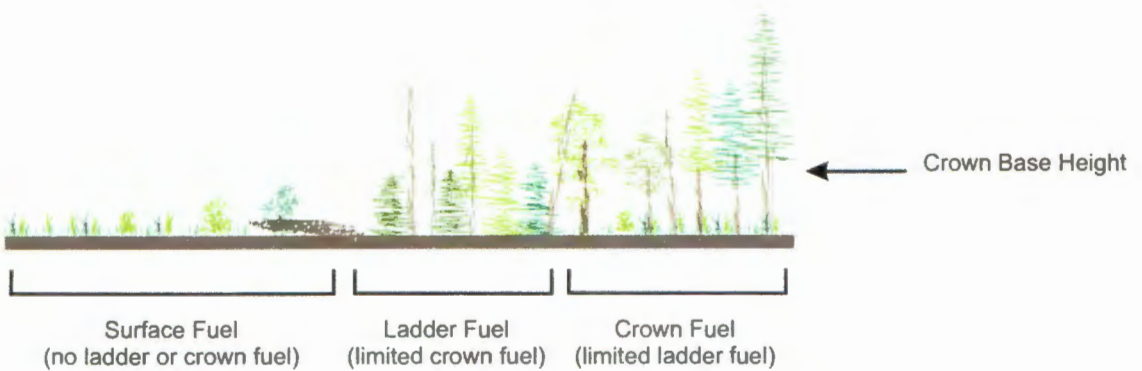


Figure 29: Vertical fuel structures that can lead to crown fires. For fire to ladder into the crown, the surface and crown fuels must have the appropriate level of vertical connectivity and density to sustain combustion into the crown. The surface fuel must burn intensely enough to ignite and sustain ladder fuel ignition. Surface fuel burns at a given flame length and intensity, which dictates the height and density at which the ladder fuel must be available. Living and dead material can act as ladder fuel. The ladder fuel must have the density to sustain combustion and ignite the crown fuel at the crown base height. The illustration represents an environment that may not support laddering fire. (Source: illustration drawn by Author)

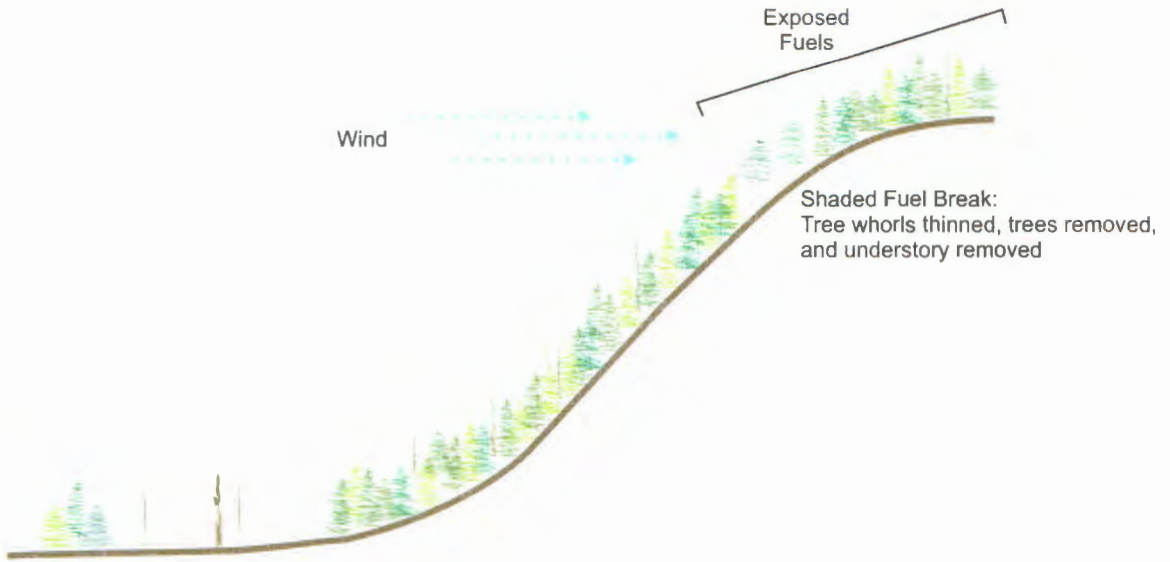


Figure 30: Shaded fuel breaks are placed at strategic locations to minimize fire's ability to ladder into tree crowns. Areas with heavy fuel loads and low canopy base heights and tall understory vegetation are likely areas for fire to ladder into the canopy. (concept by Rothermel 1983, Agee 1999, illustration drawn by Author)

The NRMP concludes that the relative abundance of hardwood stands within the park provides similar fire protection as shaded fuel breaks because the fuel composition changes and would therefore impede fire movement. There has been no active management within the hardwood stands of the park. Therefore, the surface and ladder fuels are still present and contiguous throughout the various stands. The shaded fuel break theory proposed in the NRMP will be tested by the fire simulations. The plan also recommends that conditions be reassessed on a ten year schedule. The fieldwork completed for this research was conducted exactly ten years after the NRMP studies.

Summary

The events that led to the establishment of Forest Park were both deliberate and serendipitous. A visionary design for a city-wide park system and subsequent failed land deals created a unique and rare park setting. Development has inched up to the boundary of the park over the last fifty years, but the interior has remained untamed. Although the species mix has been altered from that of a native wildland, the forest has followed the typical succession pattern for its location and orientation in the Western Hemlock Vegetation Zone.

The study area has experienced more frequent fires of varying intensity than would be expected in a similar wildland area based on the fire cycle studies presented in Chapter 3. The increased fire activity is likely contributable to the historic landuse of the area, especially the logging activity. Understanding Forest Park's inimitable place among the nation's city parks, the City of Portland has developed a natural resource management plan that has a long-term vision for maintaining the forest. The need to better understand the role of fire in achieving the city's vision is a goal of this study.

CHAPTER 5: MODEL IMPLEMENTATION: STEPS AND RESULTS

Fire behavior simulation has opened new avenues in research by analyzing forest fires without having to burn down the forest. Many different types of fire simulation models have been developed, all of which require the same basic inputs of terrain, weather, and fuel. Farsite is the fire behavior model used in this study. The process begins with field work to collect the fuel data that will support the custom fuel model and crown fuel inputs to Farsite. In order to develop a fuel map of the study area the entire landscape must be classified accordingly. Multi-spectral remote sensing imagery was used to apply a vegetation index that would simplify the process and improve the fuel map accuracy. At the end of this process the basic fuel map was complete, and could be used as the basis for other fuel layers.

Fire Model History

Publications regarding fire behavior, fuel analysis, and fire weather in the West date back to the 1920s. In 1913, USFS Forester J.A. Larsen began gathering meteorological data while conducting silviculture studies at the Priest River Experimental Forest in Idaho. He discovered a correlation between weather and fire behavior and in 1921 published several reports about the influence of precipitation, relative humidity, wind, and temperature on forest fires.

In 1928, Harry Gisborne, a USFS Forest Examiner, published the first technical report comparing duff and wood moisture content with various weather elements. Gisborne later developed a fire danger meter and related administrative system that provided action plans for current or probable fire danger. Gisborne's

system was implemented in 1931, but not used nationally until 1934 (USDA, Forest Service, Rocky Mountain Research Station).

L.G. Hornby developed the standards and instructions for fuel type mapping in 1933. By the 1930s the primary concern of the USFS was fire control planning. Fuel classification was used to gauge how difficult a fire would be to suppress. In 1935 Hornby developed a fuel classification system that formalized the description of rate of spread and resistance to control into classes of low, medium, high, and extreme.

In the Hornby model the potential rate of spread and the 'resistance to control' class ratings were determined based on the 'average worst' burning conditions. Average worst conditions were defined as burning conditions typical of the worst part of the average fire season. Rate of spread was estimated through statistical analysis of individual fire reports. Resistance to control was estimated by measuring the amount of time needed to construct a fireline by hand. The Hornby system was the fuel mapping standard for over 40 years (Anderson 1982, Sandberg, Ottmar, and Cushon 2001).

W. R. Fons had pioneered the mathematical representation of fire spread in the 1940s by focusing on the heating dynamic at the fire front. He theorized that fire spread can be visualized based on a series of successive ignitions across a fuel bed, the rate of which is determined by ignition time and distance between fuel particles. Frandsen in 1971 applied the conservation of energy principles to a unit of fuel ahead of an advancing fire in a homogenous fuel bed.

It was not until 1972 that Richard Rothermel introduced for the first time a mathematical model for the quantitative evaluation of both the rate of surface fire

spread and intensity based on in-situ fuel and weather inputs. Rothermel developed two basic fire spread equations; rate of spread (ft/min), and reaction intensity (Btu/ft² min.). Each equation had sub-equations. He also developed a list of 11 input parameters that would be either collected directly from field data or derived from field data in a laboratory. Ultimately, Rothermel's equations were used to create the first standard set of fuel models based on various vegetation regimes. However, Rothermel's model did not account for firebrands (spotting) or vertical spread into the canopy and crown fire (Rothermel 1972).

The advent of computers with powerful computational and graphical ability enabled fire prediction to move beyond tables and graphs. Fire simulation can be presented in three-dimensional multi-angle scenes displaying the fire spread across the topographic details of a landscape. A fire simulation system combines the fire behavior model with a fire simulation technique (Albright and Meisner 1999). There are multiple types of fire behavior models and simulation techniques that have been developed over time and incorporated in a variety of fire simulation applications.

There are four types of fire behavior models: physical, physical-statistical, statistical, and probabilistic.

Physical models predict fire spread based the physics of combustion regarding heat transfer from conduction, convection and radiation. Physical models require large amounts of detailed data about distribution and density of fuel across a fuel bed (Albini 1986).

Physical-statistical models use both physics and statistical correlation to generate fire behavior formulas. Rothermel's equations based on the conservation of

energy principles and statistical data from laboratory experiments are an example of this type of model.

Statistical models use test fire data to derive fire behavior equations of best fit. In statistical models, rate of spread, fuel consumption, and fire intensity are independent variables and the physical relationships between parameters is not considered.

Probabilistic models are based on contingency tables of discrete categories each representing an environmental variable. The probabilities in the table are then used to simulate the likelihood of fire spread from one location to the next. Probabilistic models are usually used for predicting a series of hypothetical fires over a wide area instead of the rate of spread for a specific fire (Albright and Meisner 1999).

Fire simulation techniques use probability of occurrence or mathematical functions in addition to the fire behavior model to simulate fire spreading across a defined landscape. There are three simulation techniques: bond percolation, cellular automaton, and elliptical wave propagation (Figure 31).

Bond percolation uses a lattice of square, hexagonal or triangular cells to represent the landscape. Fire spread through out the cell lattice is based on probability of spread from cell to cell.

Cellular automaton also represents the landscape in a cellular fashion. Each cell has set values for fuel and environmental parameters. Fire spread is based on rules that are applied to all cells. The rules relate the future state of one cell to its initial state and the state of neighboring cells at given time steps.

Elliptical wave propagation projects the landscape as a continuous surface. This technique requires no local tuning based on the assumption that the fuels, weather, and topography in the area where the input parameters were recorded are uniform (Albright and Meisner 1999).

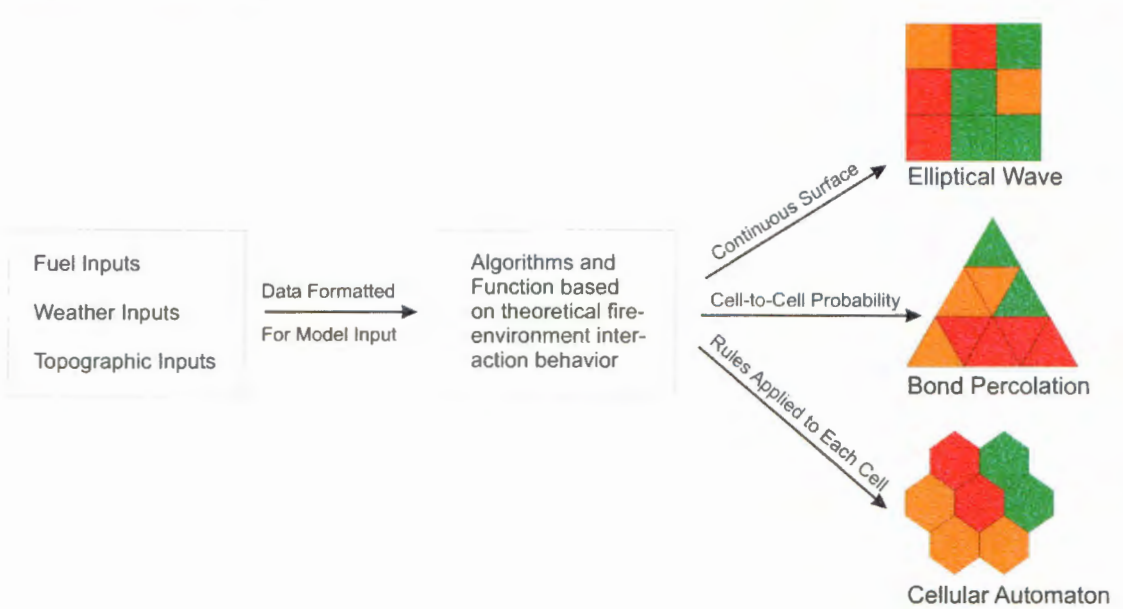


Figure 31: Fire simulation model types, inputs, and output generation schematic. The cell shapes of each model depicted in the diagram represent common cell shape for the model type. However, the actual cell shape for each model may vary. For example, a bond percolation model can have rectangular cells. (Source: diagram by Author)

There are some practical advantages to using elliptical wave propagation models. First, they have been developed most recently and therefore can be used on a PC platform. Earlier models were primarily developed and compiled on UNIX workstations. Furthermore, the PC-based applications have been continually updated. Many of the UNIX-based applications have not been maintained. Additionally, the older fire models have fixed spatial resolution, which is not the case for the elliptical wave, PC-based applications.

Fire Modeling Applications

In this study a series of computer applications were used to develop the datasets used in the test simulations. The first was Firemon, which is a field collection protocol, database, and reporting tool developed for monitoring effects of recent wildland fires and effectiveness of treatments (Appendix B). The Firemon protocol was established by a consortium of government agencies and a non-profit research corporation, USFS Firelab, NASA, USGS, and Systems for Environmental Management. The output from Firemon reports is used for further data creation using Fuelcalc and Farsite.

Fuelcalc is a prototype application under development by the USFS. It is used to calculate canopy fuel characteristics.

The roots of fire behavior estimation lie in Rothermel's equations. Fuel bed characteristics used in this study are based on the format of fire behavior models used in Farsite. A fuel model refers to the surface fuel characteristics used for fire behavior. The fuel model parameters are the same for Anderson's (1982) 13 standard fuel models and user-defined custom fuel models as the described in Table 5.

Table 4: Description of fuel model fields derived from Firemon and Behave output.
(Source: Finney 2004)

Fuel Model Fields			
Field	Description	Data Type	Metric Units
FMod	Fuel Model number: number 1-13 is reserved for the standard fuel models (Anderson 1982). Custom fuel models use numbers 14 through 50.	Integer	Number 1-50
1H	1 hour timelag fuel load (woody litter under 0.6 cm diameter)	Decimal	Tons/hectare
10H	10 hour timelag fuel load (woody litter under 2.5 cm diam.)	Decimal	Tons/hectare
100H	100 hour timelag fuel load (woody litter under 8 cm diam.)	Decimal	Tons/hectare
LiveH	Live herbaceous plants	Decimal	Tons/hectare
LiveW	Live woody plants	Decimal	Tons/hectare
DSAV	Dead fuels surface area to volume ratio	Integer	1/cm
LHSAV	Live herbaceous fuels surface area to volume ratio	Integer	1/cm
LWSAV	Live woody fuels surface area to volume ratio	Integer	1/cm
Depth	Depth of the fuel bed	Decimal	Cm
XtMoist	Moisture of extinction, percent moisture content of the fuels 0.6 cm in diameter or less where the fire will not continue to readily burn.	Integer	Percent
DHt	Heat content in Joules for dead fuels	Integer	J/kg
LHt	Heat content in Joules for live fuels	Integer	J/kg

Farsite enables a user to initialize a custom fuel model from a standard fuel model using an automated worksheet. The process of developing a custom fuel model is more complex than just filling in the worksheet. Once the parameter values have been set, a fuel model must go through a process of evaluation and revision (Andrews, Bevins, and Seli 2003).

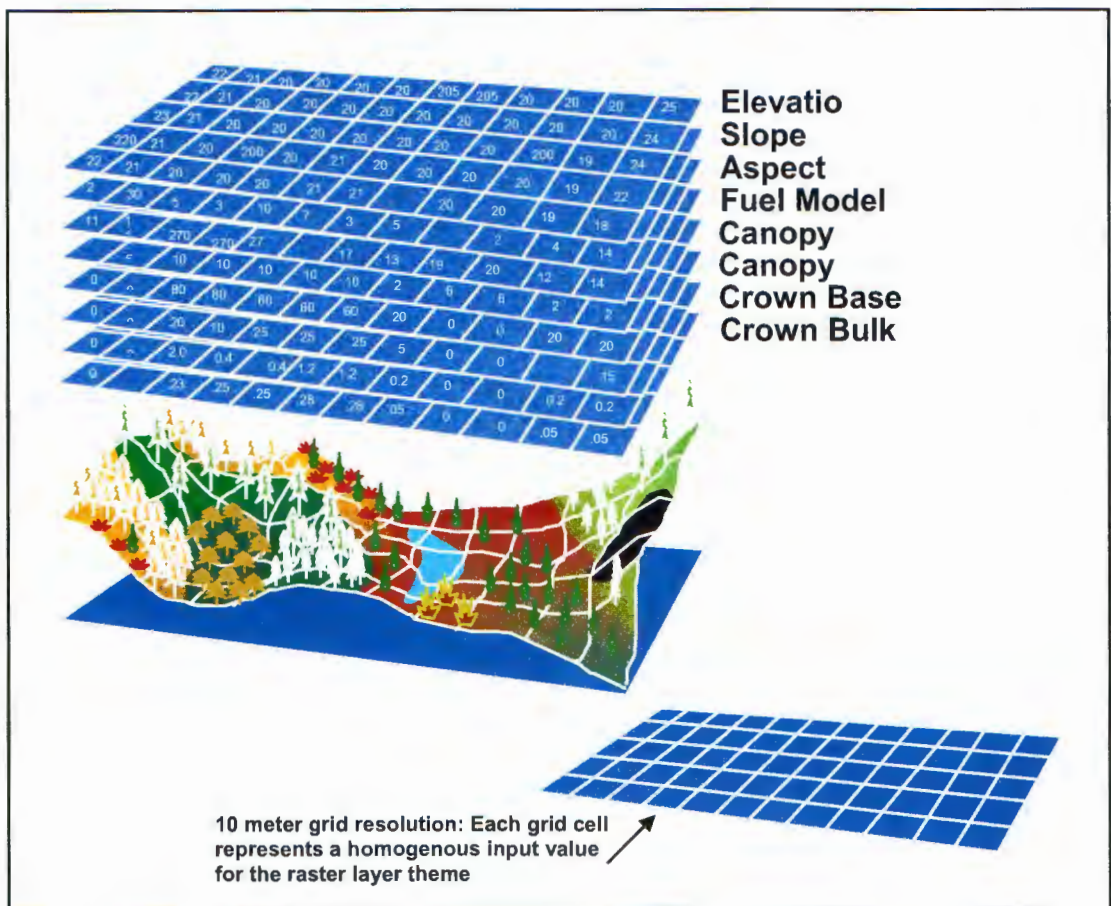
Farsite is fire simulation software used to visualize fire spread over landscape data layers developed in ArcGIS. Farsite consists of a set of fire behavior algorithms that calculate fire spread and intensity across a continuous landscape based on various fuel, weather, and topographic inputs (Appendix A). Separate fire behavior models

are used for surface fire, crown fire, spotting fire acceleration. Each model is calculated in a two-dimensional plane, but together the behaviors are an abstraction of a three-dimensional process (Finney 2004). The linkage of the models relies on an assumed sequence of events starting in the substrate fuels (surface fire). Based on model inputs the fire may achieve a spread rate that enables it to transition to burning aerial fuels and laddering out of the understory (surface fire) and into the overstory (crown fire).

The Farsite model uses two-dimensional surfaces as the inputs into the equations that predict fire behavior and spread over a landscape (Figure 32). Topographic, as well as surface and aerial fuel data are developed into raster layers in ArcGIS (Table 6). Raster resolutions of 25-50 meters are widely available for topographic and remote sensing data and provide an acceptable level of detail (Finney 2004). However, since the area of interest for this study is small relative to most wildland fire simulations, the raster resolution of the data layers have been reduced to 10 m (Figure 32). Ten meter USGS digital elevation models (DEMs) were used for this study.

Table 5: Explanation of the raster inputs to Farsite (Source: Finney 2004).

Raster Theme	Units	Usage
Elevation	m	Used for adiabatic adjustment of temperature and humidity from the reference elevation input with the weather stream.
Slope	percent	Used for computing direct effects on fire spread, and along with Aspect, for determining the angle of incident solar radiation (along with latitude, date, and time of day) and transforming spread rates and directions from the surface to horizontal
Aspect	Az	See Slope
Fuel model		Provides the physical description of the surface fuel. Fuel model parameters are described in detail in Table 2.
Canopy cover	percent	Used to determine an average shading of the surface fuels that affects fuel moisture calculations. It also helps determine the wind adjustment factor that decreases windspeed from the reference velocity of the input stream (6.1 m above the vegetation) to a level that affects the surface fire.
Canopy height	m	Affects the relative positioning of a logarithmic wind profile that is extended above the terrain. Along with canopy cover, this influences the wind adjustment factor, the starting position of embers lofted by torching trees, and the trajectory of embers descending through the wind profile.
Crown base height	m	Used along with the surface fire intensity and foliar moisture content to determine the threshold for transition to crown fire
Crown bulk density	kg m ⁻³	Used to determine the threshold for achieving active crown fire



Rate of Spread: $R = I_R \xi (1 - \Phi_w + \Phi_s) / \rho_b \epsilon Q_{ig}$

$R =$ forward steady state spread rate (m min^{-1})

$I_R =$ reaction intensity ($\text{kJ min}^{-1} \text{m}^{-2}$)

$\xi =$ the propagating flux ratio

$\Phi_w =$ **wind coefficient (result of wind-slope vector and wind speed)**

$\Phi_s =$ **slope coefficient (result of wind-slope vector and radian azimuth)**

$\rho_b =$ *ovendry bulk density (kg m^{-3})*

$\epsilon =$ dimensionless effective heating number (proportion of fuel mass that must be raised to ignition temperature)

$Q_{ig} =$ heat of pre-ignition (kJ kg^{-1})

Fire Intensity: $I_b = hwR/60 = (I_R/60) * (12.6R/\sigma)$

$I_b =$ fire intensity at leading edge

$h =$ *heat yield of the fuel, total heat less the energy required to vaporize moisture (kJ kg^{-1})*

$w =$ **weight of the fuel per unit area (kg m^{-2})**

$R =$ leading edge steady state spread rate (m min^{-1})

$I_R =$ reaction intensity ($\text{kJ min}^{-1} \text{m}^{-2}$)

$\sigma =$ **surface area to volume ratio of fuel bed (m^{-1})**

Ladder Fire: $I_o = (0.010 * \text{CBH}(460 + 25.9M))^{3/2}$

$I_o =$ threshold for transition to crown fire

CBH = crown base height that incorporates the presence or effect of ladder fuel

M = foliar moisture content (percent on dry weight basis)

Crown Fire Rate of Spread: $\text{RAC} = 3.0 / \text{CBD}$

$\text{RAC} =$ active crown fire spread rate

$3.0 =$ *empirical constant defining critical mass flow rate through the crown for continuous flame ($0.05 \text{ kg m}^{-1} \text{ s}^{-2}$) and a conversion factor (60 s min^{-1})*

CBD = crown bulk density (kg m^{-3})

Crown Fire Intensity: $I_c = 300 (I_b / 300R = \text{CFB} * \text{CBD}(H - \text{CBH})) * R_{\text{Cactual}}$ or R

$I_c =$ crown fire intensity

H = crown height

Heat content of surface and crown fuels is assumed to be $18,000 \text{ kJ kg}^{-1}$

Max. Crown Spread Rate: $R_{\text{Cmax}} = 3.34 * R_{10} * E_1$

$R_{\text{Cmax}} =$ maximum crown fire spread rate

3.34 = *coefficient to minimize accounting for individual tree torch or the possibility that spotting could be accounted for twice*

R_{10} = forward steady state spread rate for fuel model 10 using 0.4 wind reduction factor

E_i = fraction of the forward crown spread rate achievable at the i th perimeter vertex given orientation of the vertex to the maximum spread direction and elliptical dimension of the crown fire

Crown Burned: $CFB = 1 - e^{-ac(R-R_o)}$

CFB = crown fraction burned

e^{-ac} = exponent where $a_c = -\ln(0.1) / 0.9 (RAC - R_o)$

R_o = critical surface fire spread rate where $R_o = I_o (R /)$

Spread Distance per timestep: $D_t = R (T_t + (e^{-aaT_t} / a_a) - (1 / a_a)) + D_{t+1}$

D_t = spread distance require to achieve the current spread rate under current conditions

R = forward steady state spread rate ($m \text{ min}^{-1}$)

T_t = time required to achieve the current spread rate under current conditions

a_a = *constant that determines the rate of acceleration (set to 0.115 or 0.300) Crown fires use equation $a_a = a_a - 18.8 * CFB^{2.5} e^{(-8 CFB)}$*

D_{t+1} = desired spread distance in next timestep

Figure 32: Farsite landscape layers developed in ArcMap and exported into ASCII. Layers represent real fuel and topographic situation of the fire area. Farsite uses the data of each layer as inputs into algorithms and functions to simulate fire spread. The key functions and parameters are listed. All parameters related to data collected in the field are bold. All parameters or constants developed from laboratory tests are *italic*. (Source: Finney 2004)

Control of the spatial and temporal resolution is critical for the fire simulation. The total length of the simulation is broken into timesteps or “iterations”. Within a single timestep each active fire polygon grows at a rate based on fire behavior equations. At the end of the defined timestep the fire polygons are merged to show the full fire extent and growth since the last timestep.

The maximum timestep, distance resolution, and perimeter resolution parameters control the spatial and temporal resolution of the simulation. The maximum timestep is based on the length of time fire spreads through environmental conditions that are assumed constant.

The distance resolution specifies the level of spatial detail required during a timestep. The distance resolution is defined as the maximum horizontal spread distance before new environmental inputs are required (i.e. radial spread direction).

The perimeter resolution is the maximum distance allowed between vertices of the fire polygon (Finney 2004). Perimeter resolution is based on the topography as related to the rate of spread. As the fire spreads over convex areas (hills or ridges) the vertices separate more quickly over time. If the maximum perimeter resolution is exceeded by the fire spread rate then a mid-point vertex is inserted in the fire polygon perimeter.

The perimeter resolution enables the fire growth to be rasterized because of the changing vertex densities along the different fire polygons. Rasterizing the spread can visualize the aggregation of sub-timesteps for each individual fire polygon as fire spread rates change due to heterogeneity of the fire environment. The end result is a

representation of the merged fire polygons for a complete timestep over varying topography (Richards 1990).

Farsite in the Field

Farsite has been used extensively by the USFS and other state and federal agencies. Farsite's versatility and features make it an appropriate application for analysis of past, present, and potential fires. The USFS used Farsite to identify and prioritize the fire management zones in New Mexico's Gila National Forest. The State of Alaska and the Kenai Peninsula Borough used Farsite in 2001 to determine the burn scenarios for their Coho fire exercise, which resulted in the managed burning of forest that had recently been attacked by bark beetle outbreak. Farsite is used as a decision support tool for just about every large-scale wildfire every year. Farsite has an extensive set of tools that enable fire managers to apply suppression strategies to currently burning fires. The NPS and USFS use the resulting suppression maps to deploy firefighters and aerial resources (Finney 2004). Farsite has also been used to analyze past fires to determine how they burned and gauge the effectiveness of fire mitigation techniques that may have been employed in the burn area. The 2000 Bitterroot fire in Montana was extensively researched using Farsite to determine spread rate and smoke emissions (Keane, et al. 2000).

Farsite has also been used in academic research. Students and faculty at schools including the University of Texas and Humboldt State University have used Farsite to predict fire behavior or assess fire dependent ecosystems. The University of California at Santa Barbara and NASA jointly manage the Southern California

Wildfire Hazard Center and use Farsite as their primary tool for fire hazard prediction (Regents of the University of California 2005).

Additionally, Farsite is a public domain application, which enables anyone to acquire and use it to analyze fire behavior in a local environment. Its use at all levels of government, acceptance in the academic community, interoperability with ArcGIS output, and no cost of ownership made it the best candidate for use in this study.

Farsite Inputs

Running a simulation in Farsite requires that the Farsite environment be set up within the application specific to the fire simulation area. The fuel, weather, and topographic inputs have been discussed previously. They are the primary inputs and are used to create the necessary Farsite files. The Farsite interface (Figure 33) provides a simple view of how the primary inputs are organized for the simulation.

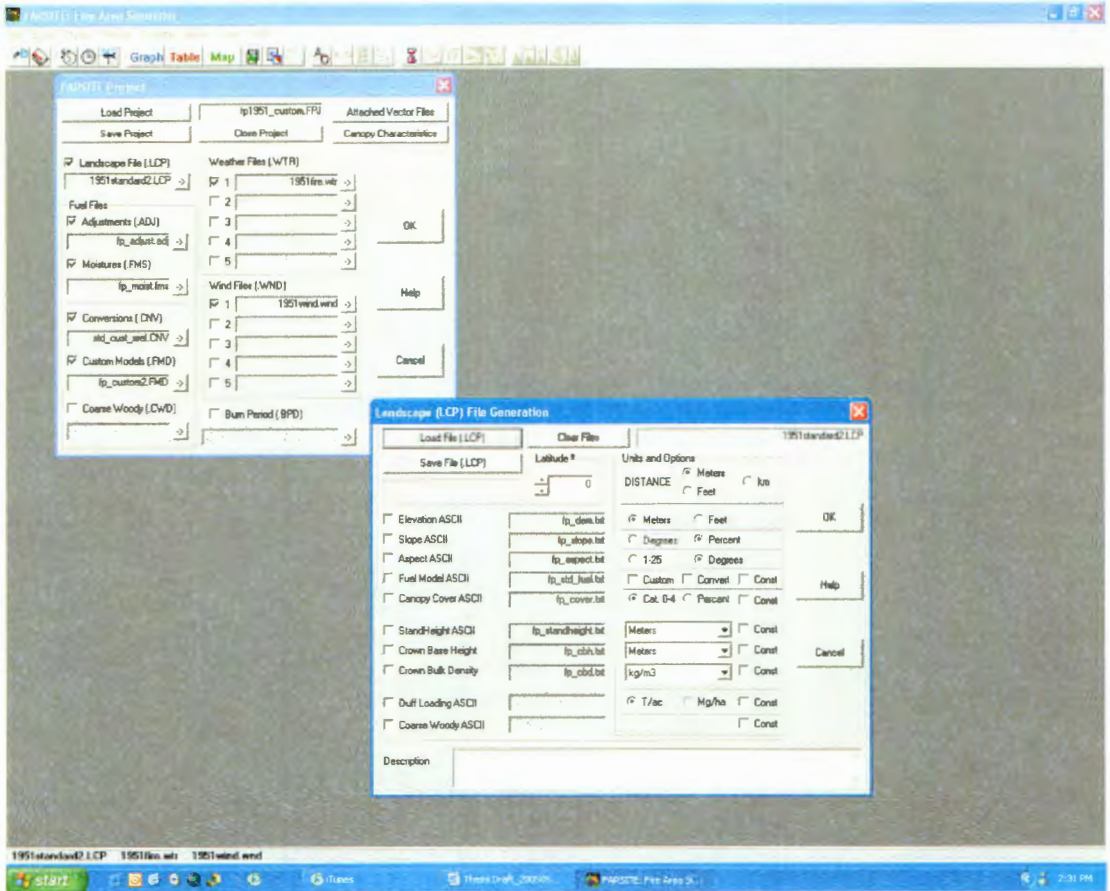


Figure 33: Farsite project view. The active dialog window is for the landscape file that contains all the topographic, fuel, and crown-fuel related inputs. (Source: screenshot by Author)

There are four types of files that make up the data inputs to run a fire simulation in Farsite. They include a landscape file, weather files, wind files, and conditional fuel files. The files are organized into a project file to which universal settings, such as the duration of the simulation can be applied. The landscape file is a combination of multiple imported geographic information system files that represent various terrain and canopy parameters. The fuel files actually adjust fuel inputs provided by the landscape file. The weather files provide temperature and humidity data that help adjust fuel moisture levels. The wind files supply the wind speed, gust,

and direction data that are used as direct inputs into the rate and spread of the simulated fire.

Wind information is input as a data stream that consists of frequent observations. The more the observation the more accurate the wind can be depicted across the simulation area. The weather files contain daily observations on temperature and humidity as well as precipitation that depict a temporal weather stream. The weather stream greatly oversimplifies actual variation in weather. However, this format is an attempt to limit to a practical level the amount of weather information required for a simulation. The file format is the same as the wind file. Both wind and weather inputs apply to the entire simulation area during the specified time of observation.

There are two conditional fuel files required for all simulations - the adjustment file and the moisture file. Both files impact how the different fuel models and associated data are used by the Farsite model. The adjustment file can reduce or accelerate the rate of spread factors for particular fuel models during a simulation. The other required conditional fuel file is the moisture file, which set the initial fuel moistures for each fuel model at the beginning of the simulation. Specific fuel moisture values provide the initial moisture percentages for the 1-hour, 10-hour, and 100-hour down woody debris, and the live woody, and live herbaceous fuels for each fuel model.

Up until now we have discussed only the text file inputs. However, in order to implement a fire simulation a geographic information system (GIS) is required to

develop several themed raster inputs, which are used to create a landscape file. A landscape file consists of all the raster data themes imported from a GIS.

There are three terrain related themes in the landscape file. The elevation theme is necessary for adiabatic adjustment of temperature and humidity and for conversion of fire spread between horizontal and slope distances. The slope theme is necessary for computing slope effects on fire spread and solar radiance. The aspect theme consists of azimuth values (degrees clockwise from north) for the slopes of the study area and is necessary for calculating the slope effects and adjustment on the prevailing wind direction and speed.

In addition to the terrain themes there are five fuel related themes in the landscape file. Two of the files are specific to the surface fuel composition and the other three pertain to the canopy fuel composition. The fuel model file is the primary surface fuel theme in the landscape file. Two fuel model files were developed for this study. One represented the custom surface fuel composition based on data collected at sampling plots located within the park. The other was based on a standard set of fuel models discussed later in this chapter. The canopy cover file is also specific to the surface fuel model. Canopy cover regulates the surface fuel moisture levels based on the amount of sunlight and wind that reaches the surface fuels. Conversely, as the canopy cover increases, humidity at the surface remains high, thus increasing the fuel moisture.

The three additional files are related to the canopy fuel composition. The first is stand height, which provides the model with the average height of the canopy as it may fluctuate over the simulation area. In the case of a crown fire the stand height

will be directly related to the flame length, probability of fire branding, and potential for spot fire ignition. The canopy base height file provides the model with the distance from the surface at which the canopy starts. A low canopy base height increases the likelihood of tree torching and crown fire outbreak. The last canopy related input is the crown bulk density file. Crown bulk density provides the model with the amount of fuel located in the crown. As crown bulk density increases more fuel is found in the crown; if a fire were to ladder into the crown it would burn longer and more intensely.

The fuel themes described above were developed from a fuel mapping process using in situ data collected from the study area and analysis of multi-spectral remote sensing data. Additional information on the Farsite inputs and specific fieldwork protocol instructions can be found in Appendix B.

Fuel Map Development: Standard Fuel Models Selection Process

Based on the vegetation stratum found at the sampling plots, five fuel classes were identified that represented the entire landscape. Each class was based on correlation between Anderson's (1982) fuel models and the observed stand composition during field data collection. The fuel models selected from Anderson's 13 standard models were intended for use in the Pacific Northwest. Table 7 defines the tree species composition of each of the sampling plots and identifies the standard fuel model that best represents the plots fuel stratum. Canopy composition was used to identify the representative fuel model of an area because aerial multi-spectral remote sensing imagery was used to develop study area fuel maps. The accuracy of

selecting the appropriate fuel model is critical, as small variations in fuel models can have significant impact on fire behavior prediction (Keane, et al. 2000).

Table 6: Stand composition of each plot. Plot 1 and 5 represent standard surface fuel model 10. Plot 2 and 4 represent fuel model 9. Plot 3, 6, and 7 represent fuel model 8. (Source: author and Anderson 1982)

Sampling Plot	Standard Fuel Model	Species	Tree/Ha	Species %
Plot 1	Model 10			
	<i>Mixed conifer with down woody debris</i>	ACMA	180	47.3%
		PSME	160	42.1%
		TSHE	40	10.5%
Plot 2	Model 9			
	<i>Western hard-woods with leafy litter</i>	ACMA	260	68.4%
		ALRU	20	5.2%
		PSME	80	21.1%
		TSHE	20	5.2%
Plot 3	Model 8			
	<i>Closed canopy mixed conifer and hardwood stands with thin litter layer</i>	ABGR	20	2.9%
		ACMA	320	47.1%
		PSME	160	23.5%
		THPL	160	23.5%
		TSHE	20	2.9%
Plot 4	Model 9			
		ABGR	20	4.0%
		ACMA	240	48.0%
		ALRU	220	44.0%
		PSME	20	4.0%
Plot 5	Model 10			
		ABGR	20	7.7%
		ACMA	40	15.4%
		PSME	100	38.5%
		THPL	40	15.4%
		TSHE	60	23.0%
Plot 6	Model 8			
		ABGR	240	44.4%
		ACMA	160	29.6%
		ALRU	20	3.7%
		PSME	100	18.5%
		TSHE	20	3.7%
Plot 7	Model 8			
		ABGR	160	27.6%
		ACMA	200	34.5%
		ALRU	40	6.9%
		TSHE	180	31.0%

Areas classified as urban were treated as non-fuel. This decision does pose some interesting questions regarding the potential for fire spread through the wildland-urban interface. Most houses and structures are flammable, but for this study all elements of development were considered non-fuel sources. This point will be revisited in the Discussion and Recommendation chapter.

Areas that had been disturbed and allowed to regenerate, such as areas under utility lines or adjacent to rail lines, had Anderson's fuel model 5 applied (Figures 34 and 35). According to Anderson (1982, 5) fires in fuel model 5 are,

generally carried in the surface fuels that are made up of litter cast by the shrubs and the grasses or forbs in the understory. The fires are generally not very intense because surface fuel loads are light, the shrubs are young with little dead material, and the foliage contains little volatile material. Usually shrubs are short and almost totally cover the area. Young, green stands with no dead wood would qualify: laurel, vine maple, alder, or even chaparral, manzanita, or chamise.

The areas represented by this fuel model in the study area may have increased volatility because of the larger and more mature shrubs, as well as an abundance of Scotch broom (*Cytisus scoparius*), which is highly flammable.



Figure 34: Anderson's photo of fuel model 5, "Regeneration shrublands after fire or other disturbances have a large green fuel component, Sundance Fire, Pack River Area, Idaho." (Source: Anderson 1982)



Figure 35: None of the sampling plots were placed in an area representing Anderson's fuel model 5. However, a visual comparison and a walk-through of these areas in the study area confirmed that fuel model 5 had appropriate fuel loading values. (Source: photo taken by Author)

Locations within the study area dominated by western hemlock or mixed conifer/deciduous stands were equated to fuel model 8 (Figures 36 and 37). Anderson describes fire movement through this type of fuel model as,

Slow-burning ground fires with low flame lengths are generally the case, although the fire may encounter an occasional “jackpot” or heavy fuel concentration that can flare up. Only under severe weather conditions involving high temperatures, low humidity, and high winds do the fuels pose fire hazards. Closed canopy stands of short-needle conifers or hardwoods that have leafed out support fire in the compact litter layer. This layer is mainly needles, leaves, and occasionally twigs because little undergrowth is present in the stand. Representative conifer types are white pine, and lodgepole pine, spruce, fir, and larch. (1982, 11)



Figure 36: Anderson's photo of fuel model 8, "Surface litter fuels in western hemlock stands of Oregon and Washington." (Source: Anderson 1982)



Figure 37: Photo taken by Author of a sampling plot selected to represent fuel model 8. The live ground cover is more abundant in the sampling plot location than in Anderson's photo representation.

Areas dominated by Douglas-fir or mixed conifer stands were equated with fuel model 10 (Figures 38 and 39). Based on Anderson's observations,

Fires [in this fuel type] burn in the surface and ground fuels with greater fire intensity than the other timber litter models. Dead-down fuels include greater quantities of 3-inch (7.6 cm) or larger limbwood resulting from overmaturity or natural events that create a large load of dead material on the forest floor. Crowning out, spotting, and torching of individual trees are more frequent in this fuel situation, leading to potential fire control difficulties. Any forest type may be considered if heavy down material is present; examples are insect- or disease-ridden stands, windthrown stands, overmature situations with deadfall, and aged light-thinning or partial-cut slash. (1982, 13)



Figure 38: Anderson's photo of fuel model 10, "Old-growth Douglas-fir with heavy ground fuels."
(Source: Anderson 1982)



Figure 39: Photo taken by Author of a maturing stand dominated by Douglas-fir. There is little old growth environment in the study area. The heavy ground fuels referred to by Anderson are rare.

Areas dominated by Bigleaf maple or deciduous stands were equated to fuel model 9 (Figures 40 and 41). Anderson describes fire spread in this fuel type,

Fires run through the surface litter faster than model 8 and have longer flame height. Both long-needle conifer stands and hardwood stands, especially the oak-hickory types, are typical. Fall fires in hardwoods are predictable, but high winds will actually cause higher rates of spread than predicted because of spotting caused by rolling and blowing leaves. Closed stands of long-needled pine like ponderosa, Jeffrey, and red pines, or southern pine plantations are grouped in this model. Concentrations of dead-down woody material will contribute to possible torching out of trees, spotting, and crowning. (1982, 12)



Figure 40: Anderson's photo of fuel model 9, "Western Oregon white oak fall litter; wind tumbled leaves may cause short-range spotting that may increase rate of spread above the predicted value." (Source: Anderson 1982)



Figure 41: The fall litter potential for this stand type in the study area is most likely less than that expected by Anderson for this fuel model. However, the dead herbaceous vegetation in the late summer and early fall would result in comparable fuel loads. (Source: Photo taken by Author)

The photos in Figures 35, 37, 39, and 41 were taken at sampling plots within the park. They may be visually compared to the photos in Figures 34, 36, 38, and 40, respectively, which are photos from Anderson’s 1982 paper that were taken to represent the standard fuel models he defined and described. The most visible difference is the quantity of ground cover found in the park photos, which has significant impact on the fuel loading of the custom fuel models. Table 8 compares Anderson’s standard fuel model loading figures with those derived for the custom fuel models.

Table 7: Comparing the fuel loading quantities between Anderson’s standard fuel models and the custom fuel model equivalents for the study area. Note the substantial difference in live vegetation quantities (the “Live Herbaceous” and “Live Woody” columns). Source: author and Anderson 1982).

Surface Fuel Model Fuel Loading Comparison						
Anderson's Fuel Models	1-hour (tonnes/ha)	10-hour (tonnes/ha)	100-hour (tonnes/ha)	Live Herbaceous (tonnes/ha)	Live Woody (tonnes/ha)	Fuel Bed Depth (cm)
8	3.36	2.24	5.60	0.00	0.00	6
9	6.55	0.92	0.34	0.00	0.00	6
10	1.66	2.80	8.00	0.00	0.00	30.5
Custom Fuel Models						
18	1.63	5.46	4.60	1.23	3.75	100
19	0.60	5.00	6.30	3.60	1.65	50
20	0.70	3.00	4.60	4.50	1.10	78

Fuel Map Development: Remote Sensing and Vegetation Index

The processed field data had to be translated into fuel themes for input into Farsite. In order to accomplish this, a fuel map representing the different fuel types for the entire park landscape had to be extrapolated from the sample data. Delineation of contiguous stands and variations in canopy was performed through a supervised

classification based on multi-spectral imagery. A relationship between the spectral response pattern (SRP) of each pixel from the classified image and the various fuel themes is the basis for propagating the fuel themes over the entire landscape. The field data sampling plots provide known fuel values at known locations and were used to train the classification process.

Only the visible red and near-infrared (NIR) bands were necessary for the analysis. Multiple spectral response classes were expected to be observed within each plot because of the variability within response pattern. In theory when SRP values are identified within a sampling plot, the plot's fuel type will be represented by the SRP values. Each pixel with a similar response pattern found within the plot area will be assigned the same fuel variable values across the entire multi-spectral image. However, the process is not that simple. Response pattern variability will cause the same SRP to be found in several plots of varying fuel types because of shadow and vegetative similarity. This dilemma is partially mitigated by applying a vegetation index to the data to better identify and differentiate the SRP of canopy types.

The weighted difference vegetation index (WDVI) was selected because of its ability to differentiate bare soil from vegetation, and because it exaggerates the differences between vegetation types (Figure 42). Traditionally WDVI uses Landsat TM red band (band 3 0.63-0.69 μm) and near-infrared (band 4 0.76-0.90 μm) data. Although TM data is not being used in this analysis, the CIR data bandwidth is almost identical. The WDVI is calculated as $\text{WDVI} = \text{NIR} - g * \text{red}$, where g is the slope of the soil line (Clevers 1988). Additional technical aspects of the multi-spectral data and the WDVI transformation are discussed in Appendix C.

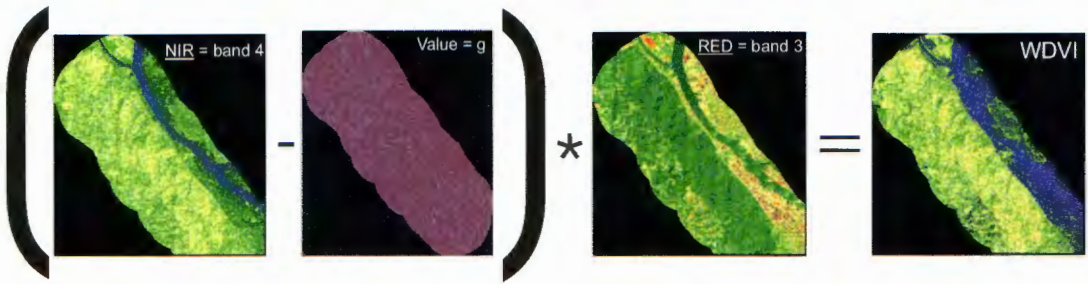


Figure 42: NIR and Red bands were extracted from the CIR image and a new raster with a soil line slope value was created to derive the WDVI surface. Illustration by author.

Fuel Map Accuracy Assessment

The goal of the multi-spectral analysis is to identify fuel model variations over the entire study area. This process will result in fuel data at a much finer spatial resolution and greater accuracy than the FP NVCS dataset. However, fire simulations using fuel themes developed from remotely sensed data have been most successful for grasslands and shrubland, with only limited success for assessing surface fuels in forested areas (Friedl, et al. 1994). To increase the likelihood of fuel assessment accuracy the multi-spectral imagery was enhanced to emphasize vegetation differences using the WDVI model. The in-situ sampling provides a priori knowledge of the area. The use of the sampling data further mitigates the limitations of relying solely on remotely sensed data.

The process of classifying the WDVI output was based on a combination of image sampling, a priori knowledge of the vegetation stratum in the park, and definitions of standard fuel model environments. About 75 sampling locations, including the locations of all the sampling plots were selected throughout the image to determine the spectral response pattern thresholds of the canopy vegetation types.

After the thresholds were identified for the canopy, classes were assigned to the image using Anderson's (1982) fuel model descriptions as guidelines. This process was the basis for the standard surface fuel model map, which served as the base fuel map for all other fuel-related themes.

The most difficult areas to class were found in deep ravines where upslope trees cast shadows down slope. The areas in shadow had similar SRP to the urban landscape class. The index range for the urban class was from 1 to 25. The index thresholds for the mixed conifer class were 26 to 56. The mixed conifer and hardwood class range was from 57 to 91. The index values for mixed deciduous class were 92 to 138. Index values above 138 were considered scrub and brush. However, no contiguous areas had an index value above 138, only pockets of a few cells scattered over areas that consisted of shrub and regenerative growth.

While the other classes performed well, the shrub class was consistently classified incorrectly. Areas such as utility corridors with woody shrub regeneration or previously harvested clearcuts had to be reclassified based on ground truth. The accuracy of the classification was reviewed using georectified 1 foot natural color imagery overlaid on the WDV (Figure 43). An error matrix was developed to assess the accuracy of the WDV classification (Table 9).

Table 8: Accuracy assessment of the WDVl classification of study area (Source: Author.)

WDVI Error Matrix	<i>Training Set Data (known cover types)</i>					<i>Row total</i>
	99	10	8	9	5	
Classification Data						
Urban/non-fuel (fuel models 99,98,0)	46	0	1	1	0	48
Mixed coniferous (fuel model 10)	7	40	3	5	1	56
Mixed conifer and hardwood (fuel model 8)	5	5	36	17	13	76
Mixed hardwood (fuel model 9)	2	1	7	58	1	69
Shrub and regeneration (fuel model 5)	0	0	0	1	2	3
<i>Column total</i>	60	46	47	82	17	252

Producer's Accuracy		User's Accuracy	
99	77%	99	96%
10	87%	10	71%
8	77%	8	47%
9	71%	9	84%
5	12%	5	67%

Overall Accuracy	72%
-------------------------	------------

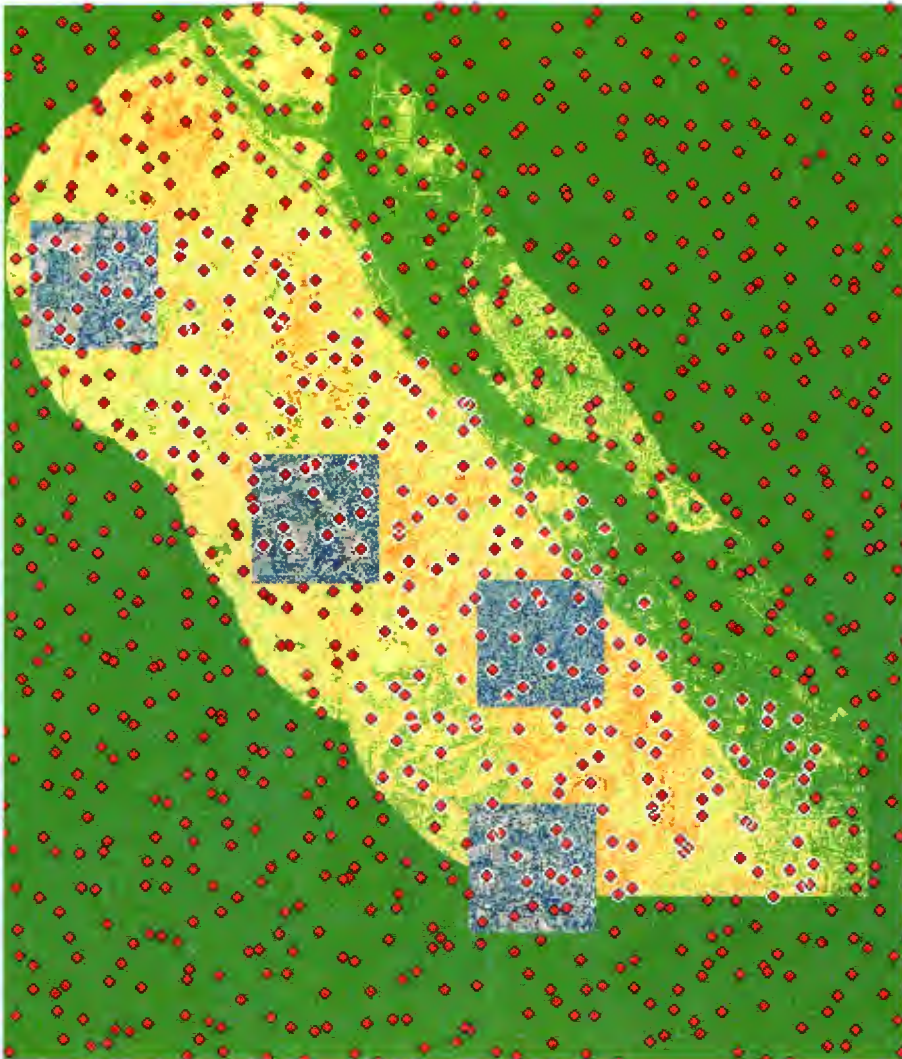


Figure 43: 1,000 points were randomly generated over the WDV image. High-resolution natural-color imagery was georectified by township and range section with the WDV image. 252 points fell within the high-resolution imagery, WDV, and areas of interest for the fire simulation. The points used for the accuracy assessment have white halos around them. (Source data from: City of Portland, Spencer B. Gross, Inc.; illustration of sampling by author)

Spatial Alignment of All Inputs

The final steps for developing the farsite inputs require that the base fuel map be resampled and reclassified. The base fuel map had a spatial resolution of 1.1 meters and represents the standard surface fuel theme based on Anderson's (1982) fuel definitions. The resolution for the simulation inputs is 10 meters and based on the DEM resolution. A 10 meter fishnet grid was developed from the DEM. A gridpoly command was then used to change the vector fishnet into a 10 meter polygon grid. The polygon grid was used as a resampling mask over the fuel map. A majority rule was applied to the 1.1 meter fuel map: whichever fuel model represented the majority of cells inside the 10 meter mask, then that fuel model was assigned to the 10 meter output (Figure 44).

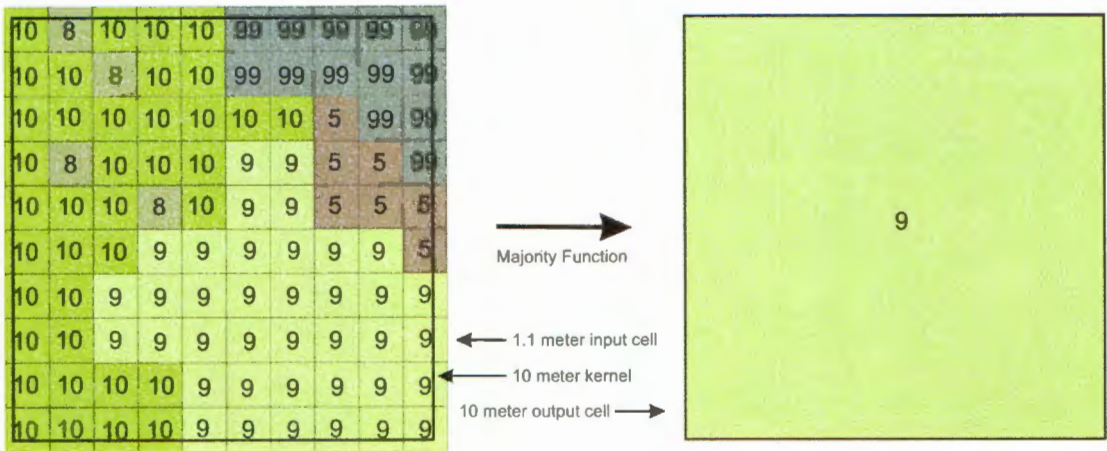


Figure 44: The majority rule processing of the 1.1 meter original fuel map to the resampled 10 meter Farsite input. For the majority kernel to include the cell value in the majority calculation the cell center must be within the 10 meter kernel. The cells must also be contiguous about the center of the filter kernel. For example, there are 38 cells with a value of ten and 38 cells with a value of nine. In the case of a tie the majority rule will apply the last value calculated that created the tie. In the case above the majority kernel started the cell count in the upper left corner, the last value input was the nine in the lower right corner. Therefore, the nine was the last value calculated and nine was applied to the 10 meter output cell. (Source: illustration by Author)

The new 10 meter fuel map is then used as the basis for the fuel theme reclassification process (Figure 45). The resampling process ensures that all the raster themes are spatially identical. Once the raster themes have been developed they are converted to the American Standard Code for Information Interchange (ASCII) format. All spatial inputs for Farsite require a space delimited ASCII format.

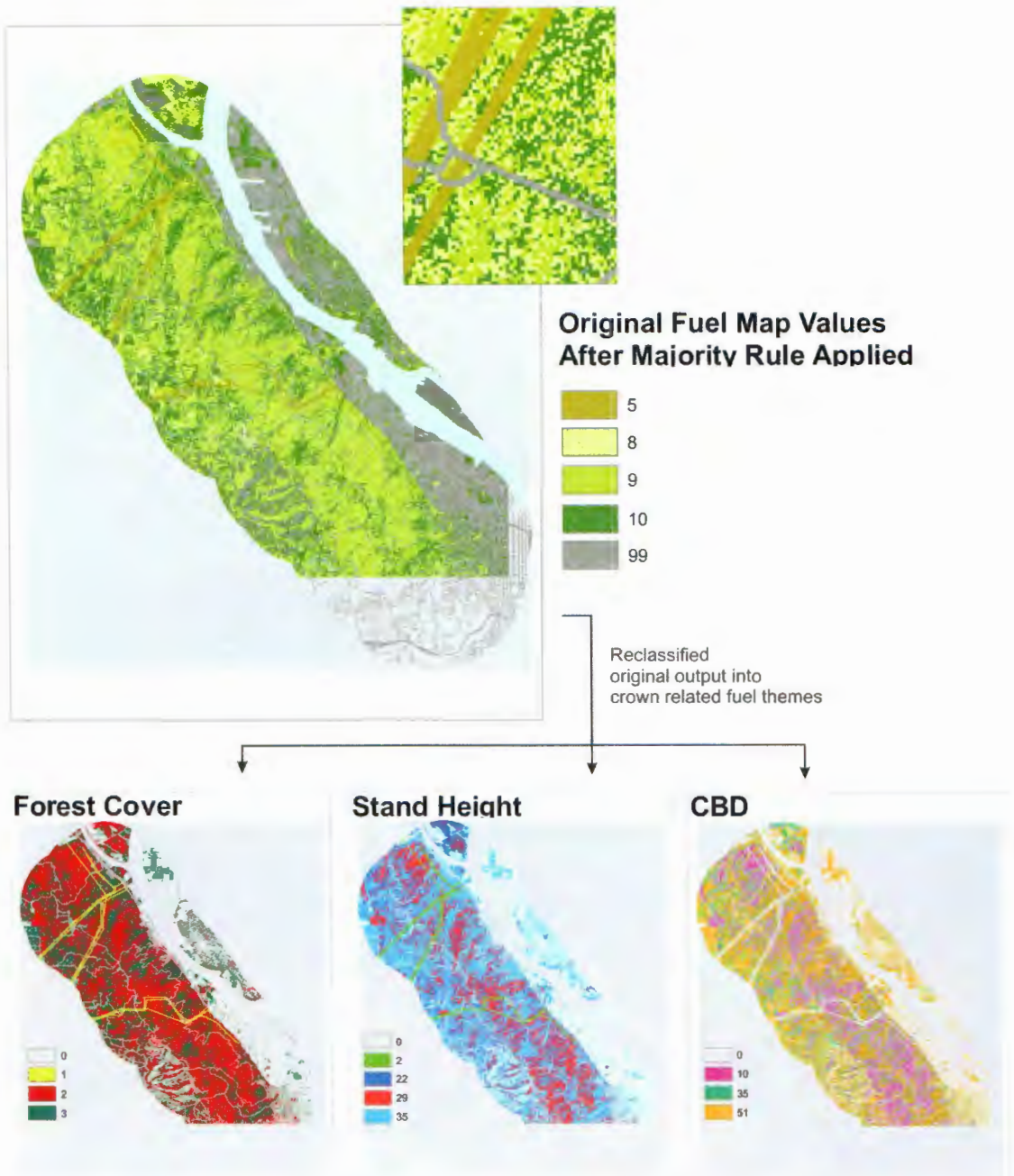


Figure 45: The output of the majority rule function applied to the classified WDVI image was used as the base fuel layer for all other fuel inputs. The raster was reclassified to create the subsequent fuel layers. For example the primary crown fuel inputs developed from the original fuel map are above. (Base map source: City of Portland, Metro RLIS, fuel themes from Author using ArcGIS)

Farsite Input Preparation and Simulation Ignition.

There are a few subjectively chosen parameters not derived from field data required for the model to run successfully. The first of these are the time step and distance parameters. For this study the time step was 15 minutes, with visible time steps set at 30 minutes. That means that each calculation result represented 15 minutes of burn time before the model acquired new inputs from the point at which the fire spread during the last time interval. Then after 30 minutes the fire behavior variables, such as the time of arrival or rate of spread are recorded permanently. The distance parameters were set to ten meters to mimic the input layer spatial resolution. By setting the maximum distance between vertices to ten meters, the simulation guaranteed that a new vertex would be inserted within a single fuel cell.

Some of the subjectively chosen settings affect fire behavior calculations. These settings include all the crown fire parameters that enable ladder fuel ignition and crown fire. Crown fire and spot fire were enabled for these simulations. When crown fire is initiated the calculation includes the lofting of embers from torching trees. With spot fire growth enabled a spotting ignition frequency and possible ignition delay must be specified. The spot fire ignition frequency for these simulations was set to 7% with an ignition delay of 5 minutes. Embers that land on consumable fuel would only ignite that fuel 7% of the time. The ignition delay further reduces the likelihood of ignition because it provides a timelag for immediate fuel heating. These values are within recommended thresholds given the initial fuel moisture conditions expected at the time of ignition (Finney 2004).

The last subjective parameters set the fire duration or length of the simulation. Since the simulations were based on the 1951 fires, the ignition time was set for 5:00 p.m. on August 17th. The simulation was allowed to run unencumbered until 12:00 a.m. August 22nd, the same amount of time that it took to bring the 1951 fire under control. The fuel conditioning period is also set with these controls. The fuel conditioning period uses the maximum and minimum daily temperatures and relative humidity to calculate daily fuel moisture fluctuation leading up to the fire.

The last item to be selected before the simulation begins is the ignition point or points. The point of ignition in 1951 was known, in fact the fire had actually been smoldering for some time before it began to spread outside of this immediate area. Therefore, a series of points was selected for ignition, instead of a single point, which would occur in the case of a lightning caused ignition. Once the ignition points were selected they were saved and reused for each subsequent simulation. After the ignition points are selected the simulation can be run with a touch of a button.

Summary

In this chapter we reviewed the origins of fire modeling and the development of fire behavior simulation applications. We narrowed the discussion to Farsite, the modeling application used in this study. We focused on the process of developing the data necessary for running a fire simulation model using Farsite. The process requires field work that is both quantitative and qualitative in nature. The field work enabled me to observe the different stand types first hand. Being in the park helped me visualize the transition between stands and see the terrain that a fire would have to

traverse. Selecting the sampling plots established permanent locations that can be revisited to quantify the fuel loads of the stand types they represent. The field data was a precursor to the lab work. In the lab the landscape could be broken down into individual themes and data layers. Using remote sensing techniques the fuel data collected and observed in the field could be propagated across the entire landscape. With landscape-wide data layers the fire simulation model is assembled in Farsite. Once the Farsite inputs are set fire simulations can be ignited and run from any point in the park.

CHAPTER 6: MODEL RESULTS

This chapter examines the results of the two fire simulations. We review the differences and similarities, and both the custom and standard models are compared in area and predicted destruction to the actual 1951 fire.

The Fire Model Results for Forest Park

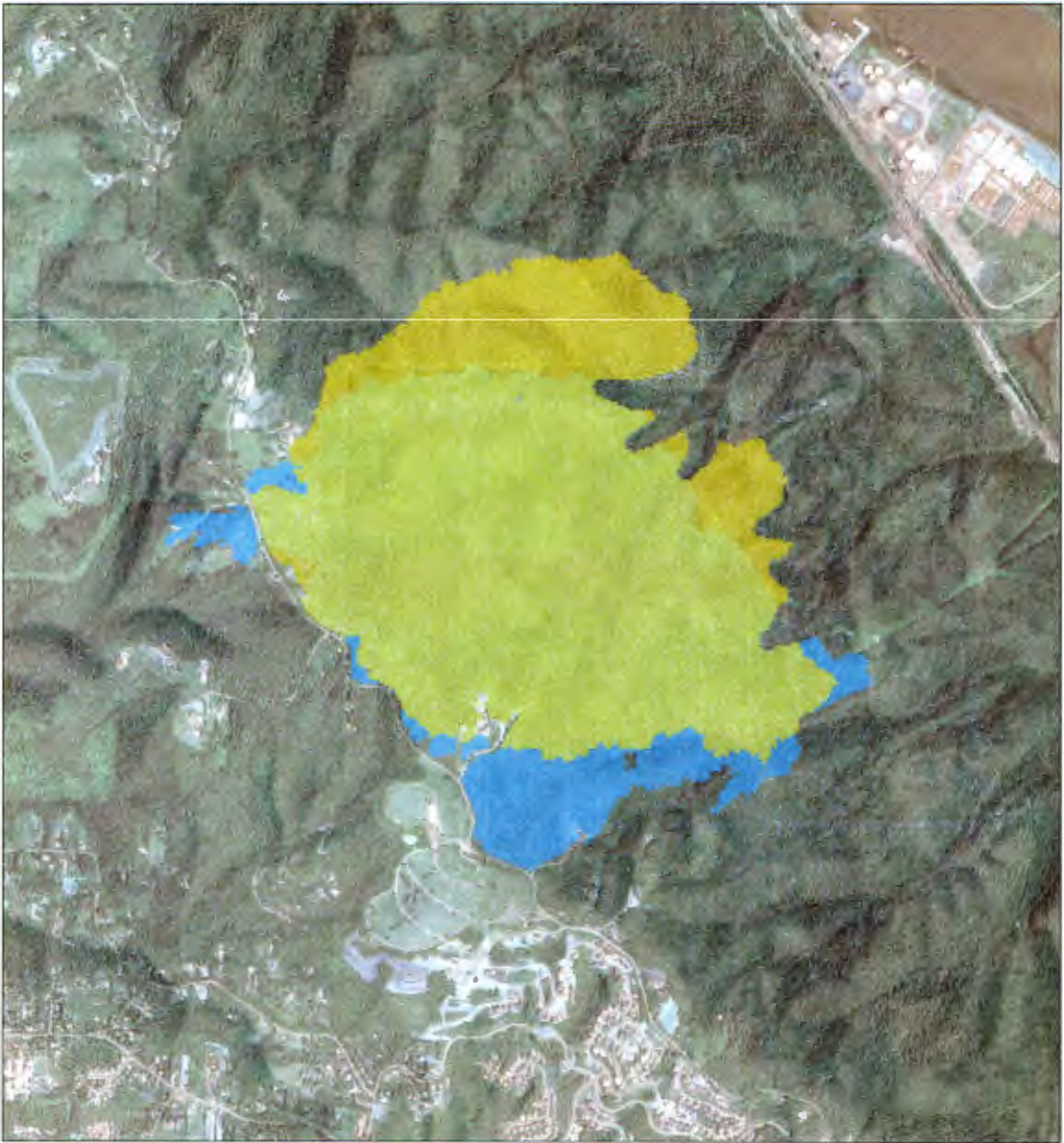
Two fire simulations were run through Farsite. Both simulations had exactly the same weather, topography, crown fuel inputs, fire behavior settings, temporal and distance parameters, and ignition points. The only difference between the initial states of the simulation models was the surface fuel inputs. The first simulation (standard simulation) used standard surface fuel model values based on standard fuel models developed by the USFS specific to the Pacific Northwest region. The second (custom simulation) used custom surface fuel model values based on in situ field work specific to Forest Park.

Each simulation took approximately two days to run on 1.53 GHz computer with 1 GB of RAM. The duration of each simulation was not typical. However, the typical spatial resolution of Farsite inputs is 30 or 50 meters. The spatial resolution of the inputs for this study was 10 meters - that's nine times the spatial information density of a 30 meter simulation, and 25-times the density of a 50 meter simulation. From a data processing perspective the duration of each simulation is understandable.

The simulation results were compared using 4 measures: rate of spread, fire and heat intensity, flame length, and final extent. Each category of comparison provides a perspective on the general behavior of the fire, as well as points in the fire's

lifecycle that would be considered most threatening. These threat points can be analyzed further to determine what combination of factors make those specific locations more dangerous than others. Once the threat points are understood, then appropriate management techniques or mitigation strategies can be adopted to deal with the specific sites.

The rate of spread is the simplest way to interpret a fire. A fire with a high rate of spread that consumes fuel and area quickly is a greater threat than a slower moving fire. While the custom simulation, by comparison, was the more threatening fire. The standard simulation demonstrated a slow-moving surface burn. However, the custom simulation rarely exhibited fire lines that were sustained, unified, and quick moving. In fact the time of arrival for both simulations was similar during the first 48 hours, with the standard simulation consuming 584 acres and the custom simulation covering 568 acres (Figure 46).



0 0.25 0.5 Miles

Figure 46: The yellow shaded area represents the burned extent after 48 hours of the standard simulation. The blue shaded area is the burned extent of the custom simulation over the same time period. The greenish shade is burnt area shared by both simulations within the first 48 hours of the simulation runs. (Base map source: City of Portland, USGS, fire data from Author using Farsite)

The custom simulation was a larger and potentially more destructive fire than the standard simulation. A comparison of the time of arrival output from the simulations paints a story of two completely different fires (Figures 47 and 48). This is most likely attributable to fuel loads. The custom simulation had fuel models that simply had more fuel. However, when comparing the rate of spread of each simulation, the fires seem to have similar behavior (Figures 49 and 50). The rate of spread similarities can again be contributed to the fuel loads. Even though the custom simulation fuel models had greater fuel quantities, a large percentage of that fuel was live. Live fuels will burn, but will not burn as readily and as intensely as dead fuel. When fire burns through live fuel loads a lot of energy is consumed in heating and drying the fuels to reach the point of combustion. This is why the custom simulation has select areas of higher rates of spread, but not a greater sustained rate of spread throughout its extent.

It is also worth noting in Figure 48 the absence of fire spread in areas occupied by houses. This may or may not be a realistic representation of where the fire would have spread in a real burn scenario. However, for these simulations it was impossible for fire to spread or ignite in an area occupied by a structure because all structures and developed areas, such as roads, were assigned non-fuel status. When reviewing the fire intensity output from the custom simulation, which is the only simulation that spread into residential areas, there were only a few locations where the fire grew intense enough to ignite a house from radiative heating. However, many embers were lofted from the main fire into residential areas through out the simulation, and many spot fires were ignited from these embers, but if those embers landed on structures it

was impossible for a spot fire to develop. This illustrates a significant shortcoming in the utility of Farsite to simulate fires in a wildland-urban interface environment. This point is discussed further in the next chapter.

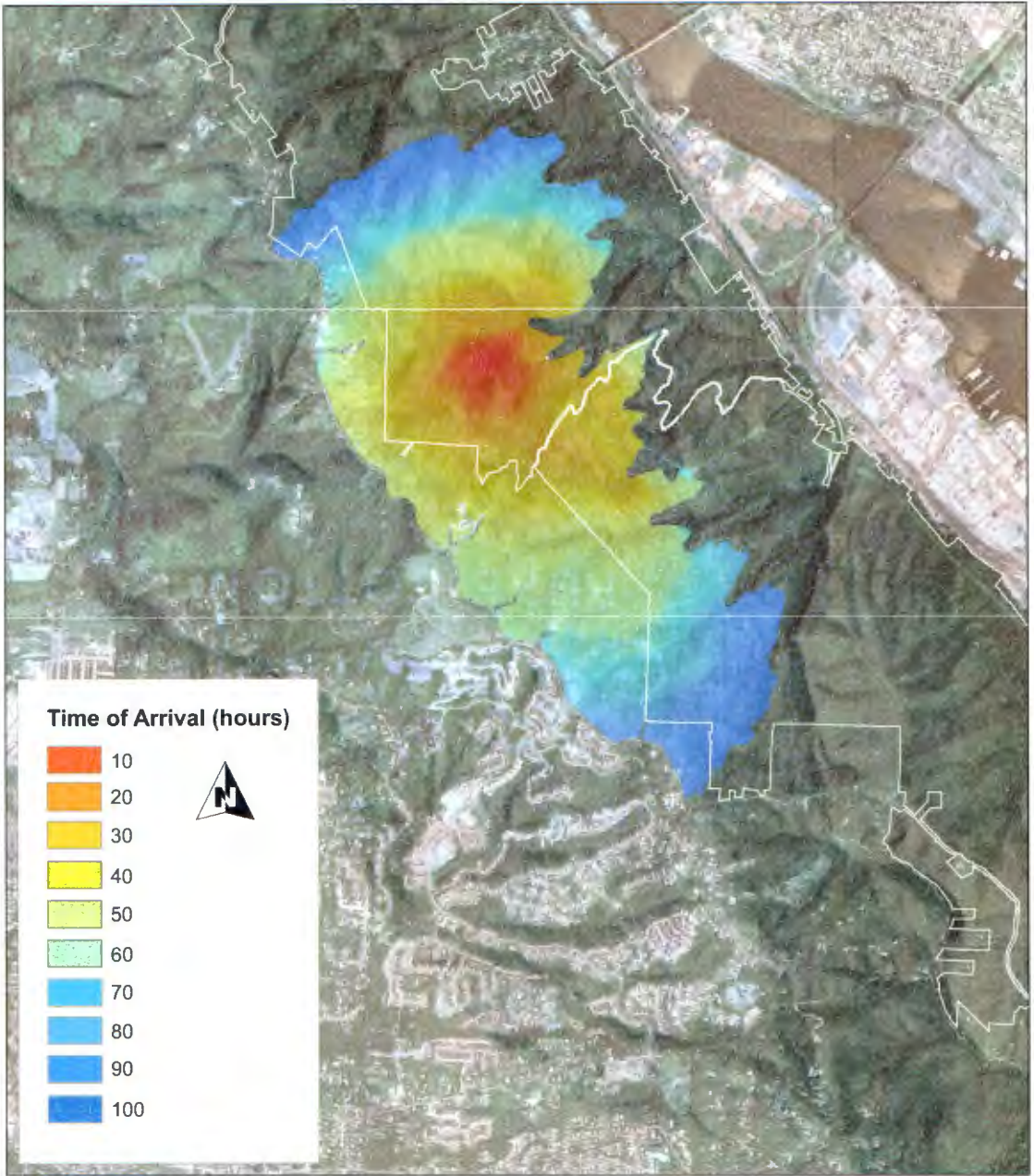


Figure 47: Time of arrival spread of the standard simulation. The white line is the park boundary. The fire spread in a consistent manner through out the simulation. This kind of spread pattern was not expected given the topography or weather inputs. (Base map source: City of Portland, USGS, fire data from Author using Farsite)

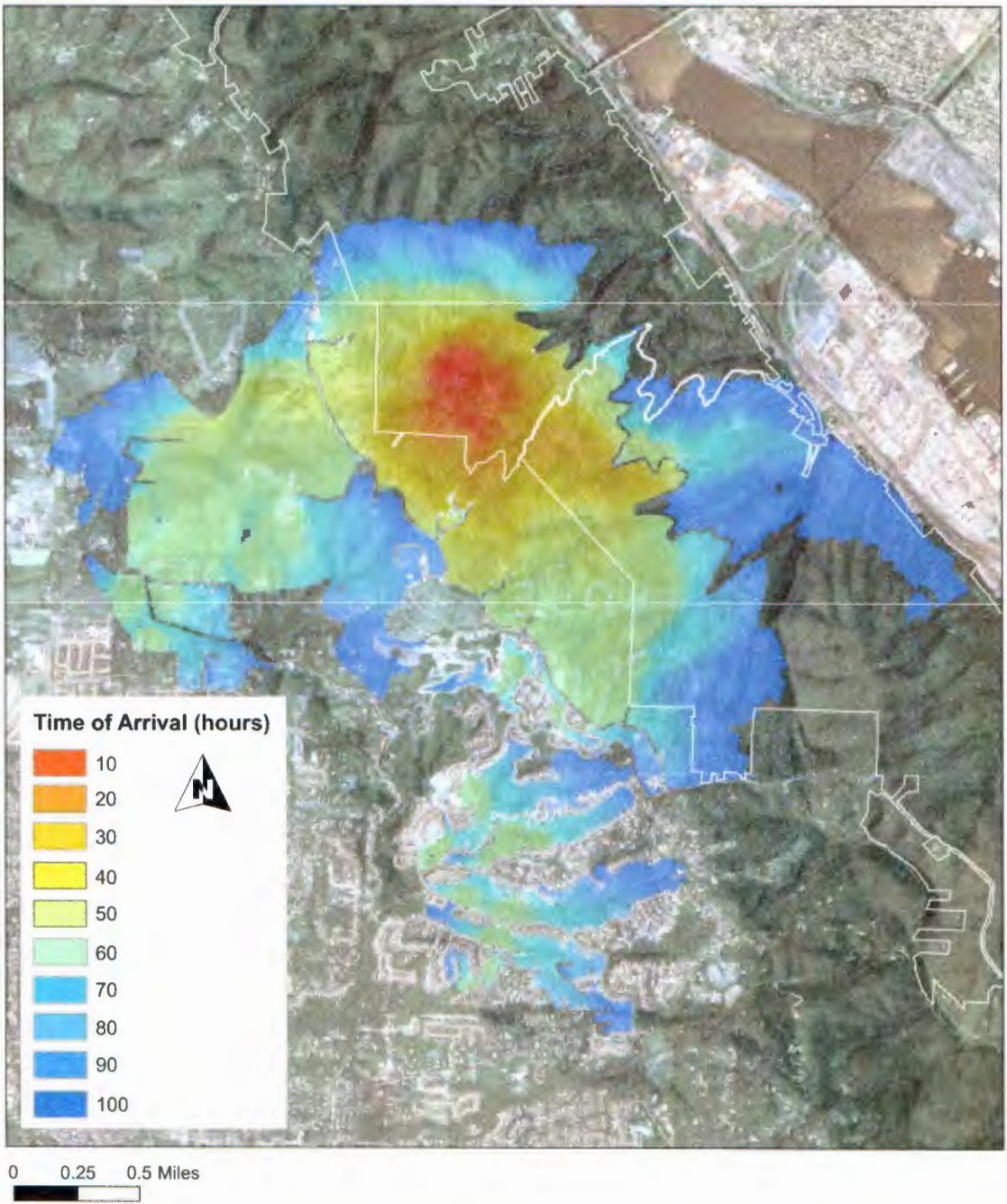


Figure 48: Time of arrival spread of the custom simulation. The white line is the park boundary. This pattern of spread is more consistent with the expected fire behavior given the topography and weather inputs. (Base map source: City of Portland, USGS, fire data from Author using Farsite)

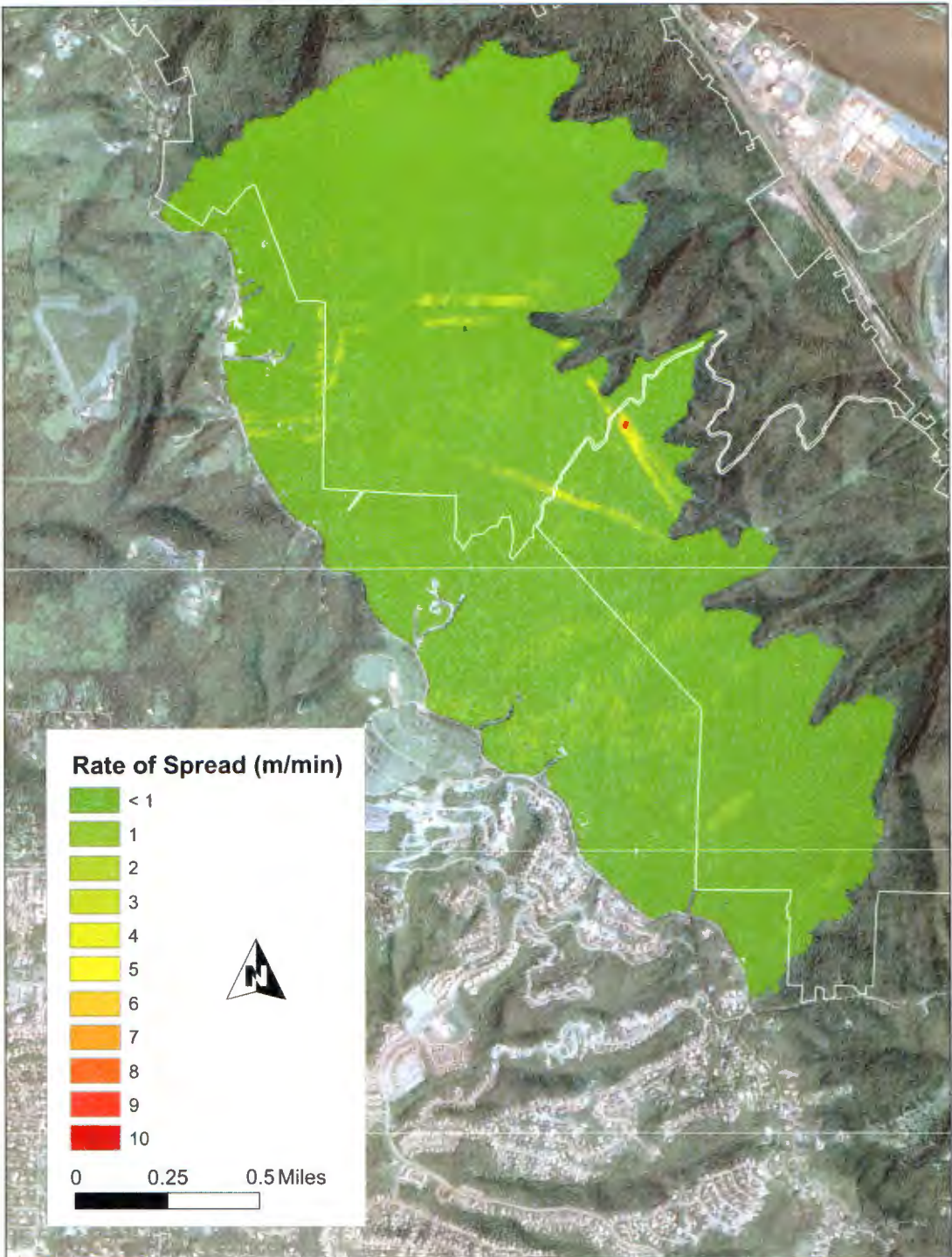


Figure 49: Rate of spread across the entire standard simulation extent. The white line is the park boundary. This image demonstrates the relatively slow advance of the fire. The areas with the highest rates of spread coincide with the utility corridors. The fuels in the corridors were among the most flammable. Excess slash and regenerative brush and shrubs (e.g. Scotch broom) occupy many corridors because of the clearing that is completed by the utility line owners. (Base map source: City of Portland, USGS, fire data from Author using Farsite)

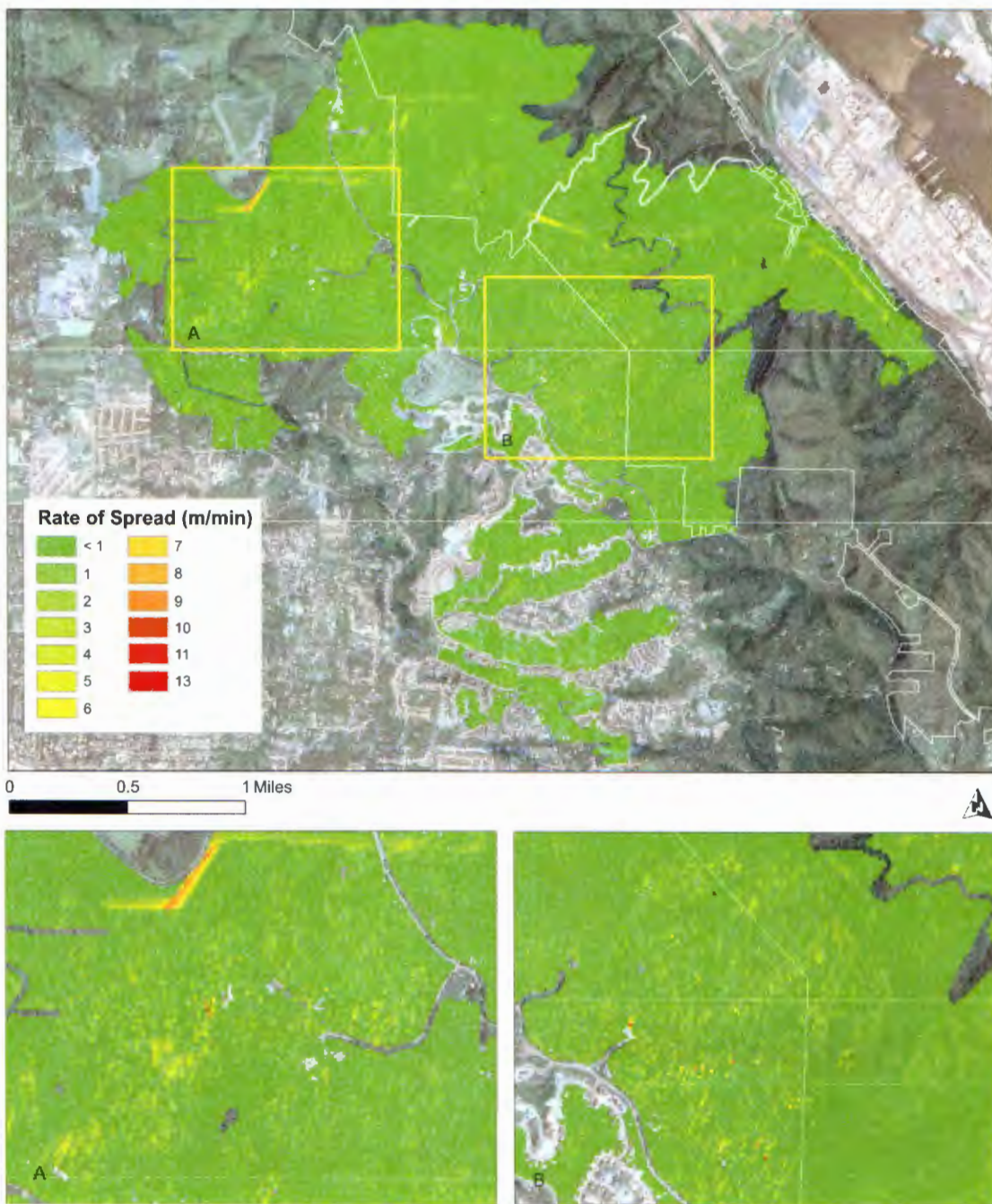


Figure 50: Rate of spread calculated for the custom simulation. The white lines are the park boundary. As in the standard simulation results the utility corridors experienced some of the highest rates of spread. Inset images A and B are areas of interest because they demonstrate increased rate of spread due to a combination of topographic features and weather inputs. Inset A also demonstrates the increased rate of spread found in the utility corridor fuels. (Base map source: City of Portland, USGS, fire data from Author using Farsite)

Two significant measures of fire intensity are the fire line intensity (FLI) and the heat produced per unit area (HPA). FLI is measured in kilowatts per meter, and HPA is measured in Kilojoules per square meter. Fire intensity is measured by two factors: the rate of spread, calculated by the number of meters burned per minute, and energy flux, the amount of kilowatts a fire generates per meter burned.

The simulations had completely different results in these categories by an order of magnitude. The custom simulation produced FLI and HPA that topped out at 71,804 kW/m and 727,683 kJ/m², respectively (Figures 51 and 52). The highest values in the standard simulation were 912 kW/m and 15,404 kJ/m². However, there are varying values suggested for the threshold intensity for an uncontrolled fire. Chapman (1999) suggests 4000 kilowatts per meter, while Hessel, Rideout and Omi (1998) suggest 1730. Regardless of which value is used, the standard simulation never reached the intensity threshold of an uncontrollable fire, while the custom simulation easily exceeded the threshold in multiple areas.



0 0.5 1 Miles

Fire Line Intensity (kw/m)
 1,730 - 71,804

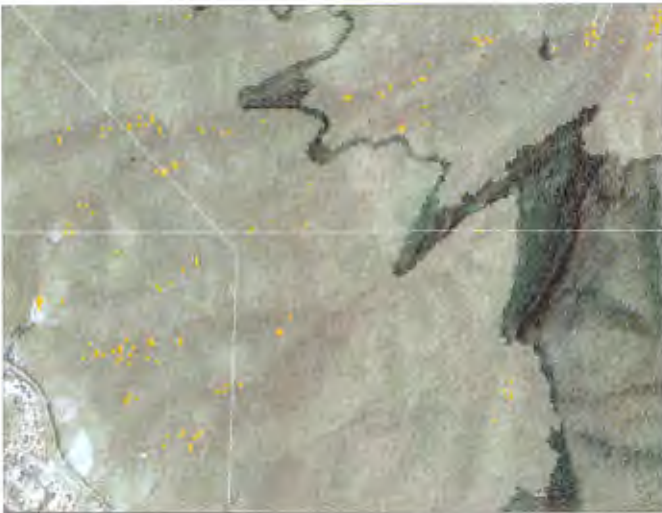


Figure 51: Fire line intensity of the custom simulation. The white line is the park boundary. The white transparent shaded area represents the final extent of the custom simulation. Substantial energy release can be seen along the utility corridors. The map inset is an enlargement of an area that experienced some of the highest energy release. The highest intensity was typically observed on Northern facing slopes and near the tops of ridges. (Base map source: City of Portland, USGS, fire data from Author using Farsite)



0 0.5 1 Miles



Heat Per Area (kJ/m²)

- 15,400 - 125,000
- 125,000 - 225,000
- 225,000 - 370,000
- 370,000 - 727,683

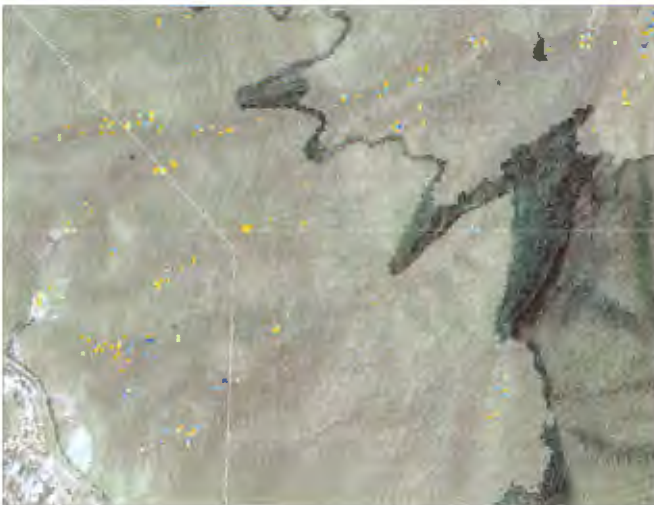


Figure 52: Heat per area of the custom simulation. The white line is the park boundary. The same areas that exhibited the highest fire line intensity in Figure 42 also produced the greatest heat. It would be safe to conclude that the fire in these areas would be uncontrollable from the ground. (Base map source: City of Portland, USGS, fire data from Author using Farsite)

To put these values in better perspective a typical gas burner on your stovetop turned to high is producing 23,000 kJ. Firewood heat output is measured in kJ per kilogram; an average for cured wood at 15% saturation is 15,400 kJ/Kg. The heat produced throughout the most of the extent of the standard simulation was intense enough to evaporate about a half gallon of water instantly. On the other hand the heat produced in a few areas of the custom simulation was intense enough to evaporate 85 gallons of water instantly. The impact of this can be understood if we note that a typical fire hose will deliver about 20 gallons per minute. However, the majority of the standard simulation experienced fire line intensities and heat production similar to or less than, that observed throughout the custom simulation. This level of heat and intensity would lead to a controllable surface fire.

At first the fire intensity and heat values observed in the custom simulation seemed like a mistake, but based on the fuel loading differences between simulations the energy release is plausible. Logically, more fuel increases the likelihood of combustion. More combustion increases flame length and fire intensity, and subsequent consumption of larger surface fuels and ladder fuels. As the flame length continues to increase, more fuel becomes available as the fire reaches into the understory fuels and begins the laddering process. The cycle reinforces itself and grows at an increasing rate, as long as the same or heavier fuel load is available ahead of the fire line.

Flame length plays a pivotal role in determining if a fire will ladder into the crown and torch small stands of trees. Flame length is a good indicator of risk of conflagration. Anderson provided a risk ranking based on his standard fuel models.

For standard fuel models 8 and 9 flame lengths of less than 2 feet (0.6 meters) were considered to have low risk of conflagration in standard weather. Standard weather is considered a 5 mph mid-flame height wind, 8% dead fuel moisture, and 100% live fuel moisture. In contrast for standard fuel model 10, a flame length greater than 4.5 feet (1.5 meters) was considered high risk. The simulation's dead fuel moisture was considerably less than 8%, more in the range of 5-6%. The mid-flame height wind was at or below 5 mph throughout most of the simulations run. Live fuel moisture was considered to be 100% across all the simulations fuels. The risk is elevated across all fuel models for the simulations because of the dead fuel moisture difference.

The difference in calculated flame lengths between the simulations was extreme. The flame length across the majority of the standard simulation was less than 1 meter and never exceeded 3 meters (Figure 53). The custom simulation had flame lengths that reached 46 meters, which means that crown fires were burning in those areas (Figure 54).



Figure 53: The flame length of the standard simulation. Most flame lengths calculated for the standard simulation represent a low risk fire. Any area not colored experienced flame lengths less than 0.6 meters. Increased flame length is observed in the utility corridors. The standard simulation exhibits increased fire behavior on the north facing slopes due to the prevailing wind direction. (Base map source: City of Portland, USGS, fire data from Author using Farsite)

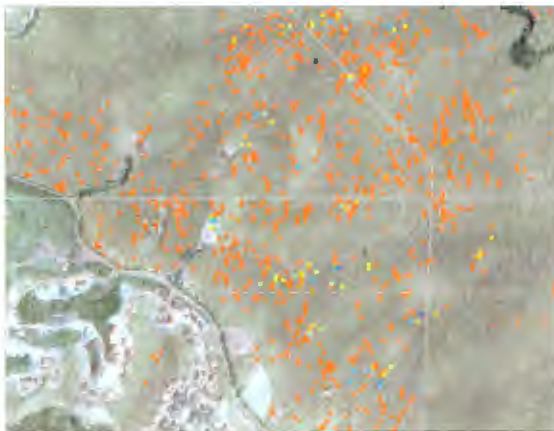
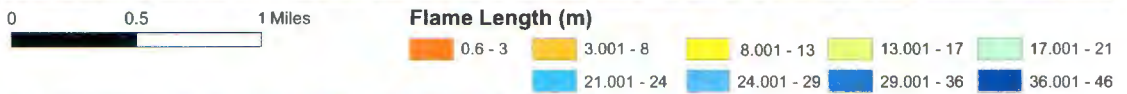


Figure 54: Flame lengths of the custom simulation. Flame lengths tended to be longer in areas with increased fire activity in the custom simulation compared to the standard simulation. The inset map shows an area where flames would have been greater than 6 feet tall at many places along the advancing fire line. (Base map source: City of Portland, USGS, fire data from Author using Farsite)

Many of the figures from the custom simulation have inset maps from a series of chutes near the ridge top. In the case of the custom simulation, this specific location was the location of the fire when the most intense winds and gusts occurred. Most of the extreme fire behavior from the simulations occurred in this environment. The simulated fire became more active and intense as it moved up the northeastern slopes and reached the tops of the chute ridges. This happened for two reasons. First, the north-northeast facing slopes were perpendicular to the oncoming wind. Second, the fuel on those slopes was primarily mixed conifer, which had greater fuel loads and lower crown base heights (Figure 55).

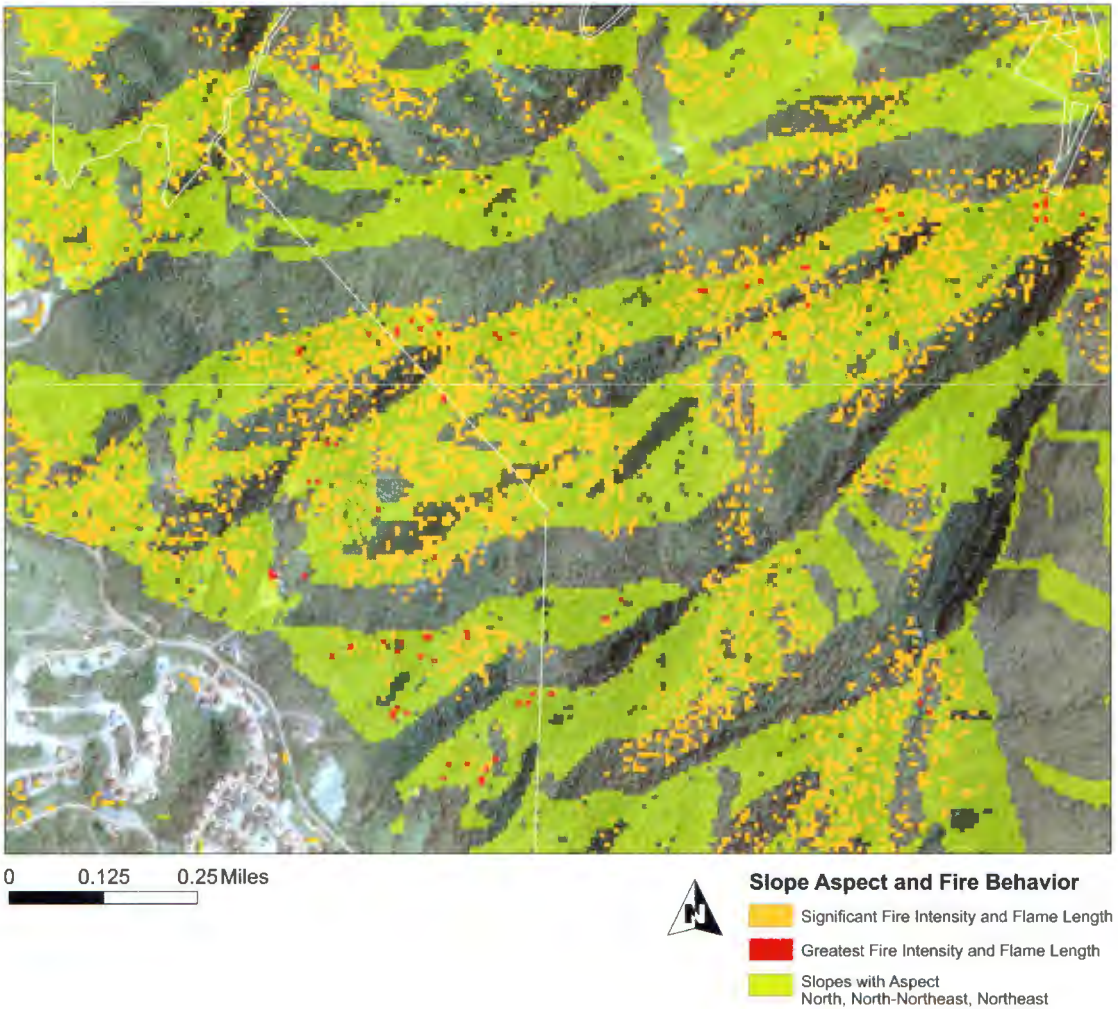


Figure 55: There is high correlation between elevated fire intensity and flame lengths that would increase the fires rate of spread and laddering probability on slopes with northeastern aspects. (Base map source: City of Portland, USGS, fire data from Author using Farsite)

Simulation Results Compared to the 1951 Fire

The simulations were allowed to run the same duration as that of the 1951 fire before they were brought under control. The 1951 fire was allowed to burn for almost three days before city resources were brought in against the advancing flames. The fire was brought under control within two days. For most of the time the fire was a slow moving surface fire. Keep in mind that a major portion of the 1951 fire overburned an area that had burned only 11 years earlier. In these areas the fire was

burning through primarily grasses and shrubs, as no trees had had time to grow back into stands. However, the areas that experienced the most significant rate of spread and intensity were heavily timbered, and caused spot fire outbreaks (Morris 1953). Figure 25 (Chapter 4) details the spread of the fire as described by Morris.

The final extents of the simulations were vastly different from one another. However, when compared to the extent of the 1951 fire, the custom simulation was closer in total area and area overlap (Figures 56 and 57). For example, during the 1951 fire when winds picked up to gusts of 40 mph, the fire spotted to the western slopes and crested the top of the ridge. The custom simulation did the same when the simulation reached that point in the weather stream. A comparison of fire behavior between the simulations and the 1951 fire reveal a closer association between the custom simulation and the actual event in acres burned (Table 9).

Table 9: A comparison of fire behavior parameters between the standard and custom simulation results and the reconstructed 1951 fire. The rate of spread for all fires was similar. However, the fire intensity and flame length calculations were dramatically different between the standard and custom simulations. The 1951 fire was 55% larger than the standard simulation result, but was only 84% of the total area consumed by the custom simulation. Source: Morris 1953, simulation data by author.

Fire Behavior Comparison				
Fire	Maximum Rate of Spread (m/min)	Maximum Fire Intensity (kw/m)	Maximum Flame Length (m)	Final Extent (acres)
1951	10	N/A	N/A	2268
Standard	10	912	2	1459
Custom	13	71,800	46	2693

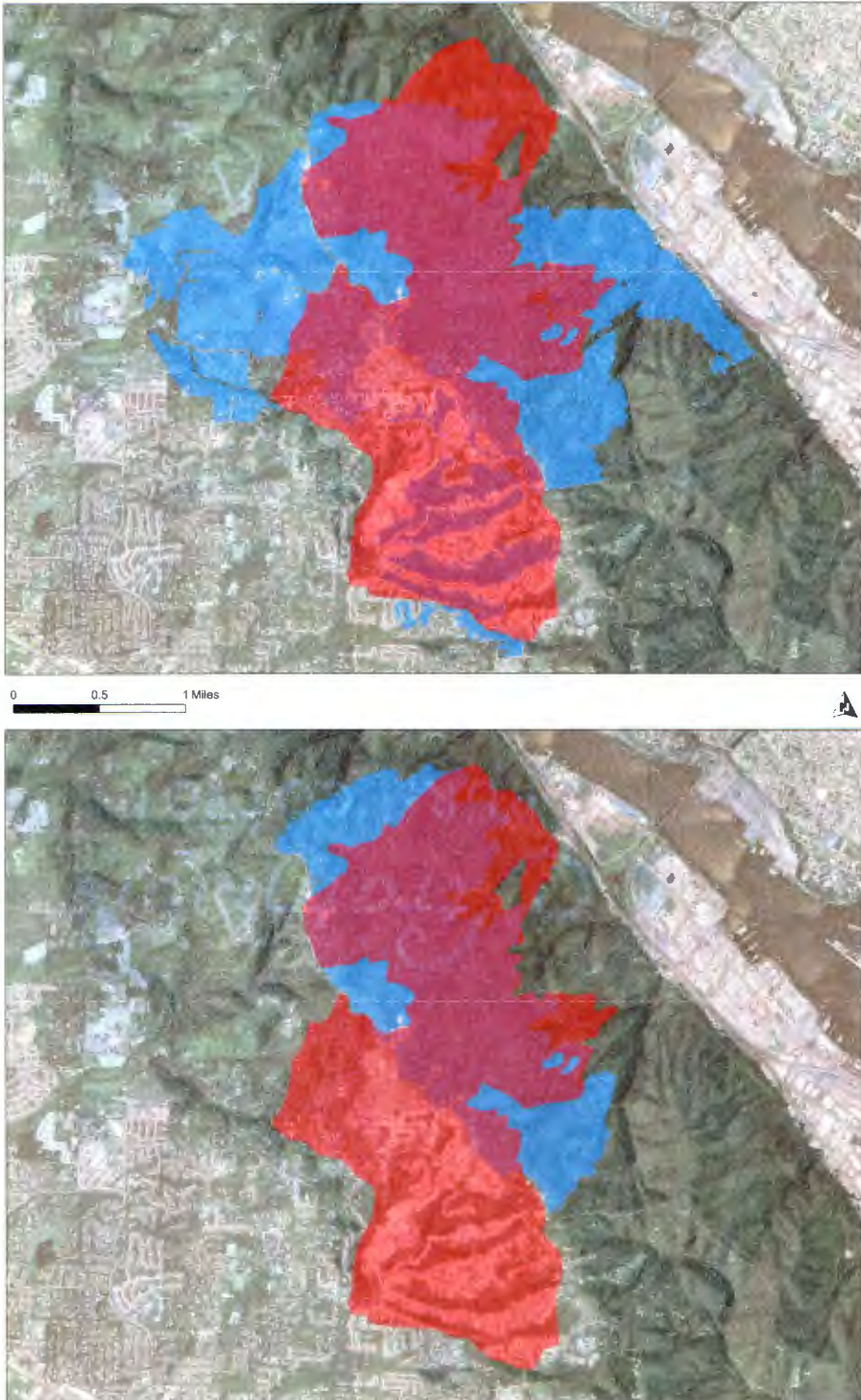


Figure 56: The red shaded area represents the reconstructed 1951 fire boundary. Blue shaded areas represent the simulation extents. The purple shaded areas represent areas that both simulated fires and the 1951 fire burned. The top image represents the 1951 and custom simulation. The bottom image represents the 1951 and standard simulation. (Base map source: City of Portland, USGS, fire data from Author using Farsite)

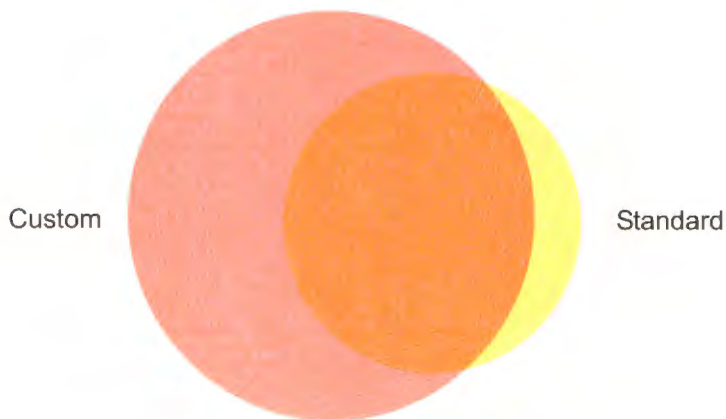
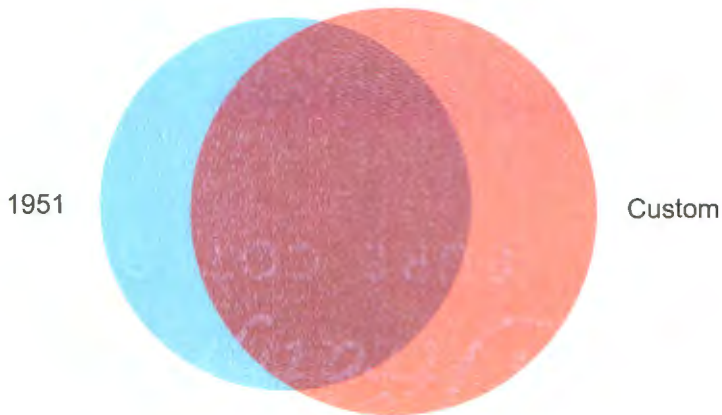


Figure 57: The circles represent the total area burned during the fires represented. The overlapping portions of the circles represent the area that both fires consumed. Even though the greatest proportion of overlap seems to be between the custom and standard simulation, the relative size difference of the fires masks the truth. The 1951 and custom simulation have the most accurate overlap. Illustration by author.

The primary reasons the 1951 and the custom simulation share similar extents were that significant spotting occurred in the custom simulation. The spotting and subsequent fires get to the heart of the difference between the simulations. The custom simulation had the right fuel load in the exact location during the time that the weather was most conducive to rapid fire spread and torching trees. This occurred at a point where the fire had reached the top of the ridge and entered into a primarily coniferous dominated area. For the next several hours the wind shifted from a Northerly flow to a Northeasterly direction and reached speeds of up to 40 mph (Figure 58). During that time the standard simulation advanced consuming 111 acres, but did not spot (Figure 59). Until the wind shifted back to the north, the custom simulation consumed 352 acres in four hours and started over 20 spot fires.



Figure 58: The images show a four hour sequence (hours 57 to 60) in the fire spread of the custom simulation. No spotting has occurred in hour 57. In hour 58 the first few spot fire have ignited and started to spread. In hours 59 and 60 the spot fires continue to grow and some of them backfire into the main fire. (Base map source: City of Portland, USGS, fire data from Author using Farsite)

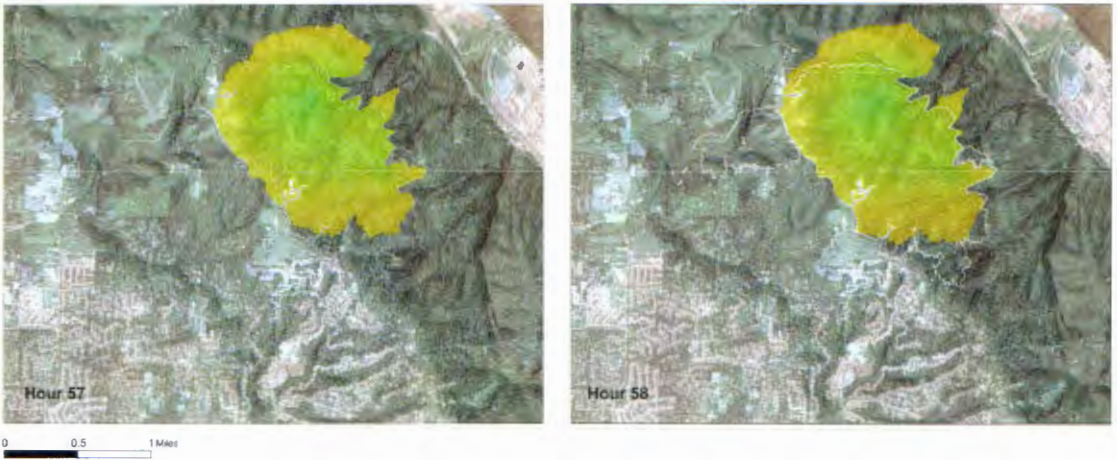


Figure 59: These images from the Standard simulation represent hours 57 and 58, no spotting occurs and the fire does not take on a new dimension as it does at this point in the custom simulation. (Base map: City of Portland, USGS, fire data from Author using Farsite)

For the purpose of comparing time of arrival rates of the 1951 fire and the simulation results a time of arrival probability map was developed for the 1951 fire. The probability map was based on Morris' descriptions of the fire, which included the time and location of his observations. Points were placed across the reconstructed 1951 fire extent; each point was given a time of arrival value based on Morris' report. The points were then used as the inputs to develop a semivariogram. A semivariogram is a mathematical form to express spatial autocorrelation. The semivariogram was used for an Ordinary Kriging model, which is applied to data that seems to have a trend. In this regard we can assume that the spread of the 1951 fire trended in specific directions, which is substantiated and fundamentally based on Morris' observations. The result of the Kriging model is a continuous surface of predicted time of arrival values. The analysis was masked with the 1951 fire extent so that the time of arrival values could be compared with the simulations. The limitation of using Ordinary Kriging is that it assumes a constant mean for the input distribution,

which is a reasonable assumption for this analysis, given that the duration of the event being modeled is known.

When comparing the time of arrival differences between the simulations and the 1951 prediction map it was clear that the custom simulation was much more similar in behavior to the 1951 fire. The custom simulation spread pattern was quite different from the described spread pattern of the 1951 fire, but the locations that the fire ultimately spread to were nearly identical. The custom simulation spreads much farther north and west than the 1951 fire before it spreads back south into the 1951 fire area. This spread pattern is the primary difference in time of arrival.

Furthermore, both the 1951 fire and custom simulation reached critical areas within similar time intervals (Figure 60). A histogram of the mapped time of arrival difference demonstrates the spatial variability of the fire spread (Figure 61). For example, the fire had reached the ridge top at the time the highest wind gusts were blowing across the ridge top in 1951. The custom simulation also reached the ridge top by that time in the weather stream. In 1951 the fire spotted down the western slopes of the ridge at this time, as did the custom simulation. Most of the spot fires that developed in the custom simulation within the 1951 fire extent did so within 4 hours of the predicted 1951 fire spread to those locations. When considering the total duration of the simulations and the 1951 fire was 108 hours, the time of arrival difference to these critical spread locations is only 4%.

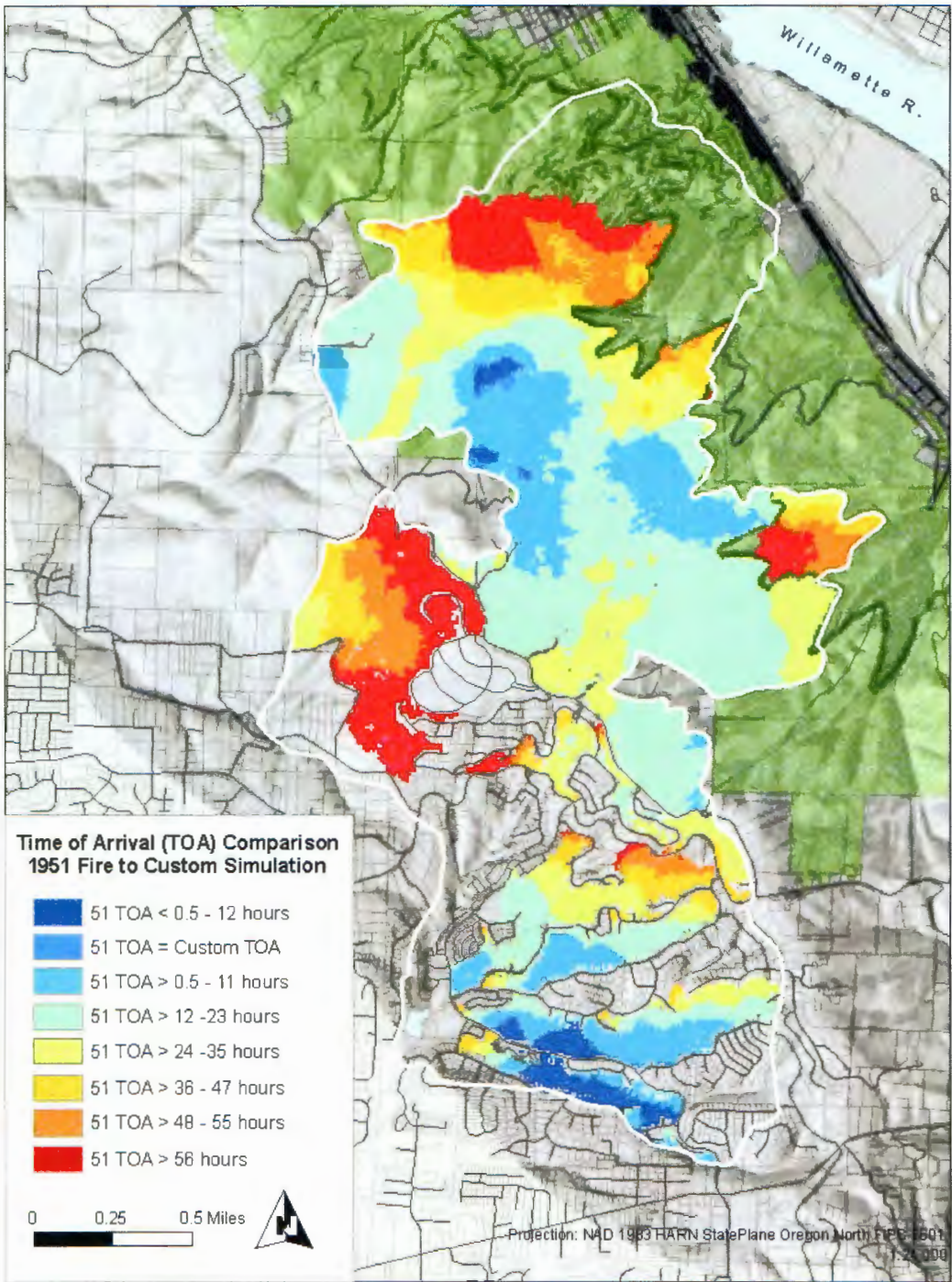


Figure 60: Time of arrival (TOA) comparison between the predicted TOA values of the 1951 fire and the TOA values of the custom simulation. Dark blue areas indicate that the custom simulation arrived at those locations between 30 minutes and 12 hours before the 1951 fire. Red areas indicate that the predicted TOA of the 1951 fire arrived at those locations 56 hours or more before the custom simulation. (Base map source: USGS, City of Portland, fire spread prediction by Author using ArcGIS)

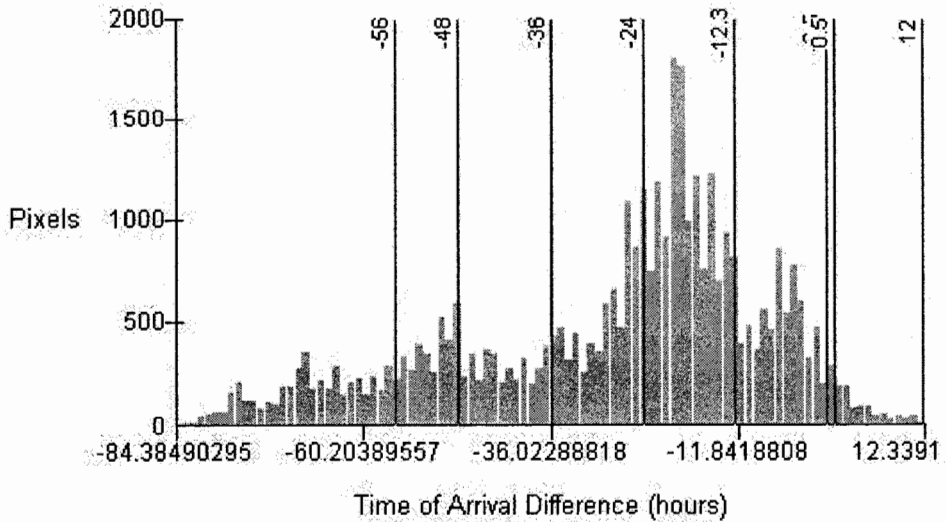


Figure 61: Histogram of the distribution of pixels for the time of arrival difference map comparing the 1951 fire and the custom simulation. The blue lines with numbers indicate the class breaks of the map. The mean value of the distribution was -28 with a standard deviation of 19.6. Histogram developed in ArcGIS by author.

The comparison between the 1951 fire spread prediction map and the standard simulation yields a substantially different result than the previous comparison. There is an increasing gap in the predicted time of arrival between the 1951 and standard simulation as the distance from the ignition point increases (Figure 62). A Histogram of the pixel value distribution further illustrates the point (Figure 63). However, given the low volatility of the fire in the standard simulation this result is not surprising. In 1951 when the fire was approaching the top of the ridge it was spreading at over 11 meters per minute, where the standard simulation experienced a rate of spread of only 3 meters per minute or less in the same area.

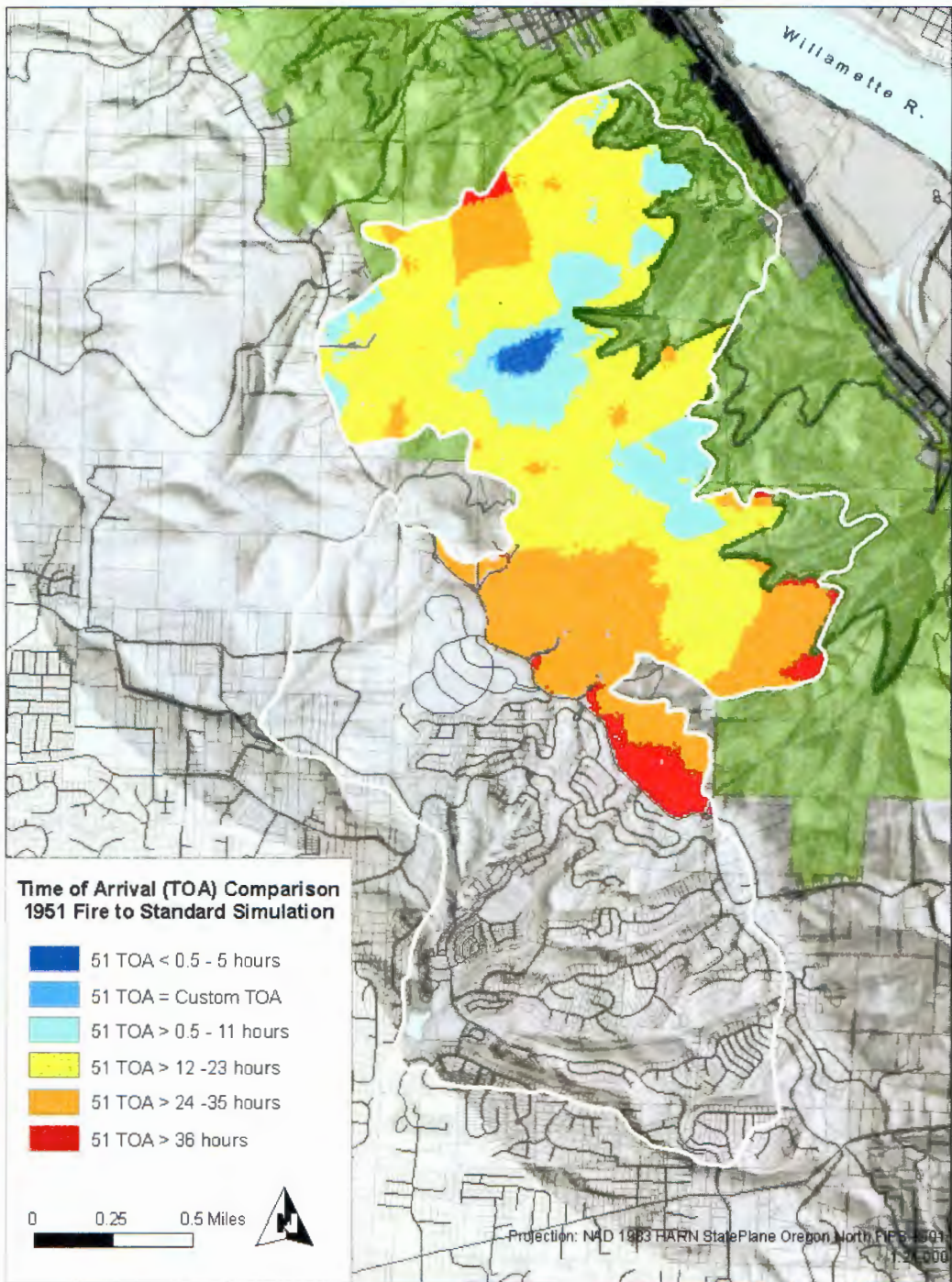


Figure 62: Time of arrival (TOA) comparison between the predicted TOA values of the 1951 fire and the TOA values of the standard simulation. Dark blue areas indicate that the standard simulation arrived at those locations between 30 minutes and 5 hours before the 1951 fire. Red areas indicate that the predicted TOA of the 1951 fire arrived at those locations 36 hours or more before the standard simulation. (Base map source: USGS, City of Portland, fire spread prediction by Author using ArcGIS)

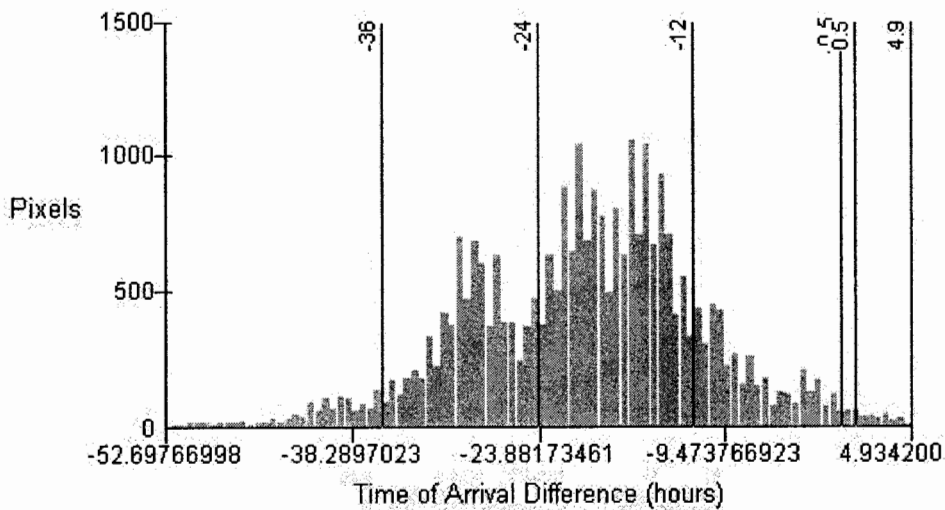


Figure 63: Histogram of the distribution of pixels for the time of arrival difference map comparing the 1951 fire and the standard simulation. The blue lines with numbers indicate the class breaks of the map. The mean value of the distribution was -20 with a standard deviation of 9. Histogram developed in ArcGIS by author.

Potential Property Loss in Forest Park's Wildland-Urban Interface

The potential for structural property loss because of wildland-urban forest fire in the developed areas around Forest Park is great. Based on the simulation analysis it is a matter of timing. The majority of both simulations consisted of controllable levels of burning. However, when the right combination of topography, weather, and fuel align, as seen in the image sequence in Figure 58, the results are dramatic. These results get to the heart of the conflict between policy and management in the wildland-urban interface.

A simple cost analysis and comparison can highlight the worst case scenario. In Table 10 the final extents of the 1951 fire and both simulations are used to calculate the total property value based on 2004 taxlot data within each boundary. The results are sobering: based on the taxlot data 1,648 structures (1,519 homes) are built within the area that burned in 1951. The total building value exceeds the real value lost in the

4th most costly urban wildfire which occurred in the Topanga Canyon area, North of Los Angeles in 1993 (values have been adjusted to 2003 dollars). The custom simulation results are less catastrophic, with the estimated loss of 756 homes, worth an estimated \$272 million. The standard simulation scenario is far more palatable, with only 36 homes lost. It is likely that none of the homes within the standard simulation boundary would be lost, given the intensity of the fire. It is just as likely that only a limited number of the estimated home losses in the custom simulation results would actually occur.

Table 10: The values in the table are based on tax assessment records and therefore do not reflect the real value of the properties, which would exceed the values given. (Source: Metro RLIS)

Current Taxlot Property within the 1951 Fire, Custom and Standard Simulation Extents					
Fire	Structures	Dwellings	Total Building Value	Total Land Value	Total Property Value
1951	129	1519	\$ 536,459,942	\$ 223,142,080	\$ 759,602,022
Custom	11	756	\$ 271,892,977	\$ 143,718,620	\$ 415,611,597
Standard	0	36	\$ 15,509,020	\$ 26,177,040	\$ 41,686,060

There are clear differences between the simulations. Even though certain fire behavior results - such as fire intensity and flame length - were similar over wide areas of the simulations, the spread of the fires was fundamentally different. The custom simulation spread over twice the area as the standard simulation. The custom fire also exhibited uncontrollable fire behavior in fire intensity and heat production. In areas where this behavior was located, the fire reached the upper canopy and spawned spot fires ahead of the advancing fire line. This type of behavior was never observed in the standard simulation. Upon comparing the simulation results with the spread of the 1951 fire, the custom simulation again behaved in a similar manner to the actual event. Unfortunately this type of behavior and spread would pose a greater threat to the

development adjacent to Forest Park. In conclusion, based on the simulation results and comparison to a real event, the custom fuel models developed for the park offered a more reliable illustration of potential fire spread and behavior than the simulation using standard fuel models.

CHAPTER 7: DISCUSSION AND RECOMMENDATIONS

In this final chapter we discuss what the results mean to the stakeholders who either live within this WUI environment or are charged with the preservation and protection of Forest Park. Potential management decisions are reviewed in the context of fuel treatment techniques and application. Two additional simulations are run based on potential accidental ignition scenarios using the custom fuel models and weather data collected during the summer of 2004. Finally, we discuss the limitations of this analysis and the future requirements to improve the use of fire simulation in the wildland-urban interface.

Summary

In this thesis I have tested the use of wildland fire simulation modeling for a wildland-urban interface environment. The results of the study support the use of custom fuel models for small scale simulations. Custom and standard fuel models were used, but the standard fuel models under-represented the live fuel components of Forest Park. The net result was homogenous fire spread and behavior regardless of changing weather and topographic inputs.

From the simulation results we learn that weather is a key factor in fire potential in the park. Drought conditions like those experienced in 1951 could create a dangerous situation because the majority of the park's plant life would lose substantial levels of moisture, leading to a significantly drier understory. As the live fuel moisture decreases, fire intensity and flame length would be greater.

Furthermore, the effect of the Tualatin ridge on easterly winds is conducive to fire spread. East winds from the Columbia gorge run into the ridge and move in a northwesterly direction down the ridge line. As east winds strengthen, the steep canyons and saddles of the Tualatin ridge enhance the chimney effect. Under this condition fire will move rapidly up and over the ridge top.

Fire Mitigation Techniques

Introducing “destructive” fire management practices, such as prescribed burning or thinning, into a wildland-urban interface environment is difficult without providing the public with feasible and tangible results. In order to mitigate the risk of fire entering or exiting an interface area, mitigation techniques need to be employed at a landscape scale. The impact of various techniques along the edges of, and within, fire-prone environments range widely. Techniques will vary depending on fuel composition, topography, and edge development density. Traditional wildland techniques such as shaded fuel breaks and prescribed burning may not work in smaller occluded environments. For extended edge environments the development of crown-fire-free-zones, stepped walls, or selective whorl pruning and vertical fuel reduction may be the only feasible approach (Scott 2002).

Mitigation techniques around structures, such as planting fire resistant ornamentals or delineating defensible spaces with fuel reduction, may reduce the probability of ignition but never eliminate the possibility. Houses ignite from a variety of sources including direct flame, radiation from other structures, and lofted

embers. Fire safe zones only reduce the risk of ignition from direct flame and radiation, but lofted embers come from further afield than a typical fire safe zone.

The situation changes dramatically, if a fire enters an urban environment as a crown fire. Crown-fire-free-zones (CFFZ) are necessary to keep fires near WUI environment out of the forest crown. The size of the CFFZ is dependent on the fuel moisture conditions, which may vary throughout the year. The less fuel moisture the more flammable the fuel. This can also be viewed from a drought condition perspective - the more severe the drought the greater the potential for fire, and the more intense the burn. A CFFZ can range in distance from a structure of 50 feet to over 800 feet. In many WUI environments the feasibility of this level of management is impossible because of land use regulations, neighborhood CC&R's (covenants, conditions, and restrictions), or the physical size of the environment (Scott 2002). Some occluded environments may be less than 200 feet across, but still pose serious fire risk.

Creating and maintaining fire-safe landscapes is a complex process (Clark 1995). Clark breaks it down into five key elements. The first is knowledge and awareness of the problem. To mitigate the risk of fire, property owners and public officials need to recognize the problem and work together to mitigate the risks at lowest level. Second, the physical infrastructure has to be in place that enables the responsible fire bureau to react and initiate their plan. Third, and more importantly, a plan needs to be in place. The responsible government agencies need to react in a prescribed and rehearsed manner in the case of an event. Fourth, structural design should be location appropriate and building code should mandate basic fire-resistant

building materials. Property owners and communities need to be aware of points of weakness in the defenses. Points at which fire fuel and structures coexist need to be treated to minimize the potential for fire to cross-over into the developed environment. Lastly, Clark advocates fuel treatment at a landscape scale. He includes pruning and removal of fuel, but most importantly fire needs to be a part of the treatment regime. Clark (1995) states, “Programs of prescribed burning must be included, despite adverse air quality effects.”

The application of fire management techniques in a wildland-urban interface can prove ecologically beneficial. Forest management in greenbelt and remnant environments is a function of scale and structure (Agee 1995). Scale is typically measured by the size of the forest and the level of fragmentation that exists. Structure is typically measured by the characteristics of the forest within the area under consideration. A significant factor in determining scale and structure is the size of the buffer, if any, that exists between the edges and the inner forest. A long and narrow environment may be composed of all edge environments. Therefore, the level and intensity of management will vary. However, the development of a buffer to limit the edge effect is important to the ecological stability and health of an urban forest. Fire is an ecological tool that can be used to improve the health of a forest.

There is an ecological component to this model. The protocol with which the fieldwork was conducted is based on ecological sampling. With additional field research on a recurring basis the fuel dataset could be developed to test vulnerability at various stages of succession. As the forest structure changes in various locations the potential impact on fire behavior can be modeled. As additional areas enter into those

stages, fire behavior can be reviewed and areas that may need treatment can be identified to increase or establish buffer. The model can also provide a way to stress test the forest. Fuel moisture scenarios can be applied that can mimic long and protracted drought conditions. Fire behavior scenarios done in advance of these conditions can help direct mitigation and response planning in the case of an actual event.

Additional Fire Simulation Scenarios within the Study Area

To mitigate the risk of fire intensity at the interface boundary, fire management plans need to be drawn at the landscape scale and need to incorporate multiple mitigation strategies that reduce intensity well before the fire reaches development. However, this may not be practical in many scenarios. Take for example, a scenario where a fire starts within a residential area green space. This type of scenario is a strong possibility given the level of development and green space adjacent to Forest Park. In Figure 64 the custom fuel models were used along with weather data collected during the summer of 2004 to perform a short-term simulation. Only the first 4 hours of the simulation are illustrated because a fire in this location likely would be quickly responded to and the full resources of the responsible fire agency would be brought to bear. The weather at the time of the simulated fire was windy with gust exceeding 20 mph and there had been no measurable rain for over a month. Since the fire took place in July, the initial fuel moisture was set at normal levels of 8 to 15% for the dead fuels. Within an hour of ignition the fire had spread and spotted across the green space gully and up to houses on both sides.

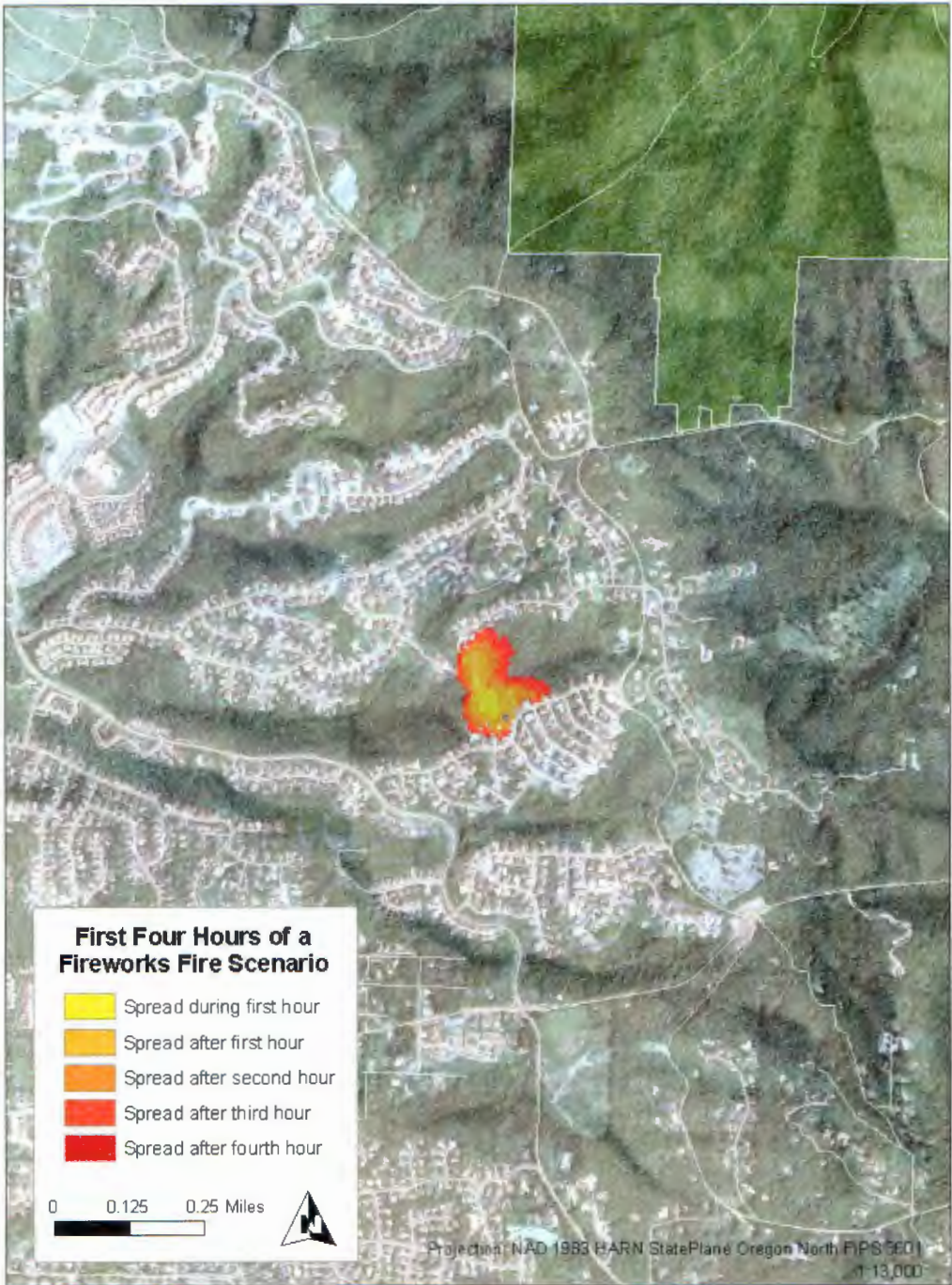


Figure 64: Accidental fire start in green belt within a residential development. The scenario of fire spreading from developed areas into the park is as likely as fire spreading from the park into developed areas. (Base map source: USGS, City of Portland, fire simulation by Author using Farsite)

The designation of houses and development as non-fuel is a significant factor in this analysis. Consider that any lofted ember that may have landed on a cedar shake roof, where the roof material is likely to ignite under these conditions is impossible in the simulation. Roof fires can quickly spread and ignite neighboring homes. Over 8 spot fires started in heavily developed areas during the custom simulation. Had houses been considered fuel, then more spot fires would have been likely. Subsequent fire spread within the neighborhoods would be much greater than the results indicate.

Another likely ignition scenario is along utility corridors occupied by high-voltage power lines (Figure 65). Several power line corridors traverse the park. Fire that may accidentally start along these lines because line-tree contacts can remain undetected while they smolder or grow in the more volatile fuels found in these utility corridors. Under the right weather and wind conditions these fires can grow and spot rapidly in locations that are relatively inaccessible for fire fighting equipment.

There are no fire hydrants or large water sources within the park. Fires will likely have to be fought by hand crews or brush units that can get close to the fire's edge via fire lanes or park roads. For an urban fire department this can pose significant challenges. As Figure 65 illustrates, the simulated fire spotted to several locations down slope and across the canyon from the point of ignition. Only the first four hours of the simulation are presented, but the fire spotted within the first hour of ignition. The point of ignition for this fire is actually in a best-case location: Saltzman Road runs parallel to the main fire and a fire lane is close to the spot fire across the canyon. The simulated fire also started between Saltzman and Leif Erickson, which would enable fire fighters to light back fires from those roads. However, there are

more areas that are less accessible in Forest Park than are accessible to fire fighters and their heavy equipment.

These two short-term simulations are not presented as definitive model runs. Rather, they are presented just to suggest how local emergency management planners might utilize the simulation tool that Farsite represents. Many additional simulations, using a variety of input parameters, would help planners gain greater insights to the likelihood and behavior of fire in Forest Park.

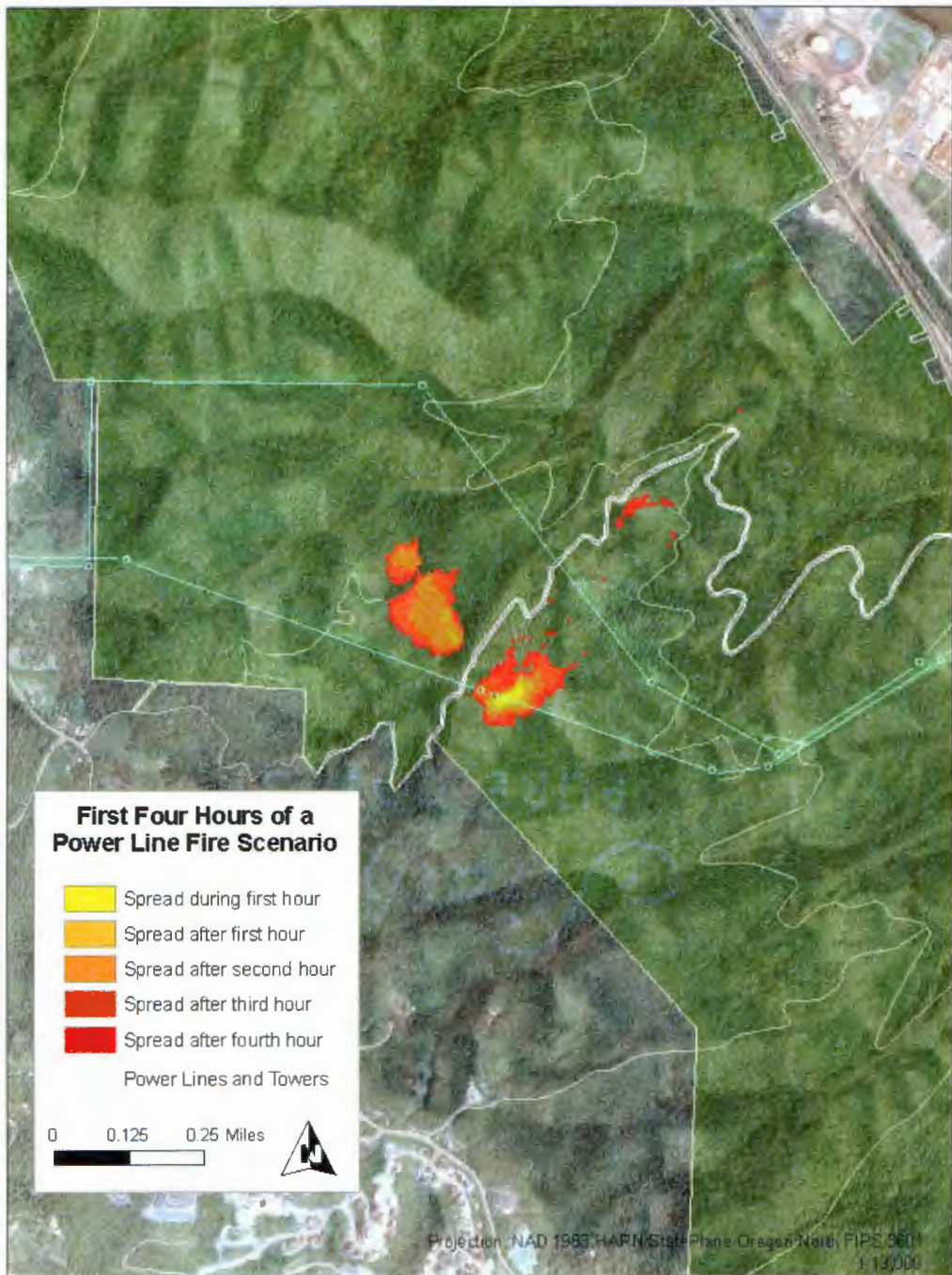


Figure 65: Accidental fire start from power line-tree contact. Power lines traverse the park at several locations. During very hot weather power lines can droop and initiate contact with vegetation that can arc and ignite. Trees can also fall or be blown across power lines causing the same arc and combustion scenario. This fire can start and remain undetected for some time and then quickly grow under the right weather and wind conditions. (Base map source: USGS, City of Portland, fire simulation by Author using Farsite)

Analysis Limitations and Recommended Model Improvements

The single most limiting aspect of using this model to assess fire behavior in the wildland-urban interface environment within the study area is the designation of houses and structures as non-fuel. A fuel model specific to houses and structures needs to be developed that will take into account the ignition thresholds of the building materials and the behavior of the structural fire. This would enable the model to be used to assess fire mitigation techniques that may be employed in the immediate vicinity of structures.

Furthermore, additional sampling plots within the study area could improve the fuel map accuracy. For example, no sampling plots were located within the utility corridors. The use of Anderson's fuel model 5 for these locations was based solely on visual assessment. Having local data for this fuel environment could impact the fire behavior of future simulations. Future fuel assessments at the permanent plots should also include substrate moisture calculations, which were not possible to record during this study because the cost of the equipment was beyond the means of the project. However, the fuel moisture values used for the simulations were based on the literature reviewed and were chosen so as to fall within a reasonable range.

Increased accuracy of the measurement of canopy height and density would also improve the crown fire portion of the simulations. This would require LiDAR (light detection and ranging) data that would provide accurate heights of the canopy as well as its cover density. This type of a data set could provide a second fuel-related base map from which to derive the fuel themes for the Farsite landscape file.

Although the standard in wildland fire simulation, a single source base fuel map was limiting given the study area's size and complexity.

The time which the simulations took to run was also a limiting factor. Even minor adjustments to the inputs required that the simulations be re-run. Each new simulation took a couple of days to complete for a matrix of cells 10 m by 10 m in size. A computer with faster processors and memory may reduce the simulation run time. However, for simulations to be used for decision support during a real event the simulation would have to run within an hour. For this to occur the spatial resolution of the inputs will need to be changed. However, the size of the study area, coupled with the location of an ignition, may not enable the model to be used as a suppression planning tool because a fire event may move too quickly through the environment.

Improved Fire Planning and Management of Forest Park

From a policy perspective it is difficult to manage to a worst case scenario. The cost associated with planning and managing for all contingencies is not feasible or fiscally responsible. Therefore, management plans must be focused on the points in the landscape that are of greatest risk.

The model as it is would be an effective tool to determine the likely spread from locations of what would be considered maximum threat. The two short-term scenarios discussed previously had points of ignition in elevated threat areas. Some of the areas of elevated threat are obvious; the utility corridors, residential areas with adjacent green space, the industrial areas adjacent to the southeastern corner of the park, and the rail lines that run along the Willamette River and most of the eastern

park boundary. However, the model could identify locations of highest threat within these higher risk areas. This model could be used to test the combination of terrain, weather, and location that represent the highest threat locations. Once identified the threat location can be targeted for mitigation.

Conclusion

Fire is a natural part of Forest Park's landscape and ecology. However, the unique orientation of Forest Park to the city of Portland presents certain challenges in establishing sustainable resource management tactics that consider the spatial distribution of the different forest stands, and their development patterns in the context of a healthy successional pattern. Counter-balancing sustainable resource planning with the potential property loss in the event of conflagration is a real issue for city officials. This research focused on demonstrating the utility of spatial modeling for decision support. The fire model provides city officials with a high-resolution fire simulation and visualization tool for Forest Park. This allows them to generate information that enables localized stand management decisions from a fire hazard perspective. This evaluation of the model will be considered successful if it can provide input to the debate and offer real data for the cost-benefit analysis of proposed restoration projects or evacuation strategies.

This study was not intended to be a policy document. Although there are policy issues discussed and management techniques introduced, I have tried not to endorse a position. The study was intended to; first, address the difference in fire simulation results when using standard and custom fuel models, holding all other

simulation inputs constant; second, illustrate the utility of the simulation model as a management tool. In this regard, the custom fuel models developed from in situ field work out-performed the standard fuel models. The standard simulation produced a fire that never reached a point of uncontrollable spread. The simulation using the custom fuel models at times burned uncontrollably, but this behavior was not sustained for very long.

The net result of my research is intended to help city officials predict and analyze fire danger. First, using the fire model appropriately, city officials can assess the conditions necessary for serious fire given an ignition event and location. Second, the model can be used as a predictive tool in assessing how a fire would likely behave under a given set of ignition conditions within Forest Park. For this model to be used accurately in the future, additional fuel assessment and weather monitoring will be required. Third, from a resource management perspective, the model predictions can be used as the basis for ecological restoration recommendations to establish and sustain a native fire-dependent ecology. Finally, this research will support the adoption of a management plan that strives to establish a healthy urban forest that will develop into a late-successional stage for future generations to enjoy.

REFERENCES

- Agee, J.K. 2000. The use of shaded fuelbreaks in landscape fire management. *Forest Ecology and Management* 127: 55-66.
- Agee, J.K. 1995. "Management of greenbelts and forest remnants in urban forest landscapes." In G.A. Bradley. ed. *Urban Forest Landscapes: Integrating Multidisciplinary Perspectives*. Seattle: University of Washington Press. Pg. 128-138.
- Agee, J.K. 1991. *Fire history of Douglas-fir forests in the Pacific Northwest*. General Technical Report PNW-285:25-33. USDA Forest Service. Portland, OR.
- Agee, J.K., and Flewelling, R. 1983. "A fire cycle model based on climate for the Olympic Mountains, Washington." *Fire and Forest Meteorology Conference Proceedings*, 7, 32-37.
- Agee, J.K. and Krusemark, F. 2001. Forest fire regime of the Bull Run Watershed, Oregon. *Northwest Science* 75:292-306.
- Albini, F.A. 1986. Wildland fire spared by radiation: a model including fuel cooling by natural convection. *Combustion Science and Technology* 45: 101-113.
- Albini, F.A. 1976. *Estimating wildfire behavior and effects*. General Technical Report INT-30. USDA Forest Service. Ogden, UT.
- Albright D. and Meisner, B. N. 1999. Classification of fire simulation systems. *Fire Management*. 59(2): 25-30.
- Anderson, H. E. 1982. *Aids to determining fuel models for estimating fire behavior*. General Technical Report INT-122. Ogden, UT: Department of Agriculture, Forest Service, Rocky Mountain Research Station. 1-20.
- Andrews, Patricia L.; Bevins, Collin D.; Seli, Robert C. 2003. *BehavePlus fire modeling system, version 2.0: User's Guide*. General Technical Report RMRS-GTR-106: 79-97. USDA, Forest Service, Rocky Mountain Research Station, Ogden, UT.
- Baker, W.L. 1992. Effects of settlement and fire suppression on landscape structure. *Ecology*. 73:1879-1887.
- Barrett, S.W., Arno, S.F. 1988. Increment-borer methods for determining fire history in coniferous forests. USDA Forest Service General Technical Report INT 244: 1-15.
- Boyd, R. ed. 1999. *Indians, Fire, and the Land in the Pacific Northwest*. Oregon State University Press, Corvallis, Oregon.
- Chapman, D. 1999. *Natural Hazard*. Oxford University Press, Melbourne.
- City of Portland. 1995. *Forest Park Natural Resource Management Plan*. By Nancy Gronowski, Jim Sjulín, Tim Brooks. Ordinance no. 168509. Portland, Oregon.
- City of Portland Archives. *City Engineer Report: Building Burma Road, 1951*. Accession No. A2000-025 project 19.
- Clark, J. R. 1995 "Fire-safe landscapes" In G. A. Bradley. ed. *Urban Forest Landscapes: integrating multidisciplinary perspectives*. Seattle: University of Washington Press. Pg. 164-171.

- Cleaves, Dave. 2001. "Fire in the Wildland Urban Interface: Dilemmas of Duality and the Role of National Science Leadership." Paper presented, Natural Disasters Roundtable, Washington D. C., January 26.
- Clevers, J. G. P. W. 1988. The derivation of a simplified reflectance model for the estimation of leaf area index, *Remote Sensing of Environment*, vol 35., pp. 53-70.
- EROS Data Center. "USGS Seamless Data Distribution Delivery System." USGS. <http://seamless.usge.gov/website/seamless/viewer.php>.
- Fahnestock, G.R and J. K. Agee, J.K. 1983. Biomass consumption and smoke production by prehistoric and modern forest fires in western Washington. *Journal of Forestry*. 81: 653-57.
- Finney, Mark A. 2004. *Farsite: Fire Area Simulator-model development and evaluation*. Research Paper RMRS-RP-4:1-47; revised version 1998 paper. USDA Forest Service, Rocky Mountain Research Station, Ogden, UT.
- Firemon. 2003. *Fuel Load Sampling Method, version 3*. Missoula, MT: Joint Fire Sciences Program. http://www.fire.org/firemon/FLv3_Methods.pdf
- Firemon. 2004. *Tree Data Sampling Method, version 3*. Missoula, MT: Joint Fire Sciences Program. http://www.fire.org/firemon/TDv3_Methods.pdf
- Forestry Canada Fire Danger Group. 1992. *Development and structure of the Canadian Forest Fire Behavior Prediction System*. Forestry Canada Information Report ST-X-3:1-63. Ottawa, Canada.
- Franklin, J.F. and Dyrness, C.T. 1973. *Natural vegetation of Oregon and Washington*. General Technical Report PNW-8. USDA Forest Service. Portland, OR.
- Friedl, M., Michaelson, J., Davis, F. W., Walker, H., and Schimel, D. S., 1994, Estimating grassland biomass and leaf area index using ground and satellite data. *International Journal of Remote Sensing*, 15:1401-1420.
- Gilvear, D. J., and Bryant, R. G. 2003. Analysis of aerial photography and other remotely sensed data. In Kondolf, G. M. and Piégay H. (eds) *Tools in Fluvial Geomorphology*, Wiley, London, p134-168.
- Hesseln, H. Rideout, D.R. and Omi, P.N. 1998. Using Catastrophe Theory to Model Wildfire Behavior and Control, *Canadian Journal of Forest Research*. 28:852-62.
- Houle, Marcy C. 1996. *One City's Wilderness Portland's Forest Park*. Portland, Oregon: Oregon Historical Society Press.
- Insurance Information Institute. 2005. "Catastrophic wildland fires in the United States, 1970-2003". Property Claim Services, ISO; Insurance Information Institute. <http://www.iii.org/media/facts/statsbyissue/catastrophes/> (accessed on April 27, 2005)
- Johannessen, Carl L., Davenport, William A., Millet, Artimus, McWilliams, Steven. 1971. The vegetation of the Willamette Valley. *Annals of the Association of American Geographers*. June: 286-302.
- Keane, R. E., S. A. Mincemoyer, K. M. Schmidt, D. G. Long, and L. Garner. 2000. *Mapping Vegetation and Fuels for Fire Management on the Gila National Forest Complex, New Mexico*. USDA General Technical Report RMRS-GTR-46-CD.

- Kenai Peninsula Borough. "Farsite computer based fire modeling." GIS Department. http://www.borough.kenai.ak.us/sprucebeetle/vegmap/coho-fire-exercise_files/frame.htm (accessed on February 6, 2005)
- Key, C. and Benson, N. 2001. The normalized burn ratio, a Landsat TM radiometric index of burn severity incorporating multi-temporal differencing. Unpublished manuscript USFS.
- Lewis, M. and Clark, W. *The Lewis and Clark Expedition*. Vol. 3. Edited by Nicholas Biddle. New York, 1961.
- Marshall, E. H. 1950. *Proposed fire protection plan for Portland city-Forest Park*. Cooperative Forest Protection State and Private Forestry Division, USDA Forest Service, Portland, OR.
- Miller, Edward. 1928. That was an eventful day in Portland. *Oregonian*, May 16.
- Miller, S.R. and Wade, D. 2003. Re-introducing fire at the urban/wild-land interface: planning for success. *Forestry* 76(2): 253-260.
- Morris, W.G. 1934. Forest fires in Oregon and Washington. *Oregon Historical Quarterly* 5:313-339.
- Morris, W.G. 1953. *Weather and fire behavior during the Portland Forest Park fire of 1951*. USDA Forest Service RF-NW Behavior General. Pacific Northwest Forest and Range Experiment Station, Portland, Oregon, USA.
- Morrison, P., and F. J. Swanson. 1990. *Fire history and pattern in a Cascade Range landscape*. USDA Forest Service General Technical Report PNW-GTR-254. Pacific Northwest Research Station, Portland, Oregon, USA.
- Munger, T. T. 1960. *History of Forest Park*. Portland, Oregon.: Forest Park Committee of Fifty.
- National Association of Realtors. 2005. "Statistics and Forecasting: Housing Statistics" [http://www.realtor.org/Research.nsf/files/Data.xls/\\$FILE/Data.xls](http://www.realtor.org/Research.nsf/files/Data.xls/$FILE/Data.xls) (accessed on April 17, 2005)
- Newton, Michael. 1968. Role of red alder in Western Oregon forest succession. In J. M. Trappe, J. F. Franklin, R. F. Tarrant, and G. M. Hansen (eds.) *Biology of Alder*. Northwest Scientific Association-Spokane, 40th annual meeting in Pullman, WA. Pacific Northwest Forest and Range Experiment Station. Portland, OR. Pg. 73-84.
- Oliver, C. D. and Larson, B. C. 1990. *Forest Stand Dynamics*. McGraw-Hill, New York, New York.
- Olmsted, John Charles. 1903. Report of the park board, Portland, Oregon: with the report of Messrs. Olmsted Brothers, landscape architects, outlining a system of parkways, boulevards and parks for the city of Portland. The Board: Portland, OR.
- Pinty, B. and Verstraete, M. 1992. GEMI: A Non-Linear Index to Monitor Global Vegetation from Satellites. *Vegetation*, 101, 15-20.
- Pyne, Stephen J. 1998. *Fire in America: A cultural history of wildland and rural fire*. University of Washington Press. Seattle, Washington.
- The Oregonian. 1889. Fierce forest fires, heavy losses reported from the hills around Portland. September 19.

- The Oregonian. 1951. It could and did happen in Portland, Skyline fire sleeping dog; officials reckoning costs. August 26.
- Regents of the University of California. 2005. "Fuel Environment Triangle." <http://www.ices.ucsb.edu/resac/right.html> (accessed on January 14, 2005)
- Richards, G.D. 1990. An elliptical growth model of forest fire fronts and its numerical solution. *International Journal for Numerical Methods in Engineering* 30:1163-1179.
- Rothermel, R. 1972. *A mathematical model for predicting fire spread in wildland fuels*. Research Paper INT-115. Ogden, UT: USDA, Forest Service, Intermountain Forest and Range Station. 41 p.
- Rothermel, R. 1983. *How to predict the spread and intensity of forest and range fires*. Gen Tech. Rep. INT-143. Ogden, UT: USDA, Forest Service, Intermountain Forest and Range Experiment Station. 161 p.
- Sandberg, D. V., Ottmar, R. D., and Cushon, G. H. 2001. Characterizing fuels in the 21st century. *International Journal of Wildland Fire*. 2001(10): 381-387.
- Scott, Joe. 2002. "Canopy fuel treatment standards for the wildland-urban interface." Paper presented, USDA Fire, Fuel Treatments, and Ecological Restoration Conference, Fort Collins, CO, April 16-18.
- Spies, T.A.; Franklin, J.F. 1989. Gap characteristics and vegetation response in coniferous forests of the Pacific Northwest. *Ecology*. 70:543-545.
- Stewart, Glenn H. 1984. Forest structure and regeneration in the *Tsuga heterophylla-Abies amabilis* transition zone, central western Cascades, Oregon. Corvallis, OR: Oregon State University. 150 p. Ph.D. dissertation.
- United States Department of Agriculture, Forest Service, Rock Mountain Research Station. 2004. "An Historical Chronology of Wildland Fire Research in the Interior Western United States (1913 - 2000)." http://www.fs.fed.us/rm/main/fire_res/fire_history.html (accessed on December 8, 2004)
- United States Department of the Interior. "National Atlas of the United States." Nationalatlas.gov. 2005. <http://www.nationalatlas.gov> (accessed on March 3, 2005)
- Unknown. 2002. *The reporter's hazardous assignment handbook: wildfires*. Anchor Point Media, Boulder, Colorado.
- Van Wagner, C.E. 1989. Conditions for the start and spread of crown fire. *Canadian Journal of Forest Research*. 7:23-34.
- Veblen, Thomas. "Key Issues in Fire Regime Research for Fuels Management and Ecological Restoration." Paper presented, USDA Fire, Fuel Treatments, and Ecological Restoration Conference, Fort Collins, CO, April 16-18, 2002.
- Vogelmann, J.E., S.M. Howard, L. Yang, C.R. Larson, B.K. Wylie, N. Van Driel, 2001. Completion of the 1990s National Land CoverData Set for the Conterminous United States from Landsat Thematic Mapper Data and Ancillary Data Sources, Photogrammetric Engineering and Remote Sensing, 67:650-652.
- Weatherford, B. F. 2002. Study supports cooperative fire protection in the west. *Fire Management*. 62(1): 8-12.

Wills, R.D. and Stuart, J.D. 1994. Fire history and stand development of a Douglas-fir/hardwood forest in northern California. *Northwest Science* 68(3):205-212.

Wilson Sinclair Albert Manuscripts, Oregon Historical Society, Portland (January 23, 1945).

APPENDIX A

Farsite Algorithms and Inputs

Farsite uses a vector or wave approach to fire growth modeling. The applications algorithms are based on Huygens' Principle using elliptical wavelets (Figure 66). Under constant conditions the wavelets would propagate uniformly over time, maintaining an elliptical shape. However, nonuniform conditions exist along a fire front. The propagation in both size and direction of wavelets is impacted by the local fuel type and orientation on the local wind-slope vector (Finney 2004).

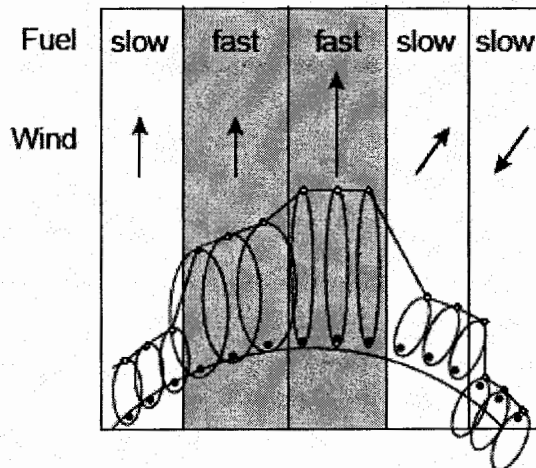


Figure A1: Wavelet size dependency on nonuniform conditions. The fire front expands most rapidly in the direction where the wind is moving directly upslope and faster burning fuel is available. Source: Finney 2004.

The fire front spreads as a continuously expanding polygon at specified time intervals (time steps). The fire polygon is defined by a series of points (vertices) with X, Y coordinates, and new polygons expand independently from each vertex based on

the landscape. The wind-slope vector determines the shape and direction of the propagating ellipses. The size of each ellipse at the leading edge of the fire is based on the various fire behavior model inputs and the time interval between steps (Finney 2004).

Farsite uses four fire behavior models to create the three-dimensional process of fire spread. The four models consist of surface fire spread, crown fire spread, fire acceleration, and spotting. The surface fire spread model is based on Rothermel's steady-state fire spread equation (Equation 1). Additionally the surface fire model uses a fireline intensity equation that describes the rate of energy release per unit length of the leading edge of the fire (Equation 2). In order for the equations to calculate appropriately fuel characteristics and moisture, windspeed and direction, and topographic slope and aspect must be available at all times at any point on the landscape. The equations are applied at every vertex along a plane parallel with the surface (Finney 2004).

All equation inputs related to data collected in the field are **bold**.

All equation inputs or constants across developed from laboratory test are *italic*.

$$\text{Equation 1: } R = I_R \xi (1 - \Phi_w + \Phi_s) / \rho_b \epsilon Q_{ig}$$

where:

$R =$ forward steady state spread rate (m min^{-1})

$I_R =$ reaction intensity ($\text{kJ min}^{-1} \text{m}^{-2}$)

$\xi =$ the propagating flux ratio

$\Phi_w =$ **wind coefficient (result of wind-slope vector and wind speed)**

$\Phi_s =$ **slope coefficient (result of wind-slope vector and radian azimuth)**

$\rho_b =$ *ovendry bulk density (kg m^{-3})*

ε = dimensionless effective heating number (proportion of fuel mass that must be raised to ignition temperature)

Q_{ig} = heat of pre-ignition (kJ kg^{-1})

Equation 2: $I_b = hwR / 60 = (I_R / 60) * (12.6R / \sigma)$

where:

I_b = fire intensity at leading edge

h = *heat yield of the fuel, total heat less the energy required to vaporize moisture (kJ kg^{-1})*

w = **weight of the fuel per unit area (kg m^{-2})**

R = leading edge steady state spread rate (m min^{-1})

I_R = reaction intensity ($\text{kJ min}^{-1} \text{m}^{-2}$)

σ = **surface area to volume ratio of fuel bed (m^{-1})**

There are numerous equations that make up the crown fire model in farsite.

Most of the equations are based on the work Charles Van Wagner who first researched crown scorch and the conditions necessary for crown fire ignition and spread scenarios (Van Wagner 1977). He and others in the Forestry Canada Fire Danger Group focused on crown foliar moisture as a primary indicator of whether a fire will ladder from the surface and torch a single tree or spread actively through the crowns (Van Wagner 1989, Forestry Canada Fire Danger Group 1992). The first equation incorporated into Farsite identifies the transition threshold at which surface fire will ladder into the overstory (Equation 3). The second equation determines the active crown fire spread rate (RAC) (Equation 4). The actual active crown fire spread rate is determined from a theoretical maximum crown fire spread rate (Equation 5). The maximum crown fire spread rate is determined from a correlation with the forward surface fire spread rate using a 0.4 wind reduction factor and a coefficient designed to

minimize the possibility that spotting could be accounted for twice (Equation 6). The next crown fire equation calculates the crown fraction burned (CFB) or the proportion of trees involved in the crowning phase of the fire (Equation 7). The CFB depends on an exponent that scales it to equal 0.9 when the surface fire reaches 90% of the difference between RAC and the critical surface fire spread rate and intensity that would initiate a crown fire. Crown fire intensity is the last crown fire equation and is a modification of the surface fire intensity equation that includes the combined loading of crown fuel and surface fuel consumed (Equation 8) (Finney 2004).

$$\text{Equation 3: } I_o = (0.010 * \text{CBH} (460 + 25.9M))^{3/2}$$

where:

I_o = threshold for transition to crown fire

CBH = crown base height that incorporates the presence or effect of ladder fuel

M = foliar moisture content (percent on dry weight basis)

$$\text{Equation 4: } \text{RAC} = 3.0 / \text{CBD}$$

where:

RAC = active crown fire spread rate

3.0 = empirical constant defining critical mass flow rate through the crown for continuous flame ($0.05 \text{ kg m}^{-1} \text{ s}^{-2}$) and a conversion factor (60 s min^{-1})

CBD = crown bulk density (kg m^{-3})

$$\text{Equation 5: } \text{R}_{\text{Cactual}} = \text{R} + \text{CFB} (\text{R}_{\text{Cmax}} - \text{R})$$

where:

$\text{R}_{\text{Cactual}}$ = actual active crown fire spread rate at the i^{th} vertex

R = forward steady state spread rate (m min^{-1})

CFB = crown fraction burned

R_{Cmax} = maximum crown fire spread rate

Equation 6: $R_{Cmax} = 3.34 * R_{10} * E_1$

where:

R_{Cmax} = maximum crown fire spread rate

3.34 = *coefficient to minimize accounting for individual tree torch or the possibility that spotting could be accounted for twice*

R_{10} = forward steady state spread rate for fuel model 10 using 0.4 wind reduction factor

E_1 = fraction of the forward crown spread rate achievable at the *i*th perimeter vertex given orientation of the vertex to the maximum spread direction and elliptical dimension of the crown fire

Equation 7: $CFB = 1 - e^{-ac(R-R_o)}$

where:

CFB = crown fraction burned

e^{-ac} = exponent where $a_c = -\ln(0.1) / 0.9 (RAC - R_o)$

R_o = critical surface fire spread rate where $R_o = I_o (R /)$

Equation 8: $I_c = 300 (I_b / 300R = CFB * CBD(H-CBH)) * R_{Cactual}$
or R

where:

I_c = crown fire intensity

H = crown height

Heat content of surface and crown fuels is assumed to be 18,000 kJ kg⁻¹

Farsite compares the values of the surface and crown fire equations to determine the type of crown fire expected. Passive crown fire or individual torching of trees will be exhibited in the simulation if I_b greater than or equal to I_o but $R_{Cactual}$ is less than RAC. An active crown fire will ensue if I_b greater than or equal to I_o and

R_{Cactual} is greater than or equal to RAC. Independent crown fire only occurs in conjunction with very high windspeeds, crown bulk density, and percent cover. For independent crown fire I_b is greater than I_o and R_{Cactual} is greater than or equal to RAC (Finney 2004).

Fire acceleration is represented by two equations that define the rate of increase in spread rate for a given ignition source assuming constant environmental conditions. The equations control time and space resolution. They calculate the spread distance required achieving the current spread rate at current conditions plus the spread distance in the next timestep provided a new equilibrium spread rate (Equations 9 and 10). The fire acceleration calculations eliminate instantaneous jumps to faster spread rates because of sudden environmental changes (Finney 2004).

$$\text{Equation 9: } D_t = R (T_t + (e^{-aaT_t} / a_a) - (1 / a_a)) + D_{t+1}$$

where:

D_t = spread distance require to achieve the current spread rate under current conditions

R = forward steady state spread rate (m min^{-1})

T_t = time required to achieve the current spread rate under current conditions

a_a = constant that determines the rate of acceleration (set to 0.115 or 0.300) Crown fires use equation $a_a = a_a - 18.8 * CFB^{2.5} e^{-8 CFB}$

D_{t+1} = desired spread distance in next timestep

$$\text{Equation 10: } T_t = \ln(1 - R_t / R) / a_a$$

The last set of equations used in Farsite predicts the ignition and spread of spot fires. Spotting is caused by embers lofted from torching trees and carried by wind

ahead of the fireline. The spotting distance is dependent on ember size, vertical wind speed profile, and the surface topography. The spotting function in Farsite is based on Albini's (1979) model that calculates the height to which an ember lofts as a function of the length of time a torching tree(s) creates enough buoyant flow equal to the time required for an ember to travel upward from its source (Equation 11 and 12). Farsite uses several assumptions in the application of Albini's model. Embers are assumed to originate at the top of the canopy. The base of the flame is assumed to be half the stand height. Ember shape is assumed to be cylindrical with constant specific gravity and drag coefficient. Lastly, embers are assumed to loft vertically directly above the burning tree. Only after the maximum lofting height is calculated does the program calculate downwind descent.

$$\text{Equation 11: } t_f = t_0 + 1.2 + a_x / 3 \left((b_x + (z / z_F) / a_x)^{3/2} - 1 \right)$$

where:

t_f = duration of the buoyant flow structure of torching tree

t_0 = time of steady burning of tree crowns

z_F = flame height (m)

z = ember height (m)

a_x = flame structure constant (5.963)

b_x = flame structure constant (4.563)

$$\text{Equation 12: } t_t = t_0 + t_1 + t_2 + t_3$$

t_t = time required for ember to travel upward from its source

t_0 = time of steady burning of tree crowns (dependent on species, diameters and number of trees torching in a group)

t_1 = time for ember to travel from its initial height to the tip of the flame above the torching tree

t_2 = time for ember to travel through the transition zone between the flame tip and the buoyant plume

$t_3 =$ time for ember to travel in the buoyant plume

Additional equations account for ember descent and downwind travel distance given terminal velocity and drag, density and volume loss due to burning, and ambient windspeed after the ember leaves the buoyant plume. Once the ember touches down it may ignite a new fire if three conditions are met. The ember can not fall within an already burned area. The landing site must contain combustible material. Lastly, the combustible material is ignitable given the embers thermal properties.

APPENDIX B

Weather and Wind Files

Wind information must be input as a stream of data contained in a text file.

The file contains data in columns that are in a space delimited ASCII format. The data in the file consists of the hour of observation which is specified as 0-2400, to the nearest minute. The speed specified in miles per hour. The direction specified in degrees, clockwise from north (0-360), and the cloud cover at the time of observation specified as a percentage, 0 to 100.

The data contained in the weather file consists of precipitation representing the daily rain amount specified in hundredths of an inch. The hour that corresponds to the minimum temperature was recorded (0-2400). The hour that corresponds to the maximum temperature observed followed by the minimum and maximum temperatures in Fahrenheit. The file also includes minimum and maximum relative humidity observed during the day as a percentage (0-99). The elevation at which the weather readings were taken is also included so that adjustments can be made to the data stream if the difference between the fire location and the observation post is too great. If there was precipitation during the day the time that it started and the time that it stopped is specified.

Multiple wind and weather files can be used in a single simulation by identifying the location of weather monitoring stations at particular locations on the simulated landscape. The locations are linked to individual wind and weather files customizing the resolution and spatial location of those data streams on the landscape.

In this study wind and weather data recorded and collected during the 1951 fire was used to create the wind and weather files. 1951 weather data are available from three sources: the Troutdale airport, Portland International Airport (known as the Portland airport in 1951), and a USFS forester's report of conditions at the fire.

The first weather station was located at the Troutdale airport located about 16 miles from the Tualatin ridge, at the mouth of the Columbia River Gorge. Ultimately the Troutdale data was discarded for two reasons. First, the influence of the Columbia River Gorge on the weather skewed the temperature and wind data. Second, the wind speed and direction reading were taken inconsistently at the Troutdale station.

The second weather station was located at the Portland airport, which is only 7.5 miles from the Tualatin ridge. The dataset from the Portland airport station was complete. Readings are available at regular 6-hour intervals, taken at 0400, 1000, 1600, and 2200 hours. Unfortunately this is less than the recommended wind input interval for fire simulation. The greatest elevation difference between the station and the study area was 1,200 feet, which does not pose a serious problem in using the data. The net affect on temperature or humidity over a 1,200 foot elevation difference does not warrant adjustment of the inputs. However, given the proximity and consistency of readings the Portland airport station was used as the primary source of weather and wind input for the fire simulations.

The last data source came from a fire report filed by William Morris, a USFS forester who observed the 1951 fire and took wind, temperature, and relative humidity readings throughout his observations. As the fire burned he moved to various locations within the burn area. He noted the times and locations at which he took the

readings. Although his time intervals were not consistent his observations filled in the gaps between the Portland airport data. Furthermore, during the fires greatest rate of spread he took a greater number of readings. The combination of his observations and the regular weather reports at the Portland airport enabled the development of weather and wind files with acceptable time intervals.

Conditional Fuel Files

There are four conditional fuel files – the adjustment file, the moisture file, the custom fuel model file, and the conversion file. The adjustment file can be used by an experienced modeler or in conjunction with local data to tune the simulation to observed or actual fire spread patterns. The adjustment file values for all fuel models used in this study were set to 1.0, which maintains the original spread rate for the fuel model.

The fuel moisture file provides fuel moistures required to begin the process of calculating site specific fuel moistures at each time step throughout the simulation. The initial fuel moisture is based on Rothermel's (1991) drought summer moisture content percentages for standard timelag fuel components (1h, 10h, 100h and live). For drought summer conditions and late summer severe drought condition the initial fuel moisture values for each fuel model would be:

Fuel:	Summer Drought (%)	Late Summer Severe Drought (%)
1h:	4	3
10h:	5	4
100h:	7	6
live:	78	70

For this study the summer drought moisture values were used because the summer of 1951 was considered a drought year. The fuel moisture was used to condition the fuel prior to the simulated fires. Fuel moisture is calculated based on the inverse diurnal fluctuations of relative humidity and temperature at the forest floor. Furthermore, the percentage of tree cover over an area also impacts fuel moisture. Tree cover is part of the landscape file discussed later in this section. For example, as the percentage of tree cover increases the relative humidity remains higher and the temperature lower. The result would be higher fuel moistures because less heated air flows over the fuels and they dry out at a slower rate. Weather and wind data from August 2nd, 16 days prior to the outbreak of the 1951 fire were applied to the initial fuel moisture values.

The other fuel files are only required if the simulation will use custom fuel models. Simulation in this study used custom fuel models. Therefore, a custom fuel model file was developed. A custom fuel model consists of the same fuel model parameters discussed in Chapter 5. Additionally, when the fuel map for this study was developed it was generated using standard fuel model numbers because one of the simulations tested was based on Anderson's standard fuel models. Therefore a conversion was created in order to use the custom fuel models file in a simulation. The conversion file is necessary if the fuel model numbers specified in the landscape file do not correspond directly to the fuel model numbers in the custom fuel model file.

The Landscape File

The data is imported from the GIS as a binary file (ASCII) comprised of a header and a body of short integers for each of the themes it contains. The header contains information on the bounds of the study area, the resolution of the cells, and the units of the themes. The landscape file must contain five basic themes; elevation, slope, aspect, fuel model, canopy cover. The file may also include optional files for stand height, crown base height, and crown bulk density. Files were developed for each of these themes for this study.

Landscape File: Topographic Themes

The study area spread across three 10m Quadrangle DEMs, which were subsequently put in a single mosaic. The mosaic had a mask applied to reduce the data to the park area plus a 1.24 mile buffer around the park boundary. The buffer distance was selected to account for development adjacent to the park. Since fire will not stop at the park boundary the buffer provides additional area for fire spread. The buffer enables placement of an ignition point outside of the park to see if a fire will spread into the park. The buffer is also large enough to observe where fire is likely to escape from a fire started in the park.

Landscape File: Fuel Map Development Process

The landscape file is developed from GIS raster datasets. The terrain themes are derived from USGS DEMs as discussed previously, but the fuel-related themes require a fuel map of the study area. The quickest way to inventory the fuel of an area is through the interpretation and classification of multi-spectral imagery. Therefore, multi-spectral imagery of the study area was acquired and used to develop a base fuel

map. Additionally, the original imagery was transformed using a vegetation index model.

The indexed fuel map was derived from the spectral response pattern of the canopy and therefore represents the vegetative cover of the area. Based on the canopy cover found in the area assumptions can be made about the vegetation and composition of the understory and substrate fuels. Fuel models represent the substrate fuel loads. The base fuel map represents the standard fuel models that were selected to represent the fuel types found in the study area. The following sections of this chapter explain the process of developing the initial fuel map and subsequent fuel-related themes for use in the landscape file.

The development of an accurate fuel map is critical to the success of this study, since the fuel map is the basis for all of the fuel-related raster themes. Development of the fuel map was a multi-step process (Figure B1) that began during the summer of 2004 with the identification of sampling plots within the park. These plots were used to collect data for developing the custom surface fuel models and providing canopy-related data for the simulations.

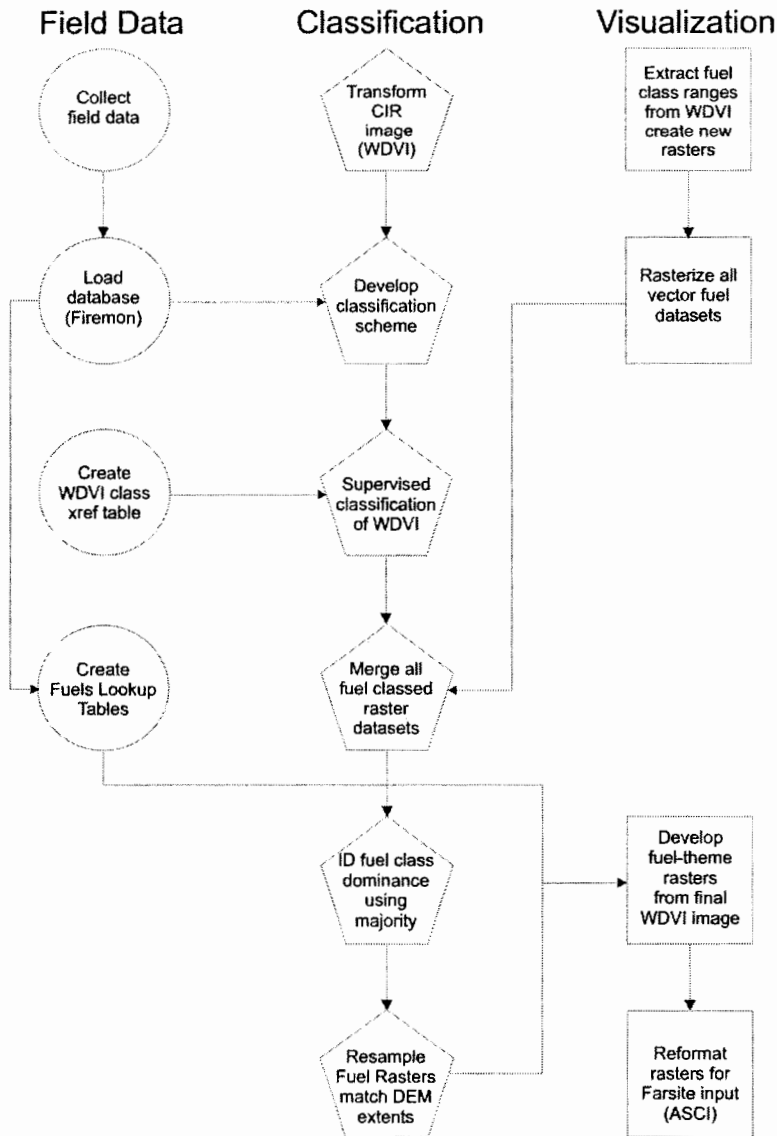


Figure B1: steps involved in fuel mapping process. (Source: flowchart drawn by Author)

The total study area includes a 1.24 mile buffer around the park boundary. The buffer was based created from a set of polygons representing the Forest Park National Vegetation Classification Standard (FP NVCS) unit data, which extends to the park boundary (Figure B2). The FP NVCS was developed by the City of Portland to study the ecology of the park. The polygon units classify areas of Forest Park into

vegetation classes and subclasses based on national vegetation classification standards. The FP NVCS is too coarse to use as the basis for fuel themes. Un-realistically “smoothed” fire spread can occur when fuel themes are too homogenized and do not accurately represent fuel variations over the simulation area (Finney 1998).

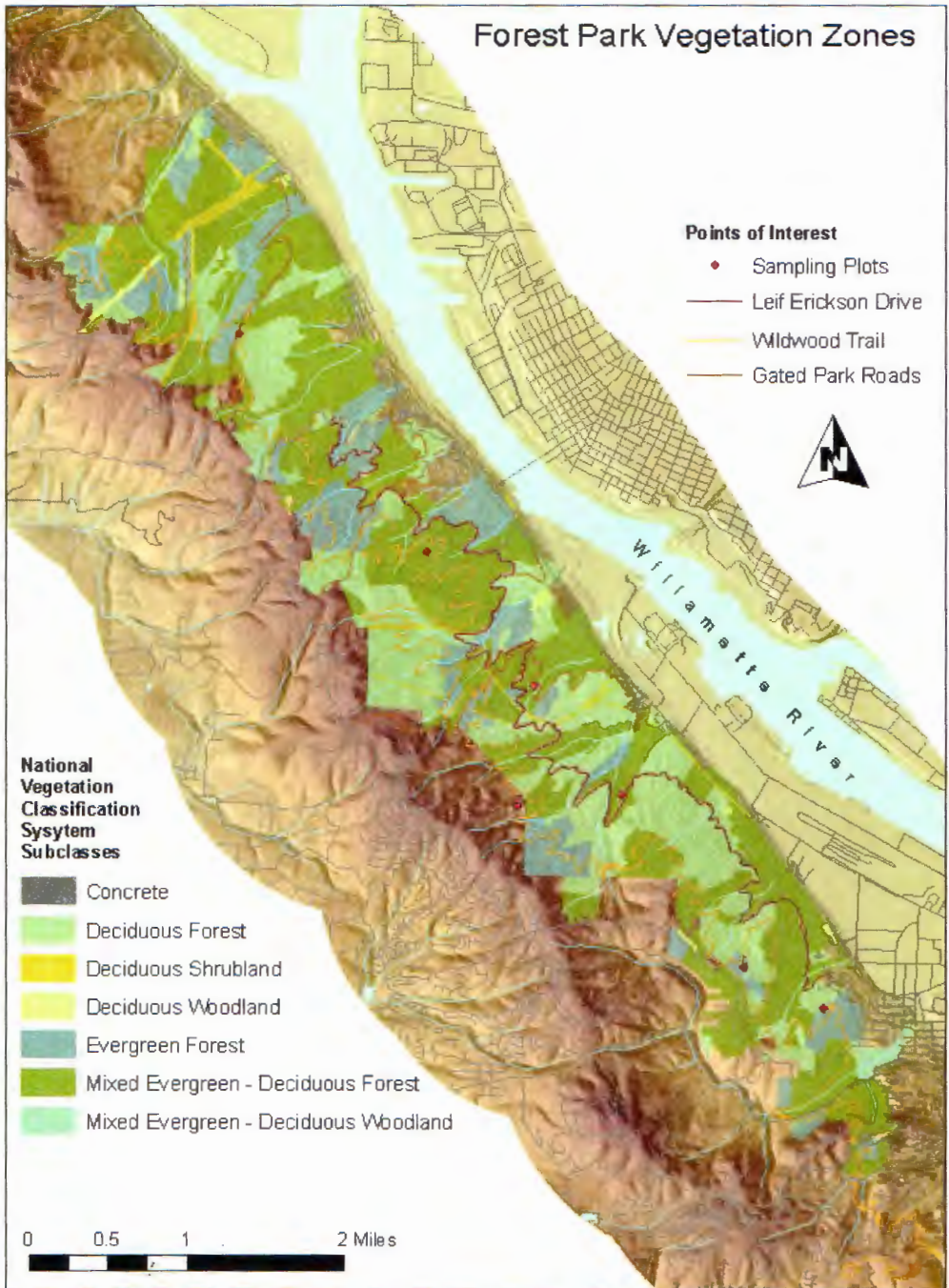


Figure B2: Forest Park vegetation zones. 1.24 mile buffer is represented by the colored image. The fuel map extends to the edge of the buffer. (Base Map Source: USGS, City of Portland, Metro RLIS)

The FP NVCS was used as a guide for conducting reconnaissance for placement of sampling plots in the park. Since the FP NVCS extended to the park boundary it was also convenient to use as the basis for developing the boundary of the simulation area. However, the multi-spectral imagery used to develop the fuel map did not extend 1.24 miles beyond the park's southeastern boundary (Figure B3). Subsequently, many of the fuel maps will have missing data in the lower-right corner.

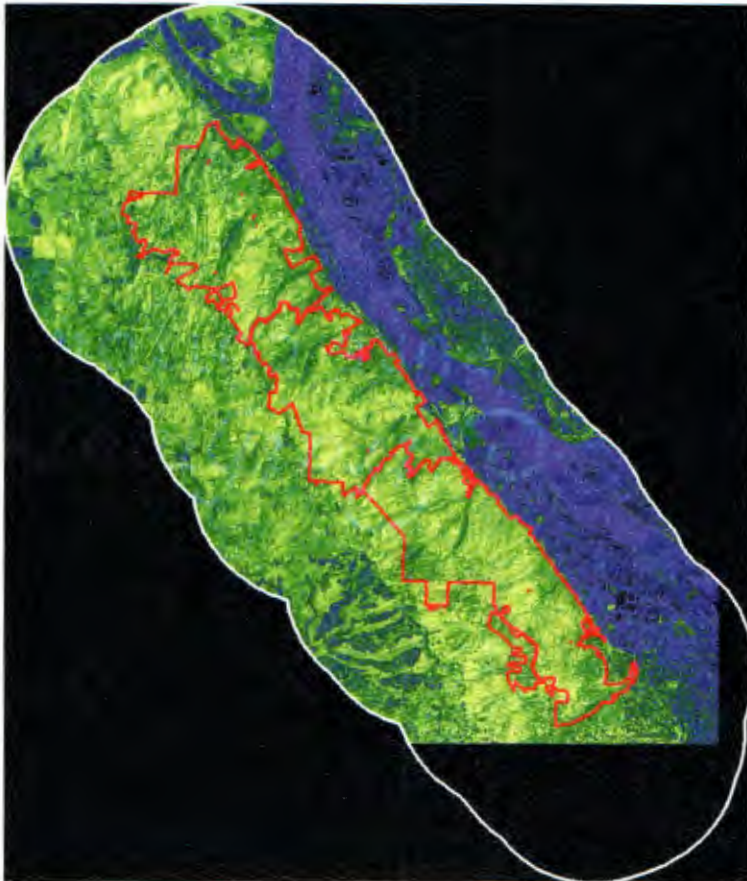


Figure B3: The extent of the multi-spectral image compared to the 1.24 mile buffer. The white line represents the 1.24 mile buffer. The red outline is the Forest Park boundary. (Base map source: City of Portland)

Landscape File: Canopy Themes

Three additional canopy-related themes were used in the landscape file. The themes included stand height, crown base height, and crown bulk density which are necessary for simulation of crown fire potential and behavior. The data used to develop the themes was based on output from the Firemon and FuelCalc applications. Stand height, and crown base height (CBH) data was calculated using data from Firemon. The crown bulk density (CBD) data was calculated using FuelCalc.

The stand height calculations were based on weighted average heights from the sampling plot tree species data. The formula used the species basal area per hectare divided by the total basal area per hectare as a weight upon which to base a representative average height for a fuel model type. For example: plot 1 represents model 10 based on tree species composition. The total basal area per hectare was 82.2 m²/ha. The weighted percentages for the plot were:

ACMA3 (bigleaf maple) basal area was 13.6

equaling a weight of $13.6/82.2 = 16.5\%$

PSME (Douglas-fir) basal area was 68.1 weight

equals $68.1/82.2 = 82.8\%$

TSHE (Western Hemlock) basal area was .5 weight

equals $.5/82.2 = .6\%$

The average species tree height was multiplied by the weighted average.

ACMA3 avg height * ACMA3 weight = $27.9 * 16.5 =$

460.35

PSME avg height * PSME weight = $47.4 * 82.8 =$

3924.72

TSHE avg hgt * TSHE weight = $7.6 * .6 = 4.56$

The sum of all weighted average heights divided by 100 equals the plot stand height to represent the associated fuel model.

Plot 1 stand height = 43.9m

The stand height for each plot were calculated this way and then aggregated and averaged to represent the appropriate fuel model.

plot 1 = 43.9 m	plot 2 = 33.7m	plot 3 = 22.3 m
plot 4 = 25.3 m	plot 5 = 27.5 m	plot 6 = 20.3 m
plot 7 = 23.5 m		

The subsequent Stand Height by fuel model was calculated for fuel models:

8 = 22 m	9 = 29.5 m	10 = 35.7 m
----------	------------	-------------

The CBH was based on sapling/snag heights found in the plots and live crown base height of the trees. The delta between the average sapling heights and the live crown base height was used as the crown base height. Since the saplings act as ladder fuel, the fire would have to be intense enough with the proper flame length to transition to the tree crowns by leaping the gap.

CBD was calculated for each sampling plot using FuelCalc. CBD density is volume of vegetation in the canopy. The greater the volume of fuel the greater the potential for higher intensity crown fire. FuelCalc's plotting tool provided a visual perspective on the average canopy height and base height. The plotted data also acted as an abstract of the profile of sampling plots vegetative stratum. For example, in sampling plot 3 (Figure B4) there was a bi-modal distribution in the vegetation stratum, the understory trees were mature and dense enough to produce significant

bulk density. In this regard the ladder capacity in that stand type would be much greater than that found in sampling plot 1 (Figure B5).

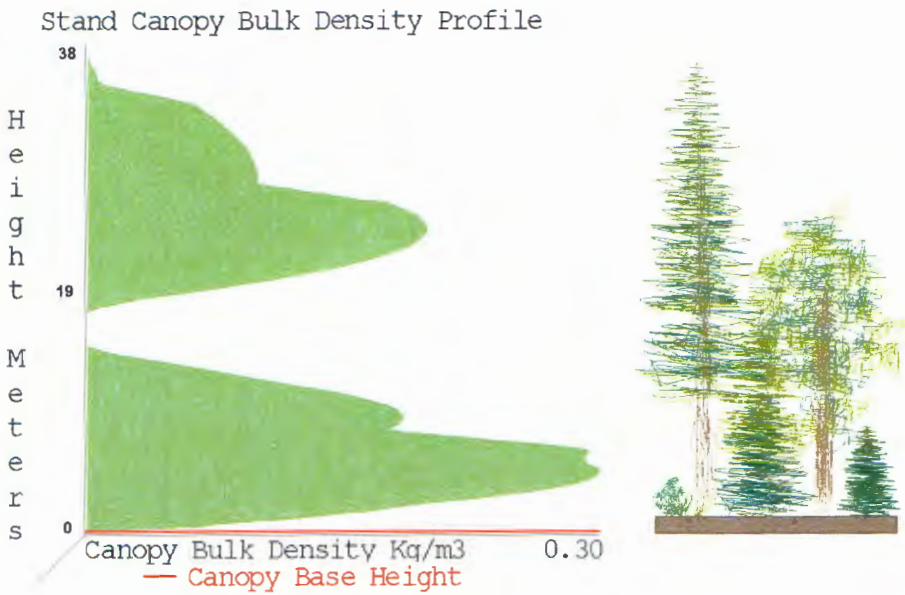


Figure B4: FuelCalc Canopy Bulk Density profiles calculated from the tree data collected at sampling plot 3. Plot 3 has a low calculated canopy base heights and significant crown bulk density from the understory to the overstory. This type of fuel stratum has high potential for laddering fire, which leads to torching trees and active crown fire. (Source: FuelCalc output, tree illustration drawn by Author)

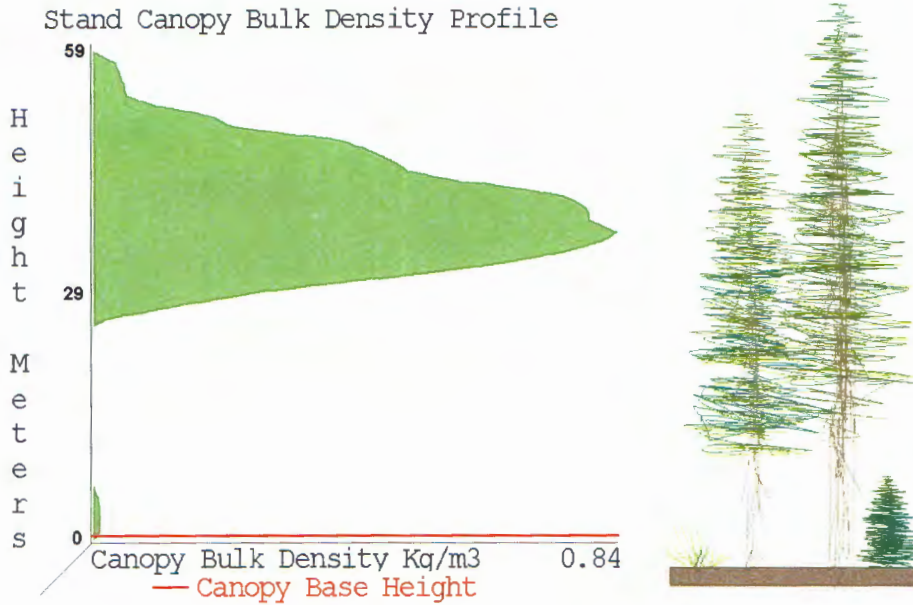


Figure B5: FuelCalc Canopy Bulk Density profiles calculated from the tree data collected at sampling plot 1. This is also a good example of how low calculated canopy base heights are not necessarily indicative of high ladder potential and crown fire. (Source: FuelCalc output, tree illustration drawn by Author)

Fieldwork Data Collection and Vegetation Sampling

Fieldwork began on August 3rd and was concluded on September 7th, 2004.

The process began by conducting reconnaissance in the area for the placement of study plots. The criteria for selecting the plots were a function of environment, time, and resources. Plots were selected based on a relevé approach, which is an ecological sampling technique similar to a stratified random sample. Plots were placed in representative portions of the stand “without preconceived bias”, meaning that the plots are located in order to represent the general conditions of a sampling stratum (Firemon 2003).

This approach is a qualitative classification method. The dominant, sub-dominant, and vegetation layers are considered homogeneous and visually

distinguishable from other sample stands. The presence and absence of species is considered more important than variations in quantity. The method relies on recurring plant assemblages from the substrate to the overstory as the primary means of classification (Mueller-Dombois and Ellenberg 2002).

Firemon standards were adopted in keeping with the theme of using only wildland fire behavior techniques to see if the same practices could be used in the urban interface. There are multiple rationales for this decision. First, analytical tools and fire models specific to urban forests do not exist. Second, given the size of the park and unmanaged growth the same field measurements and assessment procedures used for a wide-area wildland environment would be applicable. Third, the ability to design a custom fuel model based on Firemon reporting and FuelCalc tools provided the necessary inputs for Farsite. Lastly, using applications already integrated with ArcGIS minimizes the learning curve and enables the simulations to be conducted on an available and familiar platform.

The plot selection criteria considered fire history, forest composition, and topographic orientation. Plots had to vary in elevation, aspect, and slope. Forest Park has heterogeneous stand development. The heterogeneity extends to species composition and fuel strata. The number of plots was a consideration based on the time to complete the study and the availability of research assistants.

Seven suitable study plots were identified based on the selection criteria. Plot density was based on previous wildland area studies where 0.05% of the total area was sampled (Keane, et al, 2000). Plot selection was coordinated through the staff of Portland Parks. In order to retrieve the desired data from each plot, a team of three

field workers was required. The field workers had to be trained and monitored to ensure proper measurements were taken. All the data had to be collected during the fire season. The plot density of this study equated to 0.35% of total area sampled.

Each plot was marked using a permanent center marker. The plots have a radius of 12.62 meters representing an area of .05 hectares. The center of each plot was identified using a GPS (Figure B6). Establishing permanent plots has the long-term advantage of enabling the city of Portland to maintain a spatial constant for the assessment of fire hazard as the forest succession changes.

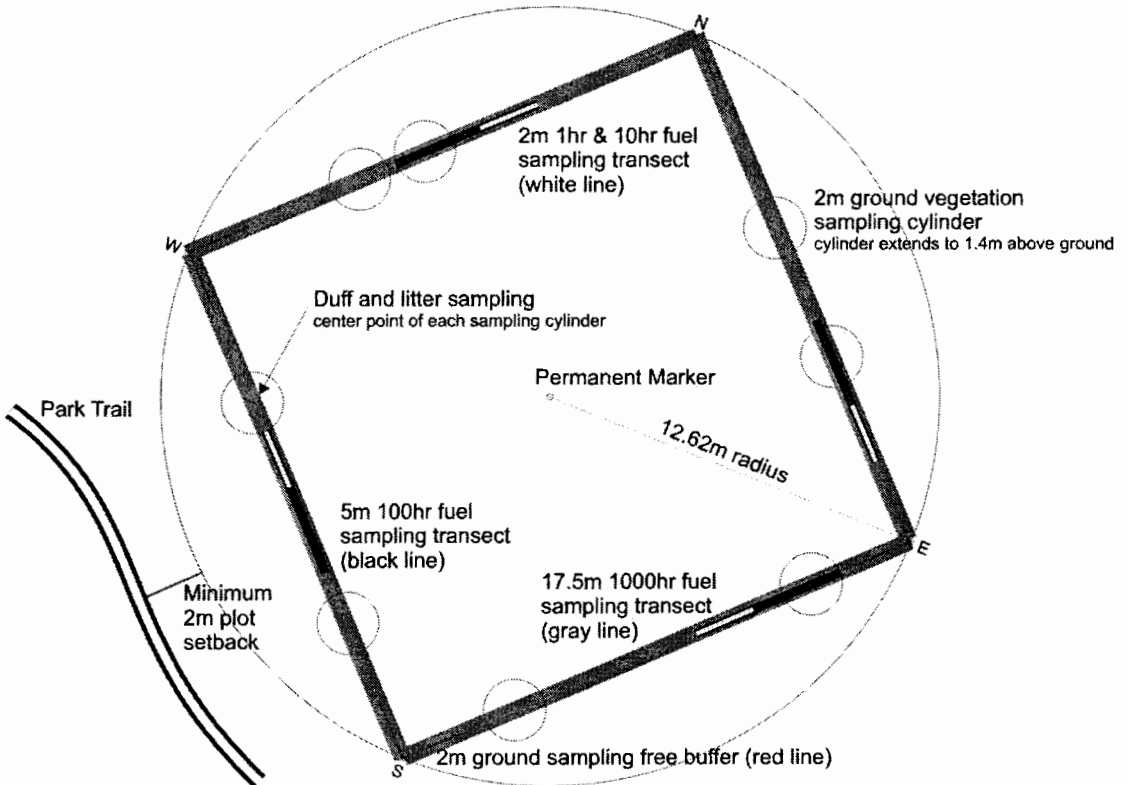


Figure B6: Example of a sampling plot and subplot sampling methods. Ground vegetation sampling cylinders, 2m (1hr/10hr) sampling transects, and 5m (100hr) sampling transects are placed randomly along the box transects. (Source: illustration drawn by Author)

The data from each plot was recorded in spreadsheets and then entered into the Firemon database. Plot-level tree summary (Figure B7a and B7d) and fuel loading summary reports were calculated and printed from Firemon. The fuel loading summary (Figure B7b) report was divided into down woody debris (DWD) and vegetation reporting. The DWD report included kg per m² for 1, 10, 100, 1000-hr timelag fuel, duff, and litter. The vegetation summary (Figure B7c) reported average shrub and herbaceous height, as well as live and dead shrub and herbaceous biomass (kg/m²). These reports were the initial inputs for the custom surface fuel models and canopy fuels.

A.
Tree Summary

RegID	ProjID	PlotID	Date	Sample Event	Trees (per ha)	Basal Area (sq. m / ha)	Avg. Live Crown Base Height (m)	Avg. Height (m)	QMD (cm)	Saplings (per ha)	Seedlings (per ha)	Total Trees (per ha)	Snags (per ha)
							Mature Trees						
fpfm	fpum	1	8/05/04	P1	380.0	82.2	18.0	34.0	52.5	120.0	.0	500.0	60.0
fpfm	fpsim	2	8/12/04	P1	380.0	63.9	12.3	24.9	46.3	240.0	.0	620.0	60.0
fpfm	fpsim	3	8/18/04	P1	880.0	49.6	11.5	22.1	30.5	340.0	.0	1020.0	120.0
fpfm	fpsim	4	8/19/04	P1	500.0	43.7	15.6	24.3	33.4	160.0	.0	660.0	100.0
fpfm	fpsim	5	9/07/04	P1	260.0	32.5	11.9	23.9	39.9	120.0	.0	380.0	100.0
fpfm	fpsim	6	8/17/04	P1	540.0	66.5	8.0	17.1	39.6	500.0	.0	1040.0	260.0
fpfm	fpsim	7	8/03/04	P1	580.0	68.6	11.9	23.2	38.8	.0	.0	580.0	180.0

B.

Fuel Loading Summary

RegID	ProjID	PlotID	Date	Sample Event	1-hr	10-hr	100-hr	1-100-hr	1000-hr Sound	1000-hr Rotten	1-1000-hr	Duff	Litter	Total	Duff	Litter	Total
					Kilograms per Square Meter											Depth (cm)	
fpfm	fpaim	1	8/05/04	P1	0.07	0.24	0.7	1.0	1.43	.8	3.2	4.3	2.0	9.5	12.4	11.4	23.8
fpfm	fpaim	2	8/12/04	P1	0.03	0.62	0.61	1.26	0.32	.2	1.8	3.2	2.1	7.1	9.4	11.9	21.3
fpfm	fpaim	3	8/18/04	P1	0.06	0.57	0.5	1.13	2.51	2.7	5.4	2.9	3.2	12.4	8.3	18.4	26.7
fpfm	fpaim	4	8/19/04	P1	0.09	0.38	0.66	1.13	0.71	.2	2.0	1.5	3.0	6.6	4.4	17.5	21.9
fpfm	fpaim	5	9/07/04	P1	0.07	0.36	0.46	0.9	6.76	2.1	9.8	3.3	1.5	14.6	9.5	8.9	18.4
fpfm	fpaim	6	8/17/04	P1	0.29	0.61	0.4	1.3	1.14	.2	2.7	2.6	3.0	8.2	7.4	17.1	24.4
fpfm	fpaim	7	8/03/04	P1	0.14	0.46	0.86	1.45	0.9	1.8	4.2	2.3	2.2	8.7	6.6	12.9	19.5

C.

Fuel Loading Vegetation Summary

RegID	ProjID	PlotID	Date	Sample Event	Shrub Cover %		Shrub Height (m)	Herbaceous Cover %		Herbaceous Height (m)	Biomass (kilograms per sq.)			
					Live	Dead		Live	Dead		Shrub		Herbaceous	
											Live	Dead	Live	Dead
fpfm	fpaim	1	8/05/04	P1	7.38	4.12	0.89	94.5	61.25	0.87	0.17	0.05	0.51	0.3
fpfm	fpaim	2	8/12/04	P1	11.5	1.25	0.46	82.0	55.0	0.56	0.24	0.03	0.38	0.23
fpfm	fpaim	3	8/18/04	P1	7.56	0.0	0.34	92.5	46.5	0.35	0.18	0.0	0.26	0.11
fpfm	fpaim	4	8/19/04	P1	3.0	0.0	0.4	71.0	51.0	0.56	0.09	0.0	0.34	0.21
fpfm	fpaim	5	9/07/04	P1	2.5	0.0	0.31	91.5	52.5	0.56	0.06	0.0	0.42	0.2
fpfm	fpaim	6	8/17/04	P1	17.88	0.38	1.08	85.5	37.0	0.54	0.51	0.0	0.38	0.15
fpfm	fpaim	7	8/03/04	P1	.56	0.19	0.17	76.75	29.12	0.52	0.0	0.0	0.34	0.11

D.

Tree Summary by Species

RegID	ProjID	PlotID	Date	Sample Event	Species	Trees (per ha)	Basal Area (sq. m / ha)	Avg. Live Crown		QMD (cm)	Saplings (per ha)	Seedlings (per ha)	Total Trees (per ha)	Snags (per ha)
								Base Height (m)	Avg. Height (m)					
Mature Trees														
fpfm	fpaim	1	8/05/04	P1	ACMA3	180.0	13.6	13.2	27.9	31.0	20.0	.0	200.0	40.0
fpfm	fpaim	1	8/05/04	P1	AEHI	0.0					20.0	.0	20.0	.0
fpfm	fpaim	1	8/05/04	P1	COCOC2	0.0					40.0	.0	40.0	.0
fpfm	fpaim	1	8/05/04	P1	ILAQ80	0.0					20.0	.0	20.0	.0
fpfm	fpaim	1	8/05/04	P1	PSME	160.0	68.1	27.6	47.4	73.6	.0	.0	160.0	20.0
fpfm	fpaim	1	8/05/04	P1	TSHE	40.0	0.5	0.8	7.6	12.4	20.0	.0	60.0	.0
fpfm	fpaim	2	8/12/04	P1	ACMA3	260.0	23.2	10.7	21.1	33.7	20.0	.0	280.0	.0
fpfm	fpaim	2	8/12/04	P1	ALRU2	20.0	2.4	15.5	24.4	39.2	.0	.0	20.0	60.0
fpfm	fpaim	2	8/12/04	P1	PSME	80.0	37.9	19.8	42.2	77.7	.0	.0	80.0	.0
fpfm	fpaim	2	8/12/04	P1	THPL	0.0					220.0	.0	220.0	.0
fpfm	fpaim	2	8/12/04	P1	TSHE	20.0	0.3	0.5	6.1	13.5	.0	.0	20.0	.0
fpfm	fpaim	3	8/18/04	P1	ABGR	20.0	0.3	2.0	9.5	13.0	20.0	.0	40.0	20.0
fpfm	fpaim	3	8/18/04	P1	ACMA3	320.0	20.7	17.3	28.7	28.7	.0	.0	320.0	20.0
fpfm	fpaim	3	8/18/04	P1	ALRU2	0.0					.0	.0	.0	60.0
fpfm	fpaim	3	8/18/04	P1	PSME	180.0	18.4	11.0	22.0	38.3	20.0	.0	180.0	.0
fpfm	fpaim	3	8/18/04	P1	THPL	180.0	9.9	0.3	9.5	28.0	260.0	.0	420.0	20.0
fpfm	fpaim	3	8/18/04	P1	TSHE	20.0	0.4	20.6	30.8	15.0	40.0	.0	60.0	.0
fpfm	fpaim	4	8/19/04	P1	ABGR	20.0	0.2	2.7	8.4	11.0	.0	.0	20.0	.0
fpfm	fpaim	4	8/19/04	P1	ACMA3	240.0	20.3	15.3	24.9	32.8	60.0	.0	300.0	20.0
fpfm	fpaim	4	8/19/04	P1	ALRU2	220.0	22.8	18.1	28.1	36.2	.0	.0	220.0	40.0
fpfm	fpaim	4	8/19/04	P1	PSME	20.0	0.5	5.8	12.8	18.5	80.0	.0	100.0	20.0
fpfm	fpaim	4	8/19/04	P1	TSHE	0.0					20.0	.0	20.0	20.0
fpfm	fpaim	5	9/07/04	P1	ABGR	20.0	0.2	3.0	8.6	11.8	40.0	.0	60.0	.0
fpfm	fpaim	5	9/07/04	P1	ACMA3	40.0	5.4	13.2	28.0	41.6	.0	.0	40.0	.0
fpfm	fpaim	5	9/07/04	P1	ALRU2	0.0					20.0	.0	20.0	.0
fpfm	fpaim	5	9/07/04	P1	COCOC2	0.0					20.0	.0	20.0	.0
fpfm	fpaim	5	9/07/04	P1	PSME	100.0	17.5	17.6	28.8	47.2	.0	.0	100.0	20.0
fpfm	fpaim	5	9/07/04	P1	THPL	40.0	0.7	0.0	7.9	15.4	40.0	.0	80.0	.0
fpfm	fpaim	5	9/07/04	P1	TSHE	60.0	8.6	12.4	28.8	42.6	.0	.0	60.0	80.0
fpfm	fpaim	6	8/17/04	P1	ABGR	240.0	7.8	4.1	13.1	20.3	180.0	.0	420.0	160.0
fpfm	fpaim	6	8/17/04	P1	ACMA3	180.0	17.7	12.9	20.3	37.6	20.0	.0	180.0	60.0
fpfm	fpaim	6	8/17/04	P1	ALRU2	20.0	3.1	11.2	25.7	44.5	.0	.0	20.0	60.0
fpfm	fpaim	6	8/17/04	P1	COCOC2	0.0					260.0	.0	260.0	.0
fpfm	fpaim	6	8/17/04	P1	CONU4	0.0					20.0	.0	20.0	.0
fpfm	fpaim	6	8/17/04	P1	PSME	100.0	37.7	10.3	21.4	69.3	20.0	.0	120.0	.0
fpfm	fpaim	6	8/17/04	P1	THPL	0.0					.0	.0	.0	20.0
fpfm	fpaim	6	8/17/04	P1	TSHE	20.0	0.2	1.4	7.9	12.0	.0	.0	20.0	20.0
fpfm	fpaim	7	8/03/04	P1	ABGR	180.0	11.6	11.3	19.8	30.3	.0	.0	180.0	80.0
fpfm	fpaim	7	8/03/04	P1	ACMA3	200.0	25.2	15.1	24.4	40.1	.0	.0	200.0	60.0
fpfm	fpaim	7	8/03/04	P1	ALRU2	40.0	3.8	18.6	29.1	34.7	.0	.0	40.0	.0
fpfm	fpaim	7	8/03/04	P1	TSHE	180.0	28.0	7.3	23.6	44.5	.0	.0	180.0	40.0

Figure B7: Firemon reports and data exports were used to develop many of the fuel related themes for the fire simulations. Fuel loading and vegetation summary data were used as direct inputs for the custom surface fuel models. The tree summary and species data served as the basis for many of the canopy-related fuel themes. See Appendix A for species code definitions. (Source: Firemon output based on data compiled by Author)

Sampling Methods. The Firemon sampling methods specific to this type of analysis are the *Tree Data (TD) Sampling Method* and *Fuel Load (FL) Sampling Method* (Keane, et al. 2000). The TD methods are used to sample individual live and dead trees within the plot area. The data is used to estimate tree density, size, and canopy characteristics for a contiguous stand's overstory. FL methods include all measurements for the substrate and understory. The FL methods are used to tally standard fire size classes for dead and down woody debris on the forest floor (Firemon 2003).

Both methods provide ecological and quantitative estimates for fire behavior inputs. Because of the subjective nature of the classification processes incorporated in each sampling method the class values are determined by committee. Each plot had minimally four people working at it at a time, usually in groups of two. Before a tree or fuel class was assigned the pair had to agree on the class value in question. The FL sampling procedure is conducted first. The TD sampling process requires a fair amount of tromping and traversing through the plot. The disturbance of the understory and substrate could adversely impact the surface fuel data. This was especially true given the slope and substrate characteristics encountered in Forest Park.

Fuel Load: Woody Debris, Substrate and Understory Vegetation. Dead woody debris (DWD) can be classified into two components, fine woody debris and coarse woody debris. The primary difference between fine and coarse woody debris is the diameter of the piece (Table B1). Fine DWD data is most associated with fire behavior because smaller twigs and sticks reach ignition temperature faster than coarse

DWD. Coarse DWD is more closely associated with fire effects because of the longer emission and combustion process. Burning logs have longer term effects on both the floral and faunal components of the ecosystem. Therefore the coarse DWD components play a reduced role in the development of surface fuel models (Firemon 2003).

Table B1: Dead woody debris components and size class thresholds. (Firemon 2003).

DWD Components		Classes	Piece Diameter (cm)	Length
DWD	FDWD	1-hr	0.0 - 0.6	undefined
		10-hr	0.6 - 2.5	undefined
		100-hr	2.5 - 8.0	undefined
	CDWD	1000-hr	8.0 or greater	1m or greater

Fine DWD is hand-counted along sub-plot transects laid out in a box shape within the sampling plot. The length of transect is based on the DWD size class. One-hour and 10-hour fine DWD size classes are counted along a 2m transect. Hundred-hour fine DWD is counted along a 5m transect. The starting point of both the 2m and 5m fine DWD transects are randomly placed at the same point along the 17.5m leg of the box transect within the sampling plot. Thousand-hour coarse DWD is counted along the entire length of the 17.5m leg (Figure B6). A measuring tape is laid down as close to the surface as possible and each piece that crosses the plane of the tape is counted and classed (Figure B8)

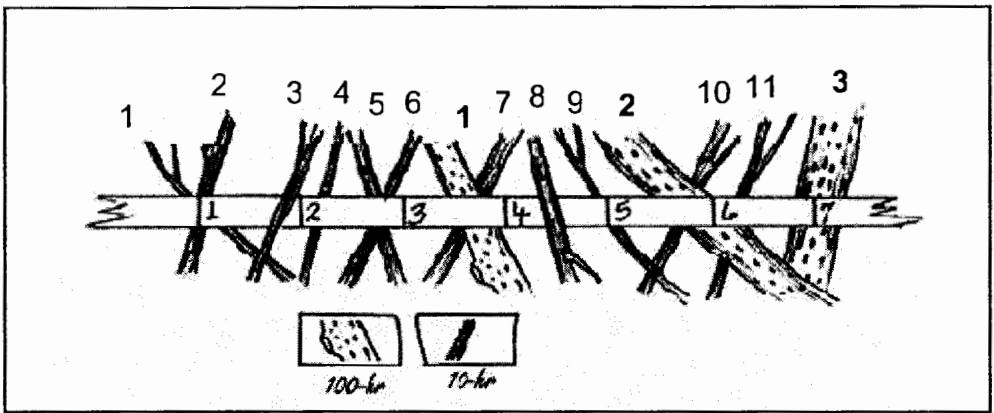


Figure B8: Example of tape placement and piece counting for fine DWD using the transect sampling method (Firemon 2003).

For each transect leg two randomly selected locations are chosen for ground cover vegetation sampling (Figure B6). The sampling area consists of a 2m cylinder with a sampling plane that extends 1.8m above the surface. Within each sampling cylinder the live and dead understory vegetation cover is recorded. The coverage area for both live and dead members of a species occupying the cylinder is recorded. For example: five sword ferns are found within the sampling cylinder, four are living and one is dead. The four living specimens cover over 90 percent of the cylinder, the dead fern covers 20 percent. Two records would be logged, one for the dead fern and one for the four living ferns. For the study area vegetation coverage within the cylinder is expected to be greater than 100%. The measurement collected from this sampling are used to calculate the tons per hectare for live herbaceous and woody plant material, as well as the surface area to volume ratio for dead fuels, and live herbaceous and woody fuels.

Duff and litter depth measurements are taken at the center points of every sampling cylinder (Figure B9). Litter is usually more closely associated with fire behavior. Duff is mostly associated with fire effects. Litter burns and helps sustain

combustion because it is loosely packed and has lower moisture and mineral content. The duff which lies beneath the litter contains more moisture and mineral content because it is comprised of more decomposed plant materials. By its very nature duff is more compacted with less exposure to air, further decreasing its combustibility (Firemon 2003). The total litter/duff profile depth and the percent litter estimation help calculate the total fuel load of the substrate.

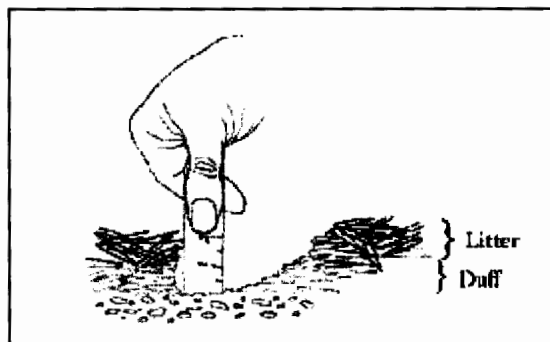


Figure B9: Example of measuring the litter/duff profile. The litter/duff delineation is identified by the decomposition state of the litter. When litter gets to the point where it can not be discerned from which plant it originated then it is considered duff. Below the duff layer is mineral soil (Firemon 2003).

Tree Data: Ecology and Canopy Measurements. Plot size was largely determined by the expected median tree diameter, height, and density. As a general rule at least 20 trees above the breakpoint diameter should occupy the plot. The breakpoint diameter is the diameter at 1.4m above the ground also known as diameter at breast height (DBH). The breakpoint diameter separates the trees classified as mature from those classified as samplings (Firemon 2004). Seedlings by definition are young trees less than 1.4m tall and were not tallied during the study. Seedling data is more associated with fire effects and ecological impact. The breakpoint diameter for this study was set at 10cm DBH. Trees with a DBH or less than 10cm were classified

as samplings and went through a different sampling method. Snags were also sampled in every plot.

After the plots had been established and the surface fuel sampling had been conducted the tree sampling could begin. The first step was to flag every tree within the plot by walking in a clockwise direction around the plot to ensure that all trees were marked in order and accounted for. Multi-color and numbered flags were used to identify the different tree classes. Red flags were used for mature trees, yellow for saplings, and orange for snags. Trees that could not be visibly classed were measured. The first measurements taken were the distance from center and azimuth from true North (Figure B10). Each tree and snag location was measured so that its location could be plotted for more detailed spatial analysis of the plot. Once again this level of detail is for fire effects purposes and ecological impact. This data was ultimately not used in this study.

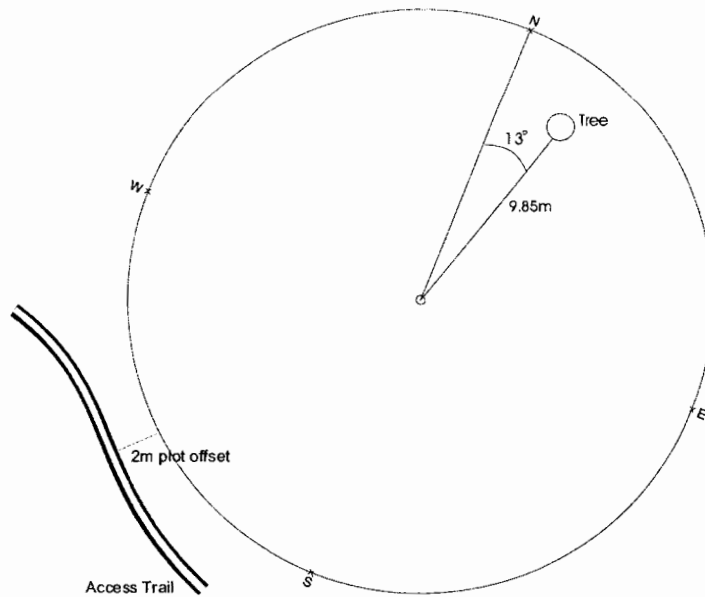


Figure B10: Example of plotting tree distance from center and azimuth from true North. The process required two people to ensure that the tape measure was held level with the slope of the plot. The person standing at center also sited the compass for the azimuth measurement. Illustration by author.

Once at the tree or snag several structural and ecological measurements are taken. The structural measurement include DBH, height, live crown ratio, crown fuel base height, canopy diameter, and crown class. The ecological characteristics recorded include species, health, mortality code or decay class for snags. The structural measurements are used to calculate a number of fire behavior inputs such as canopy bulk density, vertical fuel ladders, and height to the base of the canopy (Firemon 2004).

The first measurement taken is DBH. DBH is measured by standing on the up-hill side of the tree using a diameter tape pulled tightly around the tree at the reference height. This measurement is used in calculating the basal area of the trees. The basal

area is represented by the cross-section area of all trees in square meters per hectare. This figure is used to determine tree density and stocking in the representative stand. Tree species is identified using the FRCC - NRCS Plant Code List:

Common Name	Scientific Name	Plants Code
Grand Fir	<i>Abies grandis</i>	ABGR
Bigleaf Maple	<i>Acer macrophyllum</i>	ACMA3
Horse Chestnut	<i>Aesculus hippocastanum</i>	AEHI
Red Alder	<i>Alnus rubra</i>	ALRU2
Hazelnut	<i>Corylus cornuta var. cornuta</i>	COCOC2
Pacific Dogwood	<i>Cornus nuttallii</i>	CONU4
English Holly	<i>Ilex aquifolium</i>	ILAQ80
Douglas-fir	<i>Pseudotsuga menziesii</i>	PSME
Western red cedar	<i>Thuja plicata</i>	THPL
Western Hemlock	<i>Tsuga heterophylla</i>	TSHE

The health of the tree is determined. Health is broken down into 4 classes, healthy, unhealthy, sick or dead. Healthy trees exhibit very little biotic (e.g. insect) or abiotic (e.g. blowdown) damage. Unhealthy trees have some form of damage that will reduce growth, but not kill the tree. Sick trees have extensive damage that will likely kill the tree in the next 5-10 years (Firemon 2004). For dead trees and snag a mortality code is assigned if the cause of death can be identified. Causes include insects, fire, disease, abiotic, and harvest-related mortality. For snags decay class is recorded in the place of health. Decay class is recorded by a numerical code based on limb, bark, and sapwood retention, and the state of the top of the bole (e.g. pointed or broken).

The first crown related measurement is live crown ratio. Live crown ratio class is important in determining the ladder and torching potential of a tree (Figure B11). Numeric codes are given each tree based on a percentage of live crown. Live crown is the percent of the tree bole that is supporting live foliage. Using the trees in Figure 15 as an example; A, B, and C are considered the same ratio class because the crowns each have the same extent along the bole. Growth in A, B, and C would equate to the same biomass and ladder fuel capacity. Lone branches at the bottom of the crown that do not appear to be a part of the crown or have ladder fuel capacity are ignored during the classification process.

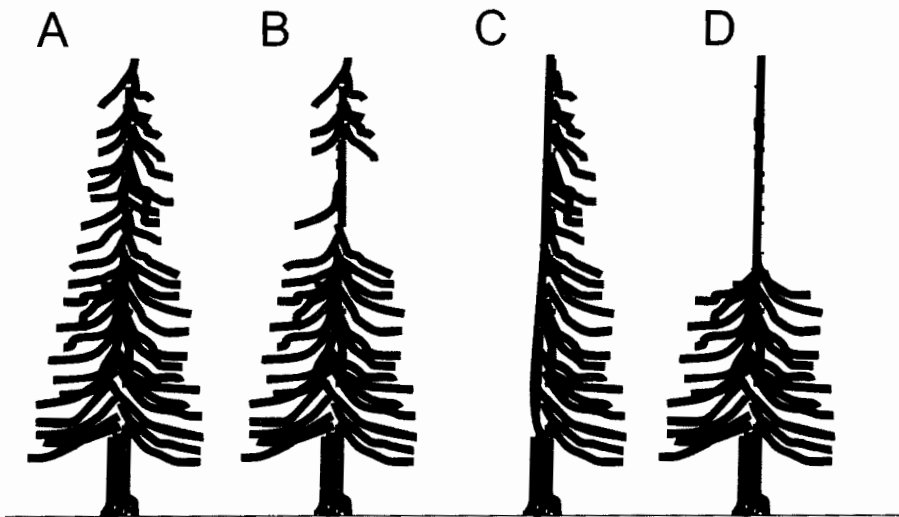


Figure B11: live crown ratio classification consists of assessing the percentage of the bole that is supporting live foliage. A, B, and C would be classed at 80%, where D would be classed at 40%. Illustration by author.

Crown class represents the position in the canopy that an individual tree occupies. The crown class assessment process attempts to analyze the amount of light that is available to the tree (Firemon 2004). For example, open grown trees are not taller than other trees, but still receive light from all directions. Crown class is broken

down into 6 classes; open grown, emergent, dominant, co-dominant, intermediate, and suppressed (Figure B12). Emergent trees are taller than any around them and have a portion of their crown above the canopy. Dominant trees will receive light from 3 to 4 directions, where co-dominant crowns will receive light from only 1 or 2 directions. Intermediate trees will receive light only on the tops of their crowns, where suppressed trees are completely shaded from direct sunlight.

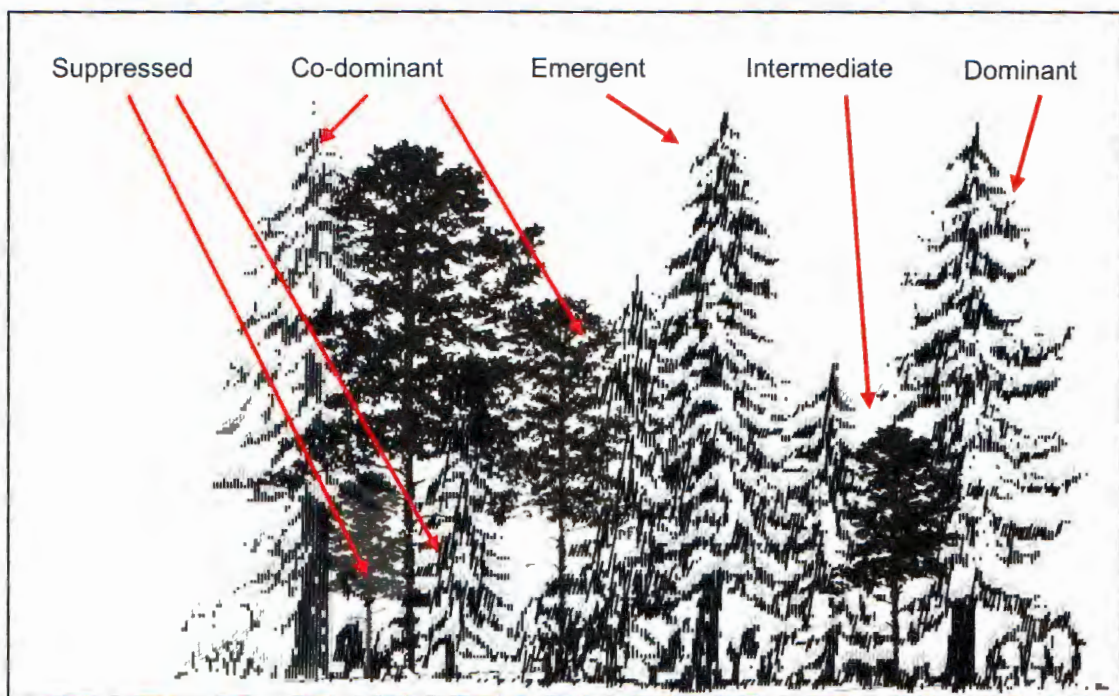


Figure B12: Examples of crown class types. Individual tree are classified based on the position in the canopy that they occupy. Illustration by author.

The height and crown base height measurements were taken using an electronic clinometer. The measuring process required multiple criteria be met before an accurate reading could be recorded. The distance between the tree bole and the clinometer had to be measured. From that vantage point the bottom of the bole and the top of the crown had to be visible. The angle from which the measurement was

taken could not exceed 60-degrees, at which point the clinometer reading became unstable. This process became time consuming under the canopy of a relatively dense forest of 25-50 meter tall trees.

APPENDIX C

Vegetation Index Technical Information

The "leaf on" image was flown between June 1st and June 20th, 2002.

Imagery was taken in 4 spectral bands; visible blue (0.41-0.49 μm), visible green (0.51-0.59 μm), visible red (0.61-0.69 μm), and near infrared (0.80-0.90 μm). Imagery was collected using GeoVantage's "GeoScanner" system on an unmodified Cessna aircraft flown at an altitude of 8,000 feet above ground, achieving a pixel resolution of approximately 1 meter. GeoScanner includes 4 discrete monochrome digital cameras with optical filters used to collect imagery in the 4 spectral bands. The cameras were mounted into a housing which included an Inertial Measurement Unit (IMU) that determines the precise acceleration and rotation of each of the cameras. The IMU, coupled with a GPS antenna, allowed for the determination of the precise altitude and location of the camera at specified imaging times. The imagery was Orthorectified and georegistered using USGS 10-meter DEMs of the mission area. Each pixel of each camera was spatially corrected, allowing for the creation of a composite mosaic image without an initial requirement for ground control points. The published multi-spectral dataset had a spatial resolution of 1.1 meters and an average horizontal error of 3.5 meters.

The soil line is a hypothetical line in spectral space that describes the variation in the spectrum of bare soil in the image. The relation between visible red and NIR spectral response pattern from bare soil is generally linear (Rondeaux *et al.* 1996). The soil line used in the WDVI function assumes that the ratio of NIR and red SRP of bare soil is constant and independent of soil moisture content. The line can be found by

locating two or more patches of bare soil in the image having different signatures and finding the best fit line in spectral space. Figure C1, C2, and C3 illustrate the process of determining the soil line slope.

The simplest way to identify the NIR-Red soil line is to make a scatterplot of the red and NIR values for the pixels in the image. Place red on the x-axis and NIR on the y-axis, and there should be a fairly linear boundary along the lower right side of the scatterplot. The straight line that points out the ratio of the NIR spectral response pattern over the red SRP of the image that best match this boundary is the soil line. The points that describe the boundary can be selected by a least squares fit or a line can be drawn that looks like the best fit (Gilvear and Bryant 2003).

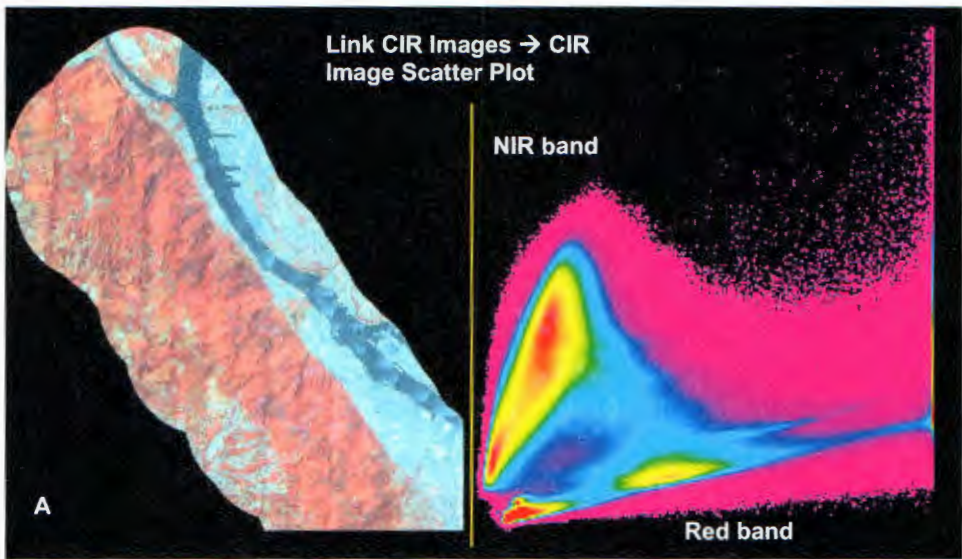


Figure C1: Linking the multi-spectral image to a feature space scatterplot (tasseled cap transformation) of the same image. The scatterplot would be best represented as a three-dimensional image. Areas green, yellow, and red indicate an increasing number of pixels with similar spectral response. The red areas would represent peaks in a three-dimensional distribution. (Source: data transformation from Idrisi and graphic by Author)

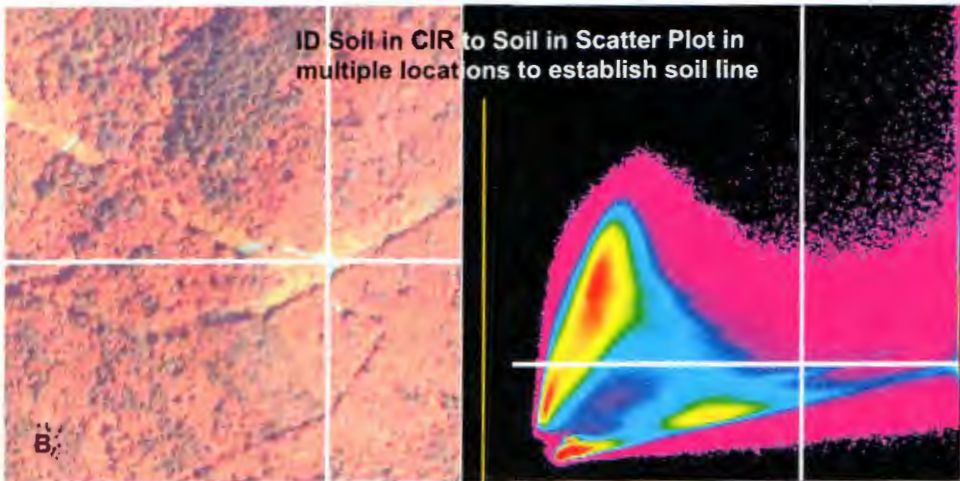


Figure C2: To establish a soil line in the scatterplot over 50 locations with exposed soil were selected within the study area. The white cross-hairs in each image represent a link between the pixel selected in the multi-spectral image and the pixel in the scatterplot. After each soil pixel was selected its location in the scatterplot was marked. Once all the samples were marked in the scatterplot a line of best fit was drawn through the marked pixels across the scatterplot. (Source: data transformation from Idrisi and graphic by Author)

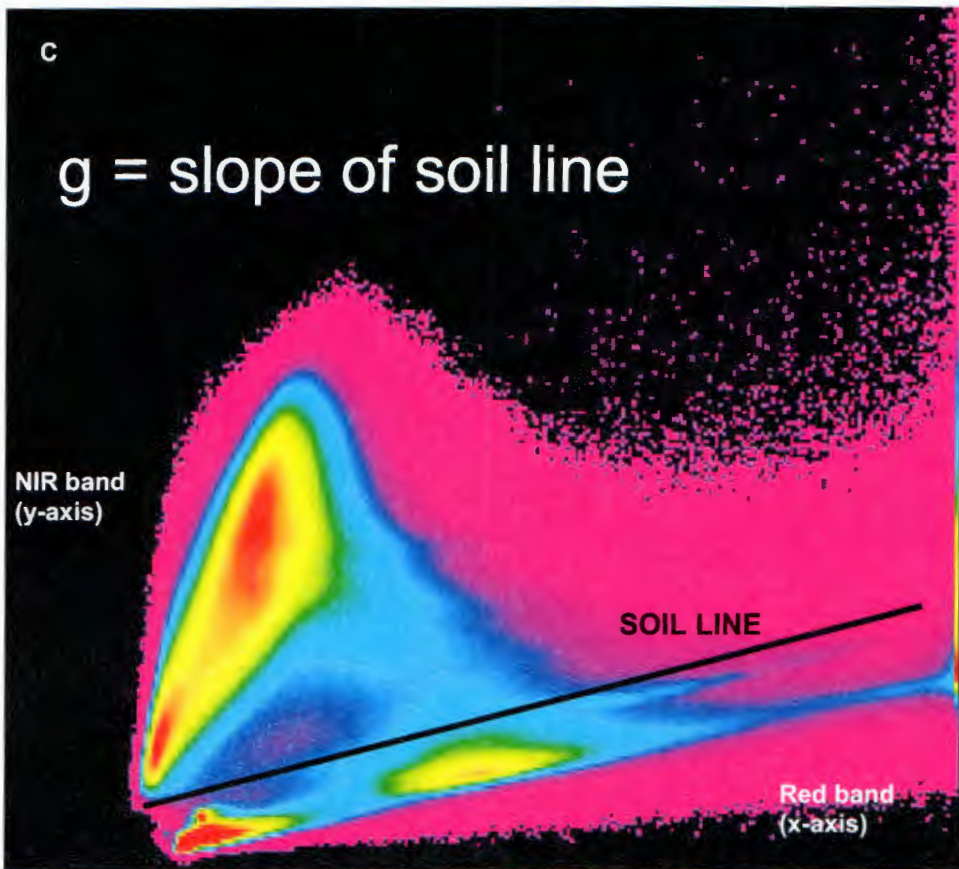


Figure C3: The soil line represents the line of best fit through sampling of bare soil pixels from the multi-spectral image. The slope of the soil line is then calculated and used in WDV equation. (Source: data transformation from Idrisi and graphic by Author)

In the tasseled cap transformation the soil line was clearly visible (Figure 81). There was a spatial component to the concentration of SRP values below the soil line. The river was the delineating feature in the image. Vegetation and bare soil values on the east side of the river were distributed in the value concentrations below the soil line. In this regard, the soil line boundary was defined by selecting multiple bare soil points on the west side of the image and drawing the line of best fit.

Many vegetation indices have been tested and used to map forest vegetation and fuels. The most commonly used is the normalized difference vegetation index

(NDVI). In 2000, Keane and his colleagues published a fuel map of the entire Gila National Forest in New Mexico. They applied NDVI to Landsat TM data. Similar methods had also been previously used to develop Farsite input layers for the Selway-Bitterroot Wilderness area. NDVI has been widely used to classify vegetation and to determine the quantity of photosynthetic biomass by using vegetation density (Pinty and Verstraete 1992).

In many respects, the NDVI is a first-order vegetation index (VI). More than 40 vegetation indices have been developed that use the principles of the Simple Ratio (SR) vegetation index and NDVI; WdVI is one of them. WdVI was selected for this study because of its soil reduction qualities. The WdVI can clearly separate the urban environment from the vegetation. Urban environments and bare soil share similar SRP characteristics. Since the park is in an urbanized environment, it was important that the urban areas be minimized during the fuel mapping process. Furthermore, Peddle, Brunke, and Hall found that WdVI was one of only a few VIs to show a moderate improvement over NDVI in its ability to predict forest biophysical parameters. They concluded that this was likely due to the inclusion of background reflectance.